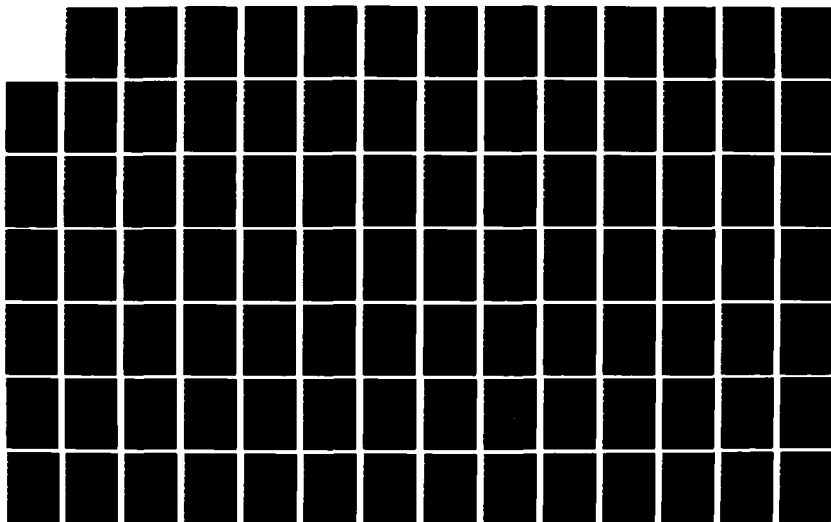AD-A171 338   OPTIMAL IMPULSIVE DIRECT ASCENT TIME-FIXED ORBITAL   1/2
               INTERCEPTION(U) AIR FORCE INST OF TECH WRIGHT-PATTERSON
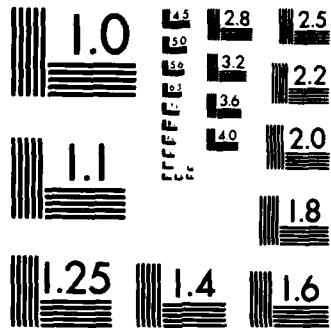   AFB OH   W G HECKATHORN 1985 AFIT/CI/NR-86-125T
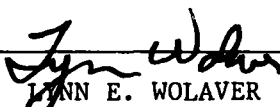
UNCLASSIFIED   F/G 22/3   NL

MICROCOPY RESOLUTION TEST CHART

NATIONAL BUREAU OF STANDARDS-1963-A

REPORT DOCUMENTATION PAGE		READ INSTRUCTIONS BEFORE COMPLETING FORM
1. REPORT NUMBER AFIT/CI/NR 86-125T	2. GOVT ACCESSION NO.	3. RECIPIENT'S CATALOG NUMBER
4. TITLE (and Subtitle) Optimal, Impulsive, Direct Ascent, Time-Fixed Orbital Interception		5. TYPE OF REPORT & PERIOD COVERED THESIS/~~DISSERTATION~~
		6. PERFORMING ORG. REPORT NUMBER
7. AUTHOR(s) William Gary Heckathorn		8. CONTRACT OR GRANT NUMBER(s)
9. PERFORMING ORGANIZATION NAME AND ADDRESS AFIT STUDENT AT: University of Illinois		10. PROGRAM ELEMENT, PROJECT, TASK AREA & WORK UNIT NUMBERS
11. CONTROLLING OFFICE NAME AND ADDRESS AFIT/NR WPAFB OH 45433-6583		12. REPORT DATE 1985
		13. NUMBER OF PAGES 104
14. MONITORING AGENCY NAME & ADDRESS(If different from Controlling Office)		15. SECURITY CLASS. (of this report) UNCLAS
		15a. DECLASSIFICATION/DOWNGRADING SCHEDULE

16. DISTRIBUTION STATEMENT (of this Report)

APPROVED FOR PUBLIC RELEASE; DISTRIBUTION UNLIMITED

17. DISTRIBUTION STATEMENT (of the abstract entered in Block 20, if different from Report)

18. SUPPLEMENTARY NOTES

APPROVED FOR PUBLIC RELEASE: IAW AFR 190-1

LYNN E. WOLAVER 13 Aug 86
Dean for Research and
Professional Development
AFIT/NR

19. KEY WORDS (Continue on reverse side if necessary and identify by block number)

20. ABSTRACT (Continue on reverse side if necessary and identify by block number)

ATTACHED.

DD FORM 1473 1 JAN 73   EDITION OF 1 NOV 65 IS OBSOLETE

ABSTRACT

A method for determining optimal impulsive trajectories is applied to minimum fuel, direct ascent, time-fixed intercept trajectories. The optimal trajectory is obtained by satisfying Lawden's necessary conditions expressed in terms of the primer vector. The vehicle is initially at rest on the surface of a spherical planet and the target is assumed to be in a circular, equatorial orbit around the planet. Results are presented and compared for two planetary models: a non-rotating planet, and one rotating with an angular velocity approximating that of the Earth. Each model is investigated for transfers in which the launch point is in the same plane as the target orbit (coplanar) and in which the launch point is not in the target orbit plane (noncoplanar). Parameters varied during the analysis include transfer time, target radius, initial position of the target in relation to the launch point, the latitude of the launch point, and the direction of the transfer trajectory, i.e. posigrade or retrograde. Cost comparisons are made between the various cases, and generalizations indicated.

QUALITY INSPECTED 1

A-1

OPTIMAL, IMPULSIVE, DIRECT ASCENT, TIME-FIXED ORBITAL INTERCEPTION

BY

WILLIAM GARY HECKATHORN

B.A.A.E., The Ohio State University, 1969
M.S., The Ohio State University, 1970

THESIS

Submitted in partial fulfillment of the requirements
for the degree of Doctor of Philosophy in
Aeronautical and Astronautical Engineering
in the Graduate College of the
University of Illinois at Urbana-Champaign, 1985

Urbana, Illinois

UNIVERSITY OF ILLINOIS AT URBANA-CHAMPAIGN

THE GRADUATE COLLEGE

AUGUST 1985

WE HEREBY RECOMMEND THAT THE THESIS BY

WILLIAM GARY HECKATHORN

ENTITLED_____ **OPTIMAL, IMPULSIVE, DIRECT ASCENT,**

_____ **TIME-FIXED ORBITAL INTERCEPTION**

BE ACCEPTED IN PARTIAL FULFILLMENT OF THE REQUIREMENTS FOR

THE DEGREE OF_____ **DOCTOR OF PHILOSOPHY**

_____
Director of Thesis Research

_____
Head of Department

Committee on Final Examination†

_____
Chairperson

Edward J. Scott

Harry H. Hilton

Julian Palmore

† Required for doctor's degree but not for master's.

ACKNOWLEDGMENTS

v

TABLE OF CONTENTS

LIST OF SYMBOLS

a	semi major axis length
c	effective exhaust velocity (eqn 2-2)
	chord length
Co	planet/moon surface
Cf	target orbit
$\underline{e}$	eccentricity vector
E	eccentric anomaly
$\underline{g}$	gravitational acceleration vector
$G(\underline{r})$	gravity gradient matrix
$\underline{h}$	angular momentum vector
H	Hamiltonian function
I	identity matrix
J	cost functional
	characteristic velocity
M,N,S,T	partitions of the state transition matrix
m	spacecraft mass
$\underline{N}$	contact force/unit mass of planet surface on launch vehicle
$\underline{n}$	nodal vector
$\underline{P}$	primer vector
P	primer vector magnitude
	period of an orbit
$\underline{r}$	position vector
R	radius of target to be intercepted

superscripts

T	transpose of vector or matrix
+	instant after an impulse
-	instant before an impulse
-1	inverse of a matrix

subscripts

o	an initial state
f	a final state
m	an intermediate state
	a minimum energy value in the Lambert Problem
1,2	reference to number of thrust impulse
k	general numerical subscript
p	periapse
H	Hohmann condition

other

$\cdot$	first derivative
$\cdot\cdot$	second time derivative
$\lvert\ \rvert$	magnitude of vector
∂	partial derivative
d	noncontemporaneous variation

CHAPTER 1

INTRODUCTION

The increased use of the Space Transportation System (STS) or space shuttle, has increased attention on the area of optimal space trajectories. Of special concern are minimum fuel trajectories. If less propellant (fuel plus oxidizer) can be carried, then more payload weight can be thrust into orbit, fuel can be saved, a smaller spacecraft can be used, or any combination of these.

The impulsive thrust approximation is valid if the thrust is large enough that the thrust duration is negligible compared to the transfer time. Thus the problem is to enter or intercept a desired planetary orbit using impulsive thrusts which minimize propellant (hereafter called minimum "fuel"). This problem is typically called Lawden's Problem due to his extensive work in minimum fuel trajectories in an inverse square gravitational field using a variable thrust engine having constant exhaust velocity and unbounded thrust magnitude (30). The impulsive solution for an entire trajectory is composed of coasting (no engine burn) arcs separated by a finite number of impulses. Optimal impulsive solutions can also be useful as starting conditions to determine optimal finite thrust solutions.

Most research has concentrated on orbital transfer trajectories using an unspecified transfer time, i.e. time-open. However, time-open optimal solutions can require excessively long or even infinite transfer times. Recent studies have explored orbital rendezvous for a specified

transfer time, i.e. time-fixed (10, 18, 29, 37). The time-fixed case is more interesting since most manned space systems have time constraints due to life support systems. Time-fixed transfers would also be appropriate for space rescue missions.

Scarce attention has been granted the area of minimum fuel orbital interception. Rather than rendezvous with another orbiting body, i.e. match position and velocity, interception requires that the space vehicle match only position. One application would be a fly-by for visual inspection. Another would involve a typical two-payload space shuttle mission. Using a technique similar to a paperboy riding down a sidewalk on his bicycle and throwing newspapers onto porches without entering every driveway or walk, the shuttle would intercept a point in the first desired orbit and launch the first payload without actually expending fuel and entering the orbit. The shuttle would then intercept a point in the second orbit, launch the payload, and return to Earth. If it entered every orbit, the shuttle would require a minimum of five velocity changes (launch, in and out of first orbit, in and out of second orbit). By intercepting the desired orbit insertion point and allowing each payload to use its own propulsion system to enter the desired orbit, the shuttle could save fuel. Less fuel would be expended by the shuttle, which would require a minimum of two velocity changes (launch and return to Earth). Each payload would require a velocity change, but less fuel would be expended because the mass of each payload would be significantly less than that of the shuttle. Thus the two shuttle velocity changes plus the two payload velocity changes would be less than the five required if the shuttle entered each orbit. This poses a potential significant fuel savings and the possibility of increased payload.

This thesis analyzes the problem of multiple-impulse, minimum-fuel, direct ascent, time-fixed orbital interception. Following are the objectives of this study:

a) Design and construct a computer program to obtain time-fixed, minimum fuel, impulsive, direct ascent intercept trajectories.

b) Apply the method to the time-fixed, direct ascent intercept from a specified initial position on a planet or moon's surface to a specified target.

c) Show the effects of different target orbit radii and initial phase angles.

d) Show the effects of inclination of the target orbit with respect to the launch point.

e) Show the effects of planet/moon rotation on the intercept.

To obtain minimum fuel optimum intercept trajectories, the following assumptions were made:

a) The planet/moon is spherical and has negligible atmospheric effects.

b) The spacecraft has a zero velocity relative to the planet immediately before the first impulse is applied.

c) A planet-centered, inertial, Cartesian coordinate system is used.

d) Launch is from an arbitrary point on the planet/moon surface.

e) The target is in a circular, equatorial orbit.

f) The intercept must be made in a finite, fixed time.

g) The engine burn times are very short compared to the transfer time. This allows the impulsive thrust approximation to be made.

h) The body from which the launch is made is the sole gravitational source.

i) Only one target is to be intercepted, i.e. no multiple interceptions are to be made.

Two planetary models are investigated: a nonrotating planet and a planet having a rotation period which is approximately 17 times the circular orbit period at the surface (comparable to Earth). The nonrotating model approximates celestial bodies which have a very low rotation rate and virtually no atmosphere, such as the Moon (for which the rotation period is approximately 400 times the circular orbit period at the surface). The model which includes planet rotation is intended to be a first approximation to optimal Earth intercepts. It is included to illustrate the effects of planet rotation.

CHAPTER 2

NECESSARY CONDITIONS FOR AN OPTIMAL, IMPULSIVE TRAJECTORY

2.1. Introduction

General optimization theory provides conditions for which a cost functional is minimized subject to a set of constraints. The optimization problem presented herein is basically to minimize propellant (fuel) expended in an inverse square gravitational field using the impulsive thrust approximation for a fixed transfer time. Minimizing propellant used is the same as maximizing the final spacecraft mass, i.e. the change in mass is assumed to be entirely due to the consumed propellant. The necessary constraints are the differential equations of motion of the spacecraft, the terminal position of the target to be intercepted, and the initial position and velocity of the spacecraft.

2.2. Cost Functional

A general form of the cost functional to be minimized in an optimal control problem over a time interval to $\leq t \leq t_f$ is as follows:

$$J = \phi \, [\underline{X}(t_f), t_f] + \int_{t_o}^{t_f} L(\underline{X}, \underline{U}, t) dt \qquad\qquad 2\text{-}1$$

where $\underline{X}$ (t) is the instantaneous state vector of the system and $\underline{U}$ (t) is the control vector.

The impulsive thrust approximation requires the thrust durations to be short compared to the time of flight. This is the case for high thrust rocket engines where the thrust acceleration greatly exceeds

the gravitational acceleration. Ignoring the gravitational acceleration, the vector change in velocity due to the thrust impulse is

$$\Delta \underline{V} = c \ln (m_o/m_f) \underline{U} \qquad \text{2-2}$$

where m_o and m_f are the initial and final masses, c is the effective exhaust velocity of the engine, and $\underline{U}$ is the unit thrust vector, i.e. $\Delta \underline{V}$ is in the direction of the thrust. For a single impulse, maximizing m_f is equivalent to minimizing $|\Delta \underline{V}|$. Thus, for N impulses, maximizing m_f corresponds to minimizing the sum of magnitudes of $\Delta \underline{V}$, i.e.

$$J = \sum_{i=1}^{N} |\Delta \underline{Vi}| \qquad \text{2-3}$$

where

$$|\Delta \underline{Vi}| = (\Delta \underline{Vi} \cdot \Delta \underline{Vi})^{1/2} \qquad \text{2-4}$$

and J is termed the characteristic velocity.

Therefore, minimizing the fuel expended, maximizing the final mass, $m(t_f)$, and minimizing the sum of the magnitudes of the velocity changes, are equivalent optimization criteria for the impulsive thrust problem.

2.3. Equations of Motion

The equations of motion of a spacecraft, thrusting in a central force field, can be written in terms of the orbital radius vector, $\underline{r}$, as

$$\dot{\underline{r}} = \underline{V}$$
$$\dot{\underline{V}} = \underline{g} (\underline{r}) + \Gamma \underline{U} \qquad \text{2-5}$$
$$\dot{J} = \Gamma$$

where $\underline{g}$ ($\underline{r}$) is the gravitational acceleration vector, Γ is the thrust acceleration magnitude ($0 \leq \Gamma \leq \Gamma$ max), J is the characteristic velocity to be minimized, and $\underline{U}$ is a unit vector in the direction of thrust. In the impulsive case, J is the sum of the magnitudes of the instantaneous velocity changes, as discussed in the previous section. Define a state vector as

$$\underline{X} = \begin{bmatrix} \underline{r} \\ \underline{V} \\ J \end{bmatrix} \qquad\qquad 2\text{-}6$$

Rewrite the equations of motion (2-5) in first order form as

$$\underline{\dot{X}} = f\ (\underline{X},\ \Gamma,\ \underline{U},\ t) = \begin{bmatrix} \underline{V} \\ \underline{g}\ (\underline{r}) + \Gamma\ \underline{U} \\ \Gamma \end{bmatrix} \qquad 2\text{-}7$$

where the control variables are Γ and $\underline{U}$.

For a high thrust engine, one can make the impulsive thrust approximation by assuming unbounded thrust magnitude (Γmax $\rightarrow \infty$). Then the engine is either off ($\Gamma = 0$) or provides an impulsive thrust of infinitesimal time duration.

To determine a minimum fuel solution, one must solve the optimal control problem over a fixed-time interval $t_o \leq t \leq t_f$. This solution must minimize the final value of J and satisfy the equations of motion and the orbital boundary conditions of the intercept problem.

2.4. Necessary Conditions

The necessary conditions for the optimal trajectory are expressed in terms of the Hamiltonian function (8, 30):

$$H = \underline{\lambda}^T (t) \ f \ (\underline{X}, \ \Gamma, \ \underline{U}, \ t) \qquad \text{2-8}$$

where $\underline{\lambda}$ (t) is a vector of Lagrange multiplier functions, also called adjoint variables. Partitioning the adjoint vector into components similar to the state vector we get

$$\underline{\lambda} = \begin{bmatrix} \underline{\lambda}_r \\ \underline{\lambda}_v \\ \lambda_J \end{bmatrix} \qquad \text{2-9}$$

The Hamiltonian (2-8) now becomes

$$H = \underline{\lambda}_r^T \ \underline{V} + \underline{\lambda}_v^T \ [\underline{g} \ (\underline{r}) + \Gamma \ \underline{U}] + \lambda_J \ \Gamma \qquad \text{2-10}$$

Three of the necessary adjoint equations for the problem are given by Lawden (30), Bryson and Ho (8), and Prussing and Chiu (40) as

$$\underline{\dot{\lambda}}_r^T = -\partial H/\partial \underline{r} = -\underline{\lambda}_v^T \ G \ (\underline{r}) \qquad \text{2-11}$$

$$\underline{\dot{\lambda}}_v^T = -\partial H/\partial \underline{V} = -\underline{\lambda}_r^T \qquad \text{2-12}$$

$$\dot{\lambda}_J = -\partial H/\partial J = 0 \qquad \text{2-13}$$

where G $(\underline{r})$ is the symmetric gravity gradient matrix $\partial \underline{g} \ (\underline{r})/\partial \underline{r}$. The boundary conditions on $\underline{\lambda}_r$ and $\underline{\lambda}_v$ depend on the terminal state constraints, $\underline{r}$ (t_f) and $\underline{V}$ (t_f), but, because the characteristic velocity is unconstrained, the constant value of its adjoint variable is

$$\lambda_J(t) = 1 \qquad \text{2-14}$$

An additional necessary condition is the Pontryagin Minimum Principle which states that the control variables must be chosen to

minimize the instantaneous value of the Hamiltonian (8). Thus, to minimize H, we minimize the dot product $\underline{\lambda}_v^T \underline{U}$, i.e. align the thrust vector in the opposite direction of the adjoint velocity vector. Lawden termed this the primer vector,

$$\underline{P}(t) = -\underline{\lambda}_v(t) \qquad 2\text{-}15$$

Noting that the optimal thrust direction is aligned with the primer

$$\underline{U} = \underline{P}/P \qquad 2\text{-}16$$

where P is the magnitude of the primer vector, and that the adjoint to the position vector, $\underline{\lambda}_r$, equals the primer vector time derivative, $\underline{\dot{P}}$,

$$\underline{\lambda}_r = \underline{\dot{P}} \qquad 2\text{-}17$$

one notes that equations (2-11) and (2-12) can be combined to obtain

$$\underline{\ddot{P}} = G(\underline{r})\underline{P} \qquad 2\text{-}18$$

The Hamiltonian becomes

$$H = \underline{\dot{P}}^T \underline{V} - \underline{P}^T \underline{g} - (P\text{-}1)\,\Gamma \qquad 2\text{-}19$$

The primer vector satisfies the same differential equation (2-18) as the first-order variation in the position vector $\underline{\delta r}$ about a reference no-thrust orbit. For an inverse square gravitational field, convenient forms of the solution to this equation are given by Glandorf (15) and by Gravier, Marchal, and Culp (17).

From the Hamiltonian (2-19) one identifies the switching function for the thrust magnitude as (P-1). In the continuous thrust case, the Hamiltonian is minimized by choosing $\Gamma = 0$ when P<1 and $\Gamma = \Gamma$ max when P>1. For the impulsive case, $\Gamma = 0$ when P<1, with the impulses occurring at those instants where P(t) is tangent to P = 1 from below (30). An arc along which $\Gamma = 0$ is called a null-thrust (NT) arc. The only possibility for an intermediate-thrust (IT) arc for $0<\Gamma<\Gamma$ max is if P = 1 over a finite time interval. This is called a singular arc because Γ cannot be determined from the Hamiltonian (2-19).

The necessary conditions for an optimal impulsive trajectory, first derived by Lawden, can be written entirely in terms of the primer vector as follows:

1. The primer vector satisfies (2-18) and must be continuous with continuous first derivative.

2. The primer magnitude P≤1 during transfer with impulses occurring at those instants for which P = 1.

3. At an impulse time the primer vector is a unit vector in the optimal thrust direction.

4. As a consequence of condition 2, $\dot{P} = \underline{\dot{P}}^T \underline{P} = 0$ at all interior impulses (not at an initial or final time).

2.5. Primer Vector Calculation

Using the primer vector, equations (2-11) and (2-12) can be written as

$$
\begin{bmatrix} \dot{\underline{P}}\,(t) \\[2ex] \ddot{\underline{P}}\,(t) \end{bmatrix} = \begin{bmatrix} 0 & I \\[2ex] G\,(\underline{r}) & 0 \end{bmatrix} \begin{bmatrix} \underline{P}\,(t) \\[2ex] \dot{\underline{P}}\,(t) \end{bmatrix}
\qquad\qquad 2\text{-}20
$$

The solution to equation (2-20) can be expressed as

$$
\begin{bmatrix} \underline{P}\,(t) \\[2ex] \dot{\underline{P}}\,(t) \end{bmatrix} = \emptyset\,(t,\,t_o) \begin{bmatrix} \underline{P}\,(t_o) \\[2ex] \dot{\underline{P}}\,(t_o) \end{bmatrix}
\qquad\qquad 2\text{-}21
$$

where $\emptyset\,(t,\,t_o)$ is the state transition matrix for the system (2-20).
A convenient form of this state transition matrix has been derived by
Glandorf (15). Gravier developed a vector form of the solution for
the primer vector and the time derivative of the primer vector (17).
This research uses Glandorf's formulation, which is valid for generally
oriented inertial Cartesian systems, and for circular, elliptic, para-
bolic, and hyperbolic transfers, but not for rectilinear flight.

By partitioning the transition matrix into four submatrices

$$
\emptyset\,(t,\,t_o) = \begin{bmatrix} M(t,\,t_o) & N(t,\,t_o) \\[2ex] S(t,\,t_o) & T(t,\,t_o) \end{bmatrix}
\qquad\qquad 2\text{-}22
$$

the primer equations can more easily be written as

$$
\underline{P}\,(t) = M\,\underline{P}\,(t_o) + N\,\dot{\underline{P}}\,(t_o)
\qquad\qquad 2\text{-}23
$$

$$
\dot{\underline{P}}\,(t) = S\,\underline{P}\,(t_o) + T\,\dot{\underline{P}}\,(t_o)
\qquad\qquad 2\text{-}24
$$

Forcing the primer at the initial impulse time to be a unit vector in the thrust direction, one obtains

$$\underline{P}\ (t_o) = \Delta\ \underline{V}_o/\Delta\ V_o \qquad\qquad 2\text{-}25$$

However, for an intercept, no velocity change is required at the final time, yielding

$$\underline{P}\ (t_f) = \underline{0} \qquad\qquad 2\text{-}26$$

Applying (2-26) to (2-23) and (2-24) yields

$$\underline{\dot{P}}\ (t_o) = -N_f^{-1}\ M_f\ \underline{P}\ (t_o) \qquad\qquad 2\text{-}27$$

$$\underline{P}\ (t)\ = (M - N\ N_f^{-1}\ M_f)\ \underline{P}\ (t_o) \qquad\qquad 2\text{-}28$$

Thus, knowing the primer vector at the initial and final times allows calculation of the primer time derivative at the initial time, and calculation of $\underline{P}$ and $\underline{\dot{P}}$ at any time.

2.6. Constants of Motion on an Optimal Trajectory

If the gravity field is time-invariant, the Hamiltonian (2-19) is not an explicit function of time. This fact along with the other necessary conditions of optimal control theory implies that H is constant over an entire NT trajectory (8). Furthermore, H is continuous across interior impulses as shown by applying Lawden's necessary conditions. For an impulsive trajectory the Hamiltonian is

$$H = \underline{\dot{P}}^T\ \underline{V} - \underline{P}^T\ \underline{g} \qquad\qquad 2\text{-}29$$

since $\Gamma = 0$. Since $\underline{P}$, $\underline{\dot{P}}$, and $\underline{g}$ are continuous across optimal impulses, the change in H across the impulse is

$$\Delta H = \underline{\dot{P}}^T \Delta \underline{V} \qquad\qquad 2\text{-}30$$

Because the velocity change $\Delta \underline{V}$ is aligned with the primer vector $\underline{P}$, and $\underline{\dot{P}}^T \underline{P} = 0$, $\Delta H = 0$ across an optimal interior impulse. This continuity of H across interior impulses demonstrates that H is constant along the entire multiple impulse optimal trajectory.

Another constant of motion applies to an NT arc between any two impulses along a reference trajectory. Premultiply (2-18) by $\underline{\delta r}^T$ and note that G is symmetric to obtain

$$\underline{P}^T \delta\underline{\ddot{r}} - \delta\underline{r}^T \underline{\ddot{P}} = 0 \qquad\qquad 2\text{-}31$$

Add and subtract $\underline{\dot{P}}^T \delta \underline{V}$ to obtain

$$d/dt \; (\underline{P}^T \delta \underline{V} - \underline{\dot{P}}^T \delta\underline{r}) = 0 \qquad\qquad 2\text{-}32$$

Integrating yields

$$\underline{P}^T \delta \underline{V} - \underline{\dot{P}}^T \delta\underline{r} = \text{constant} \qquad\qquad 2\text{-}33$$

This is a useful equation in determining optimal trajectories.

Prussing (39) and Pines (33) have shown the existence of other constants of motion. However, equation 2-33 and the Hamiltonian, equation 2-29, were used extensively in analysis and development of computer algorithms for numerical results.

CHAPTER 3

THE MINIMIZATION PROCESS

3.1. Introduction

Based on the necessary conditions of Chapter 2, Lion and Handelsman (31) developed a procedure for obtaining optimal time-fixed solutions, which is used as a background for the optimal interception problem of this thesis. This procedure has been used by many others, including Jezewski and Rozendaal (26), Gross and Prussing (19), and Prussing and Chiu (40). Briefly, the primer vector is first evaluated along the solution which satisfies the orbital boundary conditions, enforcing the necessary conditions that the primer vector at an impulse time is a unit vector in the thrust direction and that the primer vector at the final time is zero (eqns 2-25 and 2-26).

The required velocity changes were obtained by solving Lambert's Problem (Appendix B, 2, 3, 4, 13, 27) for the given orbital boundary conditions (initial and final radii) and the specified transfer time. The following theory discusses conditions for the one and two impulse case. For more details see references 19, 26, 31, and 40.
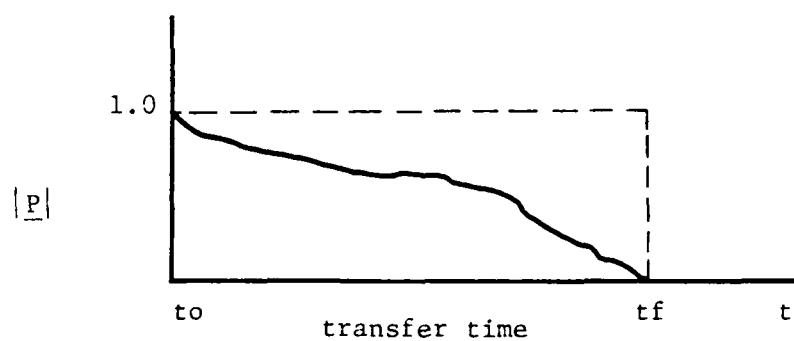
3.2. Primer on Nonoptimal Trajectory

Lion and Handelsman (31) expanded the primer definition for any two impulse segment of a nonoptimal trajectory. At each impulse on an optimal trajectory, the primer is a unit vector aligned with the vector change in velocity:

$$\underline{P}\ (t_k) = \Delta\ \underline{V}\ (t_k)\ /\ \Delta\ V\ (t_k) \qquad\qquad 3\text{-}1$$

If the velocity changes on any two impulse segment of a trajectory or the segment between an impulse time and the final time are known, so is the primer at each end of the segment. Using the partitioning of the transition matrix developed in 2-22, the time rate of change of the primer at either end of the segment is also known, and thus the primer vector, $\underline{P}\ (t)$, and its derivative, $\underline{\dot{P}}\ (t)$, are uniquely determined over the NT arc, assuming the N submatrix is nonsingular, i.e. invertible.

In general, the solution of 2-21 for different arcs can be joined together so that the primer is continuous over the entire trajectory, since $\underline{P}$ at an impulse time is a unit vector in the thrust direction. The primer rate, $\underline{\dot{P}}$, will be generally discontinuous across each impulse. In attempting to satisfy Lawden's necessary conditions, Lion and Handelsman not only extended the primer vector application as demonstrated above, but also showed how to improve the cost functional by using information available on the nonoptimal trajectory.

Based on numerical results, Lion and Handelsman's work, and the fact that for an intercept the final primer vector magnitude must be zero, certain types of primer vector time histories are possible, as shown in Figure 3-1. The existence of other types has not been disproved. Only the time history shown in Figure 3-1(a) satisfies Lawden's optimality conditions. Figure 3-1(b) indicates that an additional intermediate impulse will improve the cost, while Figure 3-1(c) indicates that an initial coast will improve cost.

(a) Optimal Trajectory
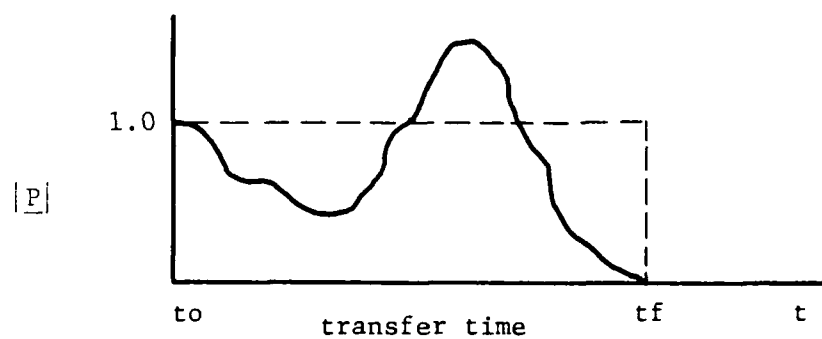
(b) Intermediate Impulse Indicated
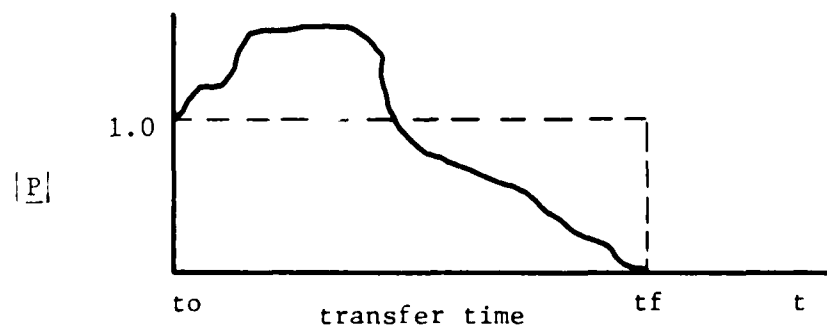
(c) Initial Cost Indicated

Figure 3-1. Typical Interception Primer Time Histories.

3.3. Additional Impulse

Assume there is a reference trajectory Γ_1 that connects the initial position $\underline{r}$ (t_o) on the body of the planet, C_o, to a final position $\underline{r}$ (t_f) on the target orbit, C_f. Γ_1 may be a one impulse intercept trajectory or a multi-impulse trajectory. Let Γ_2 be a neighboring trajectory. If Γ_1 and Γ_2 are sufficiently close, and Γ_1 does not contain any singularities, a linear variational analysis approach may be used, with higher order terms omitted. Thus the costs on Γ_1 and Γ_2 from Figure 3-2 are

$$\text{on } \Gamma_1: \quad J_1 = |\; \underline{V}_{2o}^+ - \underline{V}_{1o}^- \;|$$

and

$$\text{on } \Gamma_2: \quad J_2 = |\; \underline{V}_{2o}^+ - \underline{V}_{2o}^- \;| + |\; \underline{V}_{2m}^+ - \underline{V}_{2m}^- \;|$$

3-2

where the superscripts (+) and (−) refer to the instants immediately before and after the impulses. The subscripts (1) and (2) represent Γ_1 and Γ_2, while (o) and (m) denote the initial and midcourse impulse. For an intercept, there is no final velocity change. From the vectors at the initial time, note

$$\underline{V}_{2o}^+ = \underline{V}_{1o}^+ + \delta \, \underline{V}_o^+$$

3-3

Lion and Handelsman (31), Chiu (10), and Prussing and Chiu (40) have shown these results lead to the first order change in cost obtained by adding an impulse as

$$\delta J = J_2 - J_1 = \Delta V_m \, (1 - \underline{P}_m^{\;T} \, \underline{U}_m)$$
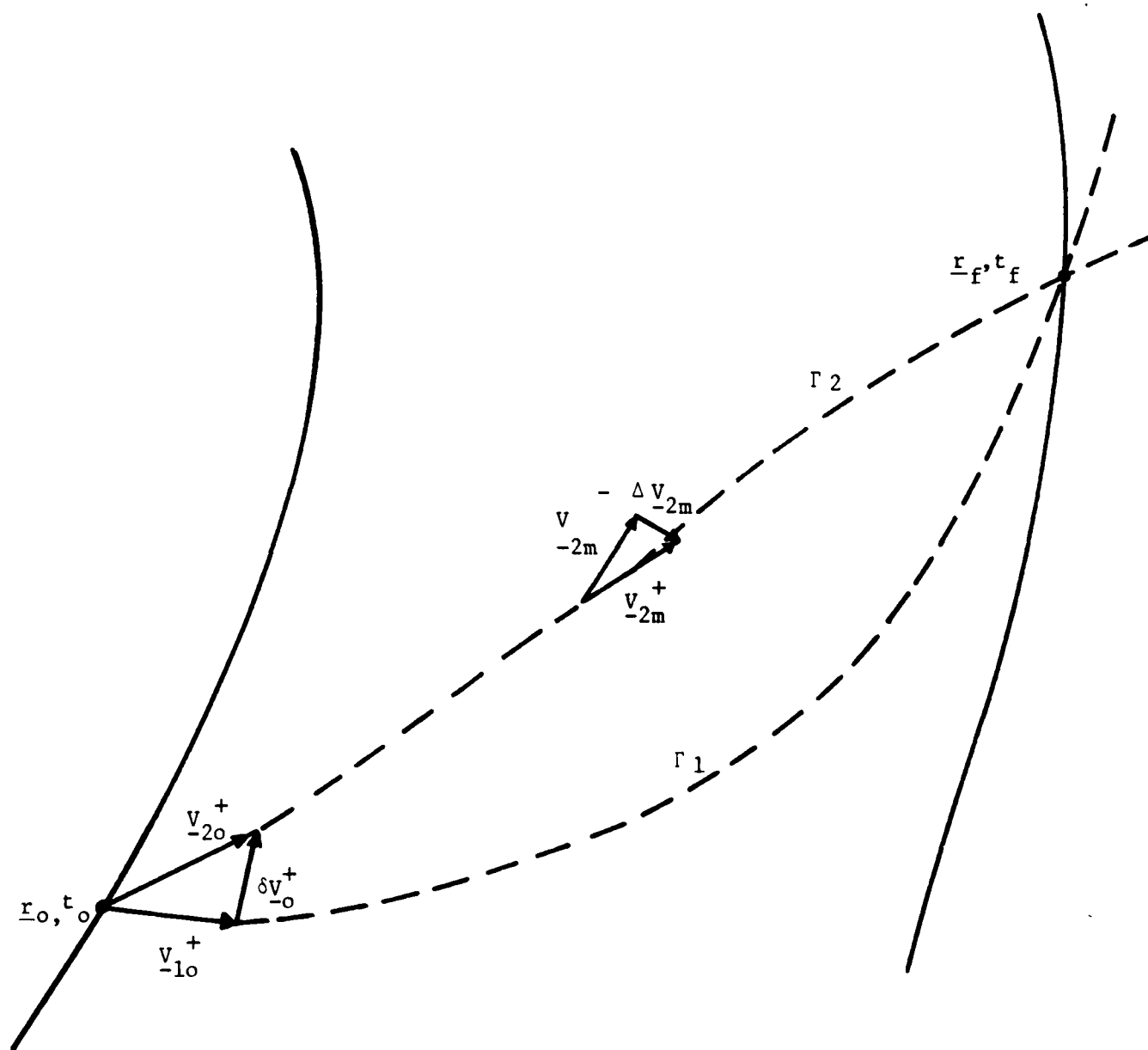
3-4

Figure 3-2. Additional Impulse Intercept Trajectories.

This change in cost can be made negative if the primer magnitude exceeds unity at any time along the two-impulse trajectory. This agrees with Lawden's condition that $P \leq 1$ on an optimal trajectory. The greatest decrease in cost occurs when t_m is such that the primer magnitude is a maximum and the impulse direction $\underline{U}_m$ is chosen to be aligned with $\underline{P}_m$.

Lion and Handelsman show that the differential cost between neighboring trajectories is

$$\delta J = (\underline{\dot{P}}^T_m{}^+ - \underline{\dot{P}}^T_m{}^-) \, d \, \underline{r}_m + (H^+ - H^-) \, dt_m \qquad \text{3-5}$$

3.4. Initial Coast

Figure 3-3 shows two neighboring trajectories: Γ_1 is a non-optimal trajectory with an impulse applied at t_o and $\underline{r}(t_o)$; Γ_2 is a nonoptimal trajectory remaining on the surface of the planet or moon, with an initial coast until time $t_1 = t_o + dt_o$ and the impulse applied at $\underline{r}(t_1)$. Both trajectories intercept $\underline{r}(t_f)$ on orbit C_f.

Since there are differences in position, velocity, and time at the initial impulse (if the planet is rotating), a noncontemporaneous variation is used, i.e.

$$d \, \underline{r}(t) = \underline{r}_2(t_1) - \underline{r}_1(t) \qquad \text{3-6}$$

where $\underline{r}_2(t_1)$ is the position vector on Γ_2 at time t_1, and $\underline{r}_1(t)$ the position vector on Γ_1 at time t. Using $dt - t_1 - t$ and $\delta\underline{r}(t) = \underline{r}_2(t) - \underline{r}_1(t)$, 3-6 becomes to first order,

$$d \, \underline{r}(t) = \delta\underline{r}(t) + \underline{\dot{r}}_1(t) \, dt \qquad \text{3-7}$$
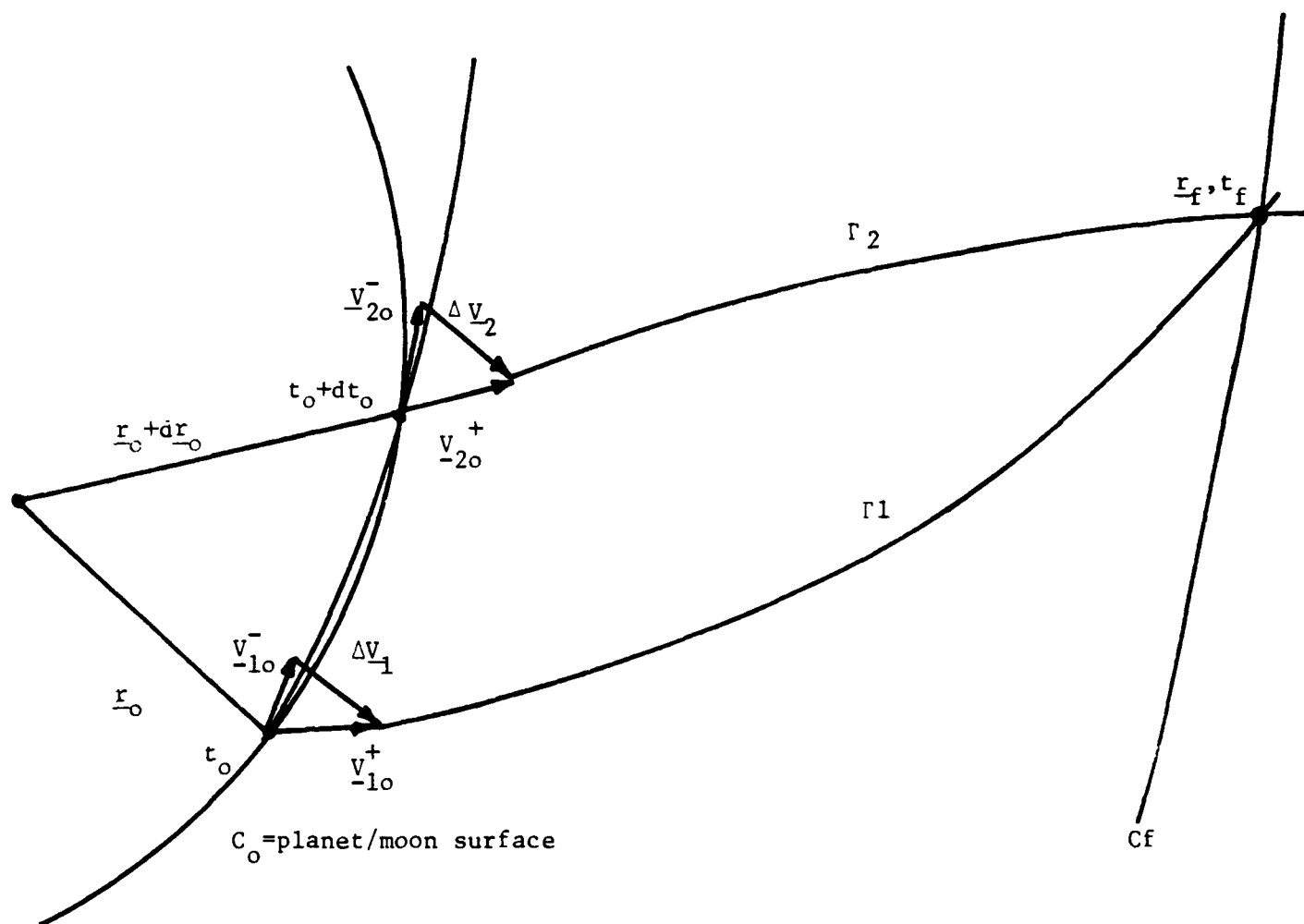
The costs on Γ_1 and Γ_2 are

Figure 3-3. Initial Coast Intercept Trajectories.

$$\text{on } \Gamma_1: \quad J_1 = |\ \underline{V}_{1o}^+ - \underline{V}_{1o}^-\ |$$

and ⟶ 3-8

$$\text{on } \Gamma_2: \quad J_2 = |\ \underline{V}_{2o}^+ - \underline{V}_{2o}^-\ |$$

For a nonrotating planet, $\underline{V}_{1o}^- = \underline{V}_{2o}^- = 0$, but they are nonzero for a rotating planet. Thus the costs become

$$J_1 = |\ \underline{V}_{1o}^+ - \underline{V}_{1o}^-\ | = |\ \Delta\ \underline{V}_1\ |$$

and ⟶ 3-9

$$J_2 = |\ \underline{V}_{2o}^+ - \underline{V}_{2o}^-\ | = |\ \Delta\ \underline{V}_2\ |$$

But

$$\underline{V}_{2o}^+ (t_1) = \underline{V}_{1o}^+ (t_o) + d\ \underline{V}_o^+ (t_o)$$ ⟶ 3-10

The difference in cost is

$$dJ = J_2 - J_1 = |\ \underline{V}_{2o}^+ - \underline{V}_{2o}^-\ | - |\ \underline{V}_{1o}^+ - \underline{V}_{1o}^-\ |$$ ⟶ 3-11

Using the fact that

$$\underline{V}_{2o}^+ = \underline{V}_{1o}^+ + d\ \underline{V}_o^+$$

and $$\underline{V}_{2o}^- = \underline{V}_{1o}^- + d\ \underline{V}_o^-$$ ⟶ 3-12

One can rewrite equation 3-11 as

$$dJ = |\ (\underline{V}_{1o}^+ - \underline{V}_{1o}^-) + (d\ \underline{V}_o^+ - d\ \underline{V}_o^-)\ | - |\ \underline{V}_{1o}^+ - \underline{V}_{1o}^-\ |$$ ⟶ 3-13

or $\qquad dJ = | \ \Delta\underline{V}_{1o} + \Delta d\underline{V}_o \ | - | \ \Delta\underline{V}_{1o} \ |$ $\qquad\qquad$ 3-14

Expanding the first term yields

$$| \Delta\underline{V}_{1o} + \Delta d\underline{V}_o \ | = [(\Delta\underline{V}_{1o} + \Delta d\underline{V}_o)^T (\Delta\underline{V}_{1o} + \Delta d\underline{V}_o)]^{1/2}$$
$$= [(\Delta\underline{V}_{1o})^T \Delta\underline{V}_{1o} + 2(\Delta\underline{V}_{1o})^T \Delta d\underline{V}_o$$
$$+ \Delta d\underline{V}_o^T \Delta d\underline{V}_o]^{1/2} \qquad\qquad 3\text{-}15$$

Ignoring higher order terms, e.g. $\Delta d\underline{V}_o^T \Delta d\underline{V}_o$, 3-15 becomes

$$| \Delta\underline{V}_{1o} + \Delta d\underline{V}_o \ | = \Delta V_{1o} \ [1 + 2 \ (\Delta\underline{V}_{1o})^T \Delta d\underline{V}_o / \Delta V_{1o}{}^2]^{1/2} \qquad 3\text{-}16$$

where $\Delta V_{1o} = | \Delta\underline{V}_{1o} | = [(\Delta\underline{V}_{1o})^T \Delta\underline{V}_{1o}]^{1/2}$.

Use the binomial series expansion

$$(1 + \varepsilon)^{1/2} = 1 + 1/2 \ \varepsilon + \text{higher order terms} \qquad\qquad 3\text{-}17$$

and drop the higher order terms to obtain

$$| \Delta\underline{V}_{1o} + \Delta d\underline{V}_o \ | \cong \Delta V_{1o} \ [1 + (\Delta\underline{V}_{1o})^T \Delta d\underline{V}_o / \Delta V_{1o}{}^2] \qquad\qquad 3\text{-}18$$

Substituting 3-18 into 3-14 yields

$$dJ = \Delta V_{1o} \ [1 + \Delta\underline{V}_{1o}{}^T \Delta d\underline{V}_o / \Delta V_{1o}{}^2] - \Delta V_{1o}$$

or $\qquad dJ = \Delta\underline{V}_{1o}{}^T \Delta d\underline{V}_o / \Delta V_{1o}$ $\qquad\qquad$ 3-19

Using the primer definition the difference in cost, to first order, between two neighboring intercepts, one with an initial coast, may be written as

$$dJ = \underline{P}_o{}^T \Delta d \ \underline{V}_o \qquad\qquad 3\text{-}20$$

or $\qquad dJ = \underline{P}_o^T \, (d \, \underline{V}_o^+ - d \, \underline{V}_o^-)$ $\qquad\qquad$ 3-21

where $d \, \underline{V}_o^+ = \delta\underline{V}_o^+ + \dot{\underline{V}}_o^+ \, dt_o$ $\qquad\qquad$ 3-22

and, because $\delta \, \underline{V}_o^- = \underline{0}$

$\qquad d \, \underline{V}_o^- = \dot{\underline{V}}_o^- \, dt_o$ $\qquad\qquad$ 3-23

From Section 2.6, it was found that

$\qquad \underline{P}^T \, \delta \, \underline{V} - \dot{\underline{P}}^T \, \delta \, \underline{r} = $ constant $\qquad\qquad$ 3-33

Applying this at the initial and final times yields

$\qquad \underline{P}_o^T \, \delta\underline{V}_o - \dot{\underline{P}}_o^T \, \delta\underline{r}_o = \underline{P}_f^T \, \delta\underline{V}_f - \dot{\underline{P}}_f^T \, \delta\underline{r}_f$ $\qquad\qquad$ 3-24

But for an intercept, $\underline{P}_f = 0$ and $\delta\underline{r}_f = 0$, simplifying 3-24 to

$\qquad \underline{P}_o^T \, \delta\underline{V}_o = \dot{\underline{P}}_o^T \, \delta\underline{r}_o$ $\qquad\qquad$ 3-25

In the case of launching from the surface of a planet, $\dot{V}_o$ is not continuous due to the contact force per unit mass, $\underline{N}$ of the planet on the vehicle before the first impulse. Rewrite equation 3-21 using equations 3-22 and 3-23.

$\qquad dJ = \underline{P}_o^T \, [\delta\underline{V}_o^+ + (\dot{\underline{V}}_o^+ - \dot{\underline{V}}_o^-)dt_o]$ $\qquad\qquad$ 3-26

Because gravitational acceleration is a function of position only and is therefore continuous, this becomes

$\qquad dJ = \underline{P}_o^T \, [\delta\underline{V}_o^+ - \underline{N} \, dt_o]$ $\qquad\qquad$ 3-27

Using equation 3-25 the cost difference becomes

$$dJ = \dot{\underline{P}}^T_{\ o} \ \delta\underline{r}_o - \underline{P}_o^{\ T} \ \underline{N} \ dt_o \qquad\qquad 3\text{-}28$$

Using the fact that on the transfer orbit

$$\delta\underline{r}_o = d\underline{r}_o - \underline{V}_o^{\ +} \ dt_o$$

and $\qquad d\underline{r}_o = \underline{V}_o^{\ -} \ dt_o$

one obtains

$$\delta\underline{r}_o = -(\underline{V}_o^{\ +} - \underline{V}_o^{\ -}) \ dt_o$$
$$= -\Delta\underline{V}_o \ dt_o$$

Substituting into 3-28 yields

$$dJ = -[\Delta V_o \ \dot{\underline{P}}^T_{\ o} \ \underline{P}_o + \underline{P}^T_{\ o} \ \underline{N}] \ dt_o \qquad\qquad 3\text{-}29$$

The first term is the usual term which indicates an initial coast on an initial orbit if $\dot{\underline{P}}_o^{\ T} \ \underline{P}_o > 0$. The second term is due to the fact that the vehicle is initially not in orbit, but at rest on the surface of a planet. Thus the cost can be decreased by an initial coast if the term in the bracket in equation 3-29 is positive.

3.5. Condition for Optimal Initial Coast

To evaluate various trajectories for optimality, the cost functional must be represented using known quantities. It can then be determined how to minimize the cost to obtain local optimality conditions. From Chapter 2, the Hamiltonian (2-29) can be written for an inverse square gravitational field as

$$H = \dot{\underline{P}}^T \ \underline{V} + \mu/r^3 \ \underline{P}^T \ \underline{r} \qquad\qquad 3\text{-}30$$

Write the cost functional as

$$J = \phi \, [\underline{X}\,(t_f),\; t_f] + \int_{t_o}^{t_f} \{L(\underline{X},\underline{U},t) + \lambda^T[f(\underline{X},\underline{U},t)-\dot{X}]\}dt \qquad 3\text{-}31$$

Bryson and Ho (8) show that

$$dJ = \int_{t_o}^{t_f} \partial H/\partial \underline{U}\;\; \delta\underline{U}\; dt + [\underline{\lambda}^T\, d\underline{X} - H\, dt]_{t=t_o} \qquad 3\text{-}32$$

One necessary condition is that $\partial H/\partial \underline{U} = 0$, yielding

$$dJ = \lambda^T_{ro}\;\; d\underline{r}_o + \lambda^T_{vo}\;\; d\underline{V}_o - H_o\, dt_o \qquad 3\text{-}33$$

In primer vector notation this becomes

$$dJ = \dot{\underline{P}}^T\, d\underline{r}_o - \underline{P}_o{}^T\, d\underline{V}_o - H_o\, dt_o \qquad 3\text{-}34$$

where $H = $ constant $= H_o$ can be obtained from 3-30. Thus the difference in cost can be obtained using the initial primer, primer derivative, radius, and velocity.

Noting that for a rotating planet with a $\underline{V}$ rot $= \underline{w}x\underline{r}_o$ rotational velocity vector, one obtains

$$d\underline{r}_o = \underline{V}_{rot}\, dt_o \qquad 3\text{-}35$$

and $\quad d\underline{V}_o = -V_{rot}{}^2/r_o{}^2\; \underline{r}_o dt_o \qquad 3\text{-}36$

Rewrite 3-32 using 3-35 and 3-36 to obtain

$$dJ = [\dot{\underline{P}}_o{}^T\, \underline{V}_{rot} + V_{rot}{}^2/r_o{}^2\, \underline{P}_o{}^T\, \underline{r}_o - H_o]\, dt_o \qquad 3\text{-}37$$

For arbitrary dt_o, dJ is minimized when the bracketed term in 3-37 is zero, i.e.

$$\dot{\underline{P}}_o{}^T \underline{V}_{rot} + V_{rot}{}^2/r_o{}^2 \underline{P}_o{}^T \underline{r}_o - H_o = 0 \qquad 3\text{-}38$$

This is an alternate form of equation 3-29 and is more convenient for numerical analysis and to allow evaluation of local optimization. Note that for a non-rotating planet, $H_o = 0$ is the condition for minimizing cost. For a rotating planet, 3-38 must be met.

3.6. Numerical Scheme and Constraints

Besides the two planetary models of the nonrotating planet and one rotating with the Earth's angular velocity, the relative position of launch point and target was also investigated. Thus a coplanar condition is one in which the target orbit and the launch point are in the same plane. An inclined condition is one for which the launch point is not in the target orbit plane. The inclined case investigated in this study was a launch latitude of 28 degrees, with the intercept in an equatorial target plane. Four additional parameters were varied: the time of flight (TF), posigrade versus retrograde orbit direction, lead angle of the target (beta), and radius of the target orbit (R).

For each data set, the first reference set of calculations for the given parameters was from the launch point at the initial time to the final position. The desired output was the optimal trajectory obtained (dJ = 0) when an initial coast was allowed. In all data cases, only one impulse was required, with an initial coast used to optimize cost.

Due to singularities and large slopes (dJ versus TF) near singularities, and due to lack of a priori slope information, the first order bisection iteration method proved most robust and useful. In

approximately 15 iterations, this method would converge on the solution to equation 3-38, i.e. where dJ = 0. This provided local optimal conditions for the given parameters. By varying TF for constant beta, R, and flight direction, the global optimum could be found. Some non-unique solutions were encountered, in which case a direct comparison of cost values was used to determine the minimum.

Chapters 4, 5, 6, and 7 will concentrate on each of the four major cases: coplanar launch point and target orbit with a non-rotating body, noncoplanar non-rotating body, coplanar rotating Earth, and noncoplanar rotating Earth. Appropriate comparisons and sample trajectories will be included in each chapter.

CHAPTER 4

OPTIMAL, COPLANAR, NON-ROTATING, TIME-FIXED INTERCEPTS

4.1. Introduction

An intercept between a launch point on a body's surface and a
point in space (i.e. target) can always be accomplished with a single
impulse. The problem is to find optimal, time-fixed, planet surface to
circular target orbit intercepts using primer vector techniques
developed in Chapters 2 and 3. Fixed transfer times allow exclusion of
excessive transfer times and would be useful in object identification,
enemy spacecraft interception, or realistic mission times due to life
support systems constraints.

The intercept geometry is shown in Figure 4-1. The launch point
is in the XZ plane, while the target orbit is in the XY plane. This is
a convenient, although totally general, choice of coordinates. From the
given geometry, optimal trajectories can be obtained by varying the
following parameters: the radius of the target's orbit, R; the latitude
of the launch point, $\emptyset_o$; the target's initial angular position, beta;
the specified transfer time, t_f; and the direction of the trajectory in
relation to the target orbit, i.e. posigrade (in the same sense as the
target orbit) or retrograde (in the opposite sense from the target
orbit).

The units for length and time were chosen to make the gravitational
constant, μ, have a unit magnitude. The reference position is the
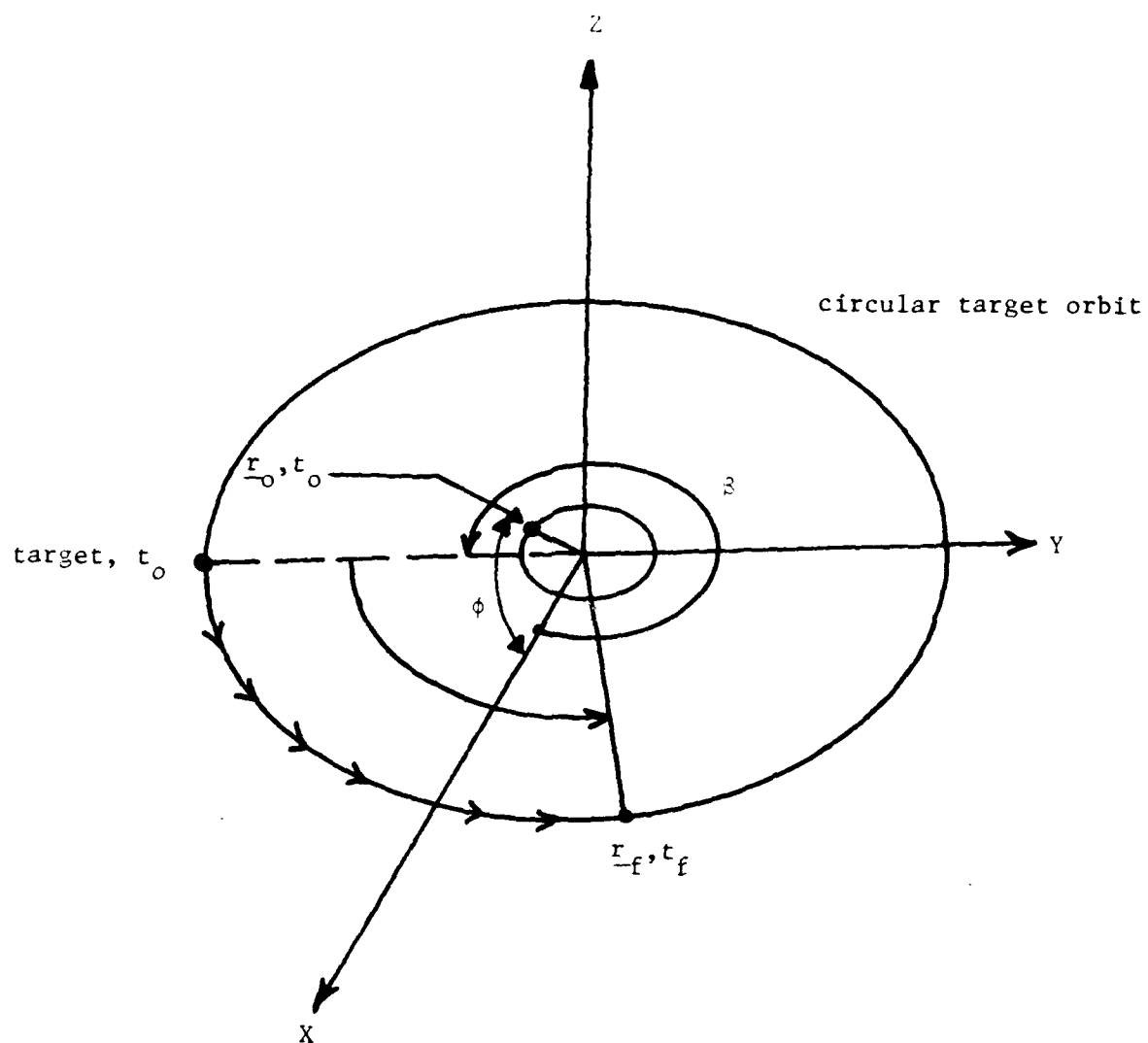
Figure 4-1.   Intercept Geometry

planet's surface, normalized to a radius of unity or one distance unit
(DU). Thus all orbits around a planet would have radii greater than
one. The reference time unit (TU) is defined for a circular orbit at
the planet's surface with a period of 2π TU. As a result, the ref-
erence velocity is the speed of a vehicle in this circular planet orbit,
i.e. 1 DU/TU. For the Earth, a DU is the Earth radius of 3963 miles
(6378 kilometers), while the TU is 13.4469 minutes.

4.2. Posigrade versus Retrograde

This study investigated the effect of the direction of the
trajectory. Figure 4-2 shows the typical case for $\beta = 270°$, $R = 1.1$,
with target and launch point in the same plane. If the primer history
indicated that an additional impulse was needed, the point is marked
with an A. Those points that violated the planet surface constraint
are marked with a C. All other points met the constraints and are
local optimums.

For times less than a certain reference value, to be discussed
later, retrograde orbits yield minimum ΔV, some having an initial coast,
some without an initial coast. For time greater than this reference
time, posigrade orbits with an initial coast yield optimum results.
This trend followed for target radii of 1.1, 2.0, 4.1721 (approximately
a 12 hour period Earth orbit), and 6.6228 (approximately a 24 hour
period Earth orbit). The target lead angles investigated were 0°, 90°,
180°, and 270°.

4.3. Coast versus No Coast

In most cases, an initial coast improved the cost, i.e. used less fuel. Again, Figure 4-2 shows a typical case. For the non-rotating body, if $T_f > T_m$ (the transfer time on the minimum energy ellipse—see Appendix B on Lambert's problem), the initial coast was possible. Thus actual flight time would equal T_m, and any excess between that t_f and the specified transfer time would become an initial coast.

In general, an initial coast also allowed the given condition to yield a local optimum primer time history. If there was no coast and $T_f > T_m$, an initial coast was indicated by the primer time history, and the no coast trajectory went inside the planet radius. In all cases, the initial coast trajectory was a local optimum, stayed outside the planet's surface, and met the cost functional requirement dJ/dt_o = Hamiltonian = 0.

4.4. Cost Comparisons

For the non-rotating case investigated in this chapter, the global optimum was analytically determined and verified using primer vector theory. The absolute minimum ΔV occurs with an initial coast such that the trajectory is rectilinear with a zero velocity at intercept. Thus the spacecraft is launched on a rectilinear orbit and just "grazes" the target at intercept. The sum of any coast time and this flight time on the rectilinear orbit is the reference time previously discussed. Figure 4-3 shows the geometry for $\beta = 270°$. At t_o, the spacecraft is on the launch pad and the target is in a coplanar orbit at 270°. At t_c, the

R=1.1 B=270 PHI=0 NO ROTATION

+----+   POSIGRADE, NO COAST
+----+   POSIGRADE, INITIAL COAST
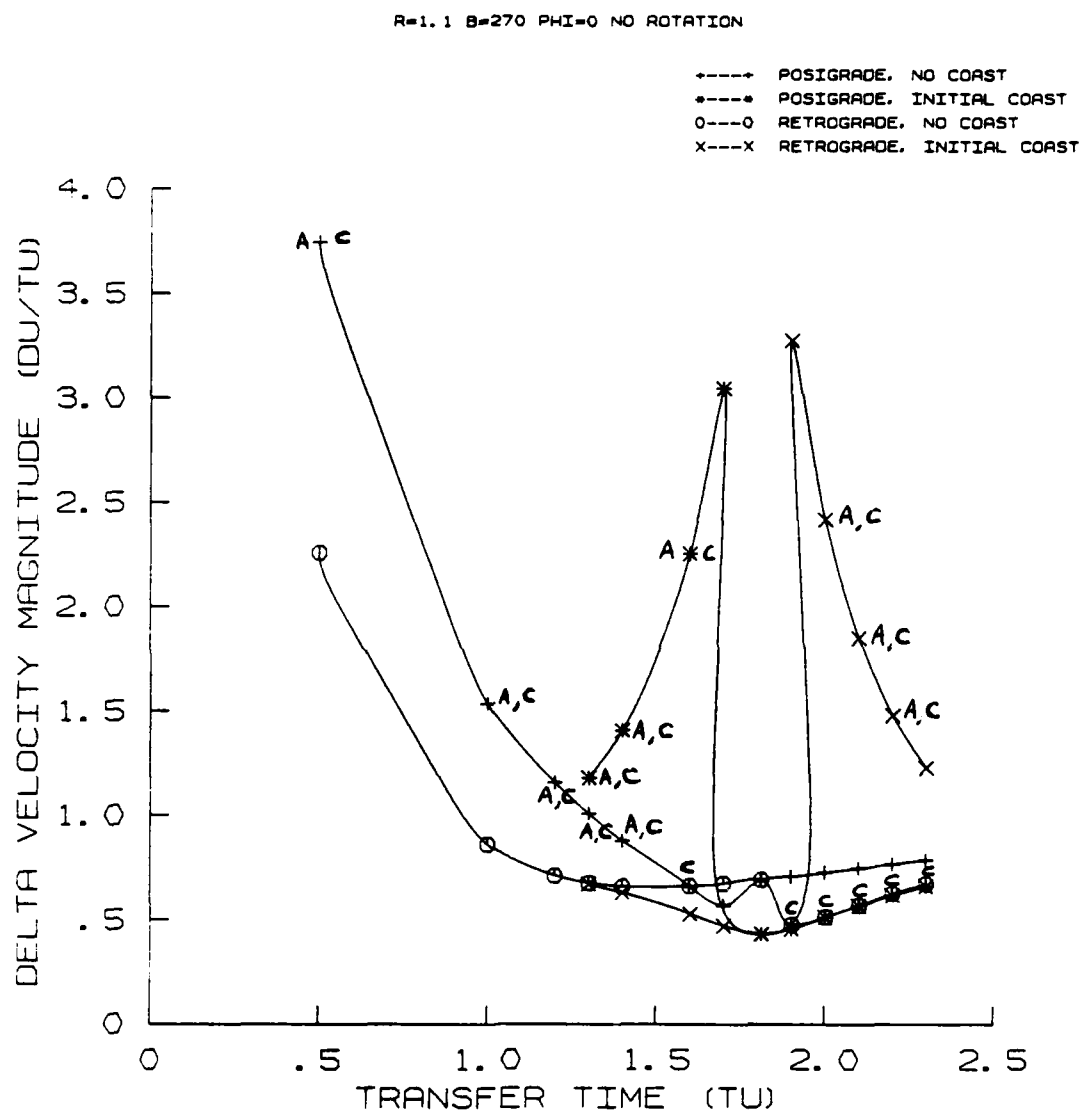O---O   RETROGRADE, NO COAST
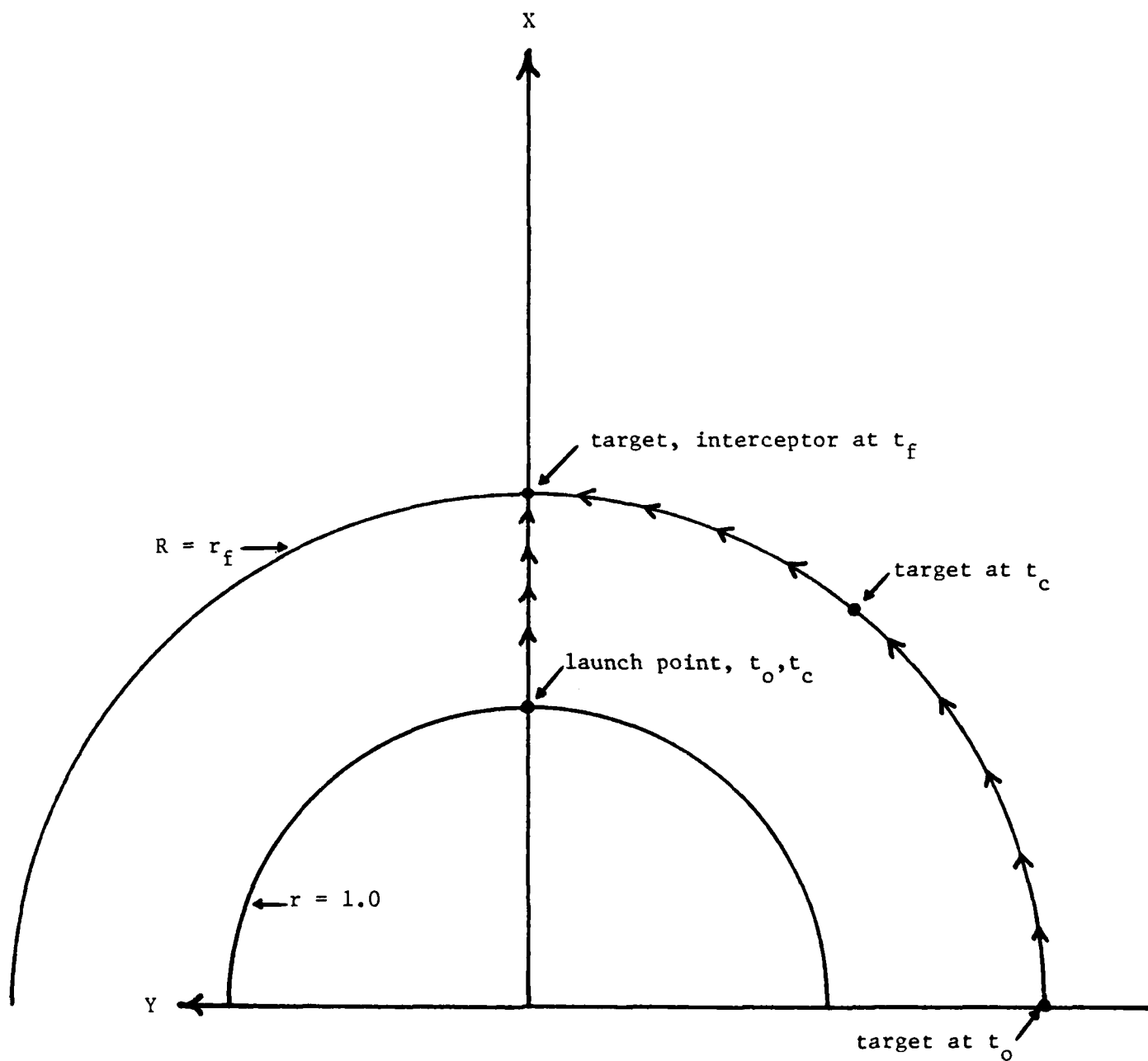X---X   RETROGRADE, INITIAL COAST

Figure 4-2.   Sample Data Case.

Figure 4-3. Optimal Geometry.

initial coast is complete and the spacecraft fires its impulse. At t_f, the intercept occurs "overhead" of the launch point.

Note that for $\beta = 0°$, the target must travel through one period to achieve the optimum intercept. For $\beta = 90°$, it must travel 3/4 of a period; $\beta = 180°$ requires 1/2 of a period; and $\beta = 270°$ requires 1/4 of a period target flight time. This reference time equals $[(360°-\beta)/360°]$ x Target orbit period, e.g. $t_f = 1.8122$ TU for $\beta = 270°$ and R = 1.1.

Figure 4-2 shows the costs for posigrade and retrograde orbits, both with and without an initial coast. The optimum ΔV curve is the bottom one, consisting of local optimum points which do not go through the planet surface. Theoretically, for a given t_f, any point with a ΔV greater than the minimum is possible. By plotting all local minima for a range of flight times, the global minimum was found. It agreed with the previously obtained theoretical value. Thus for $\beta = 270°$, R = 1.1, the global minimum occurs at $t_f = 1.8122$ TU, with a flight time of .4844 TU, a coast time of 1.3278 TU, and a ΔV of .4264 DU/TU.

Figure 4-4 shows the minimum fuel optimum curves for R = 1.1, i.e. the bottom curves on plots similar to Figure 4-2. The various beta curves are plotted separately, but all global minimum $\Delta V = .4264$ DU/TU at the reference time previously discussed. Figures 4-5, 4-6, and 4-7 show similar results for final target radii of R = 2, 4.1721, and 6.6228, respectively. The data points are labeled P for posigrade and R for retrograde orbits. The superscript + indicates an initial coast was optimal. Thus a P^+ would indicate that the local optimum for that point was a posigrade orbit with an initial coast. A point marked with a C indicates the planet surface constraint could not be met with a single-
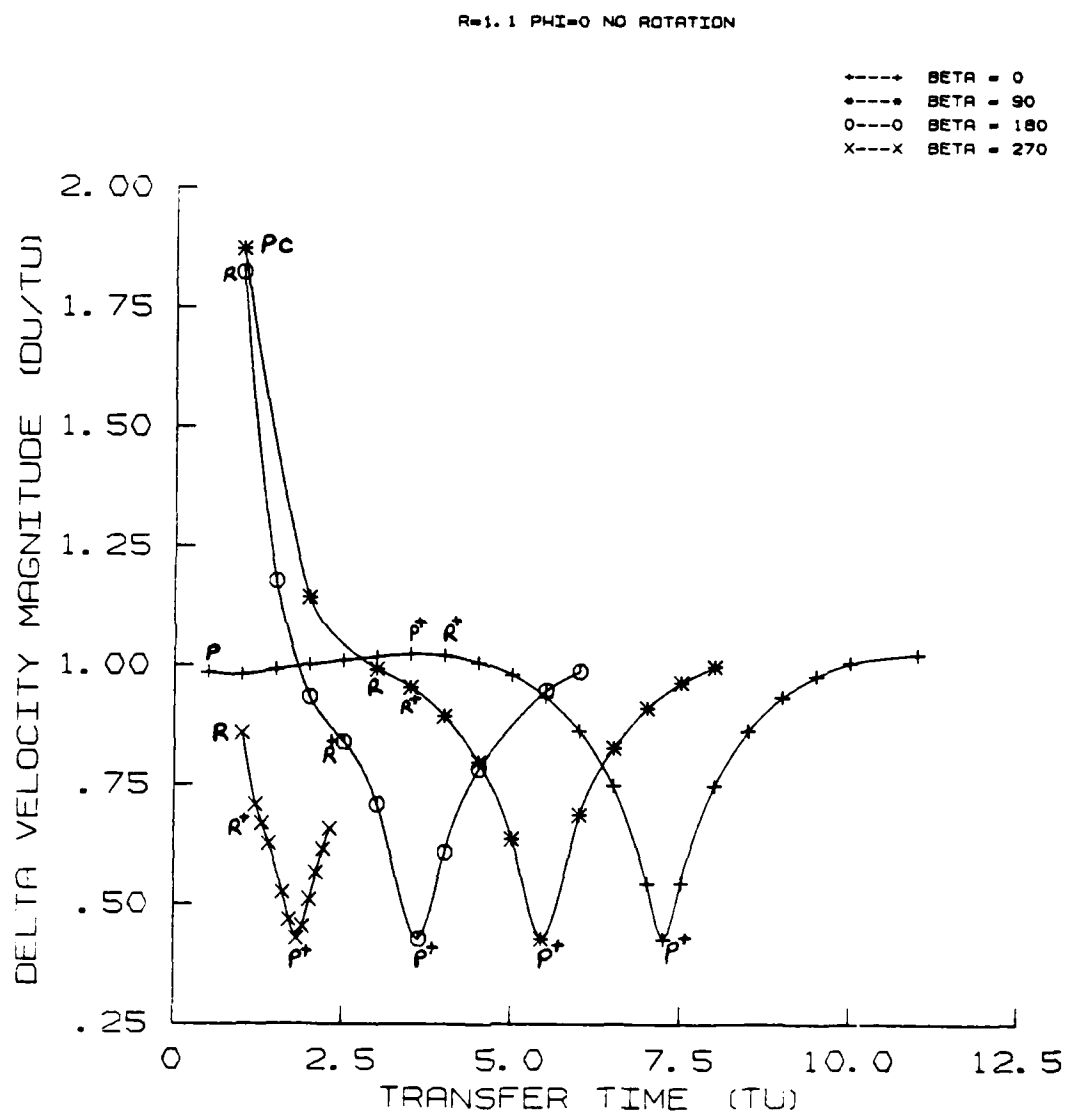
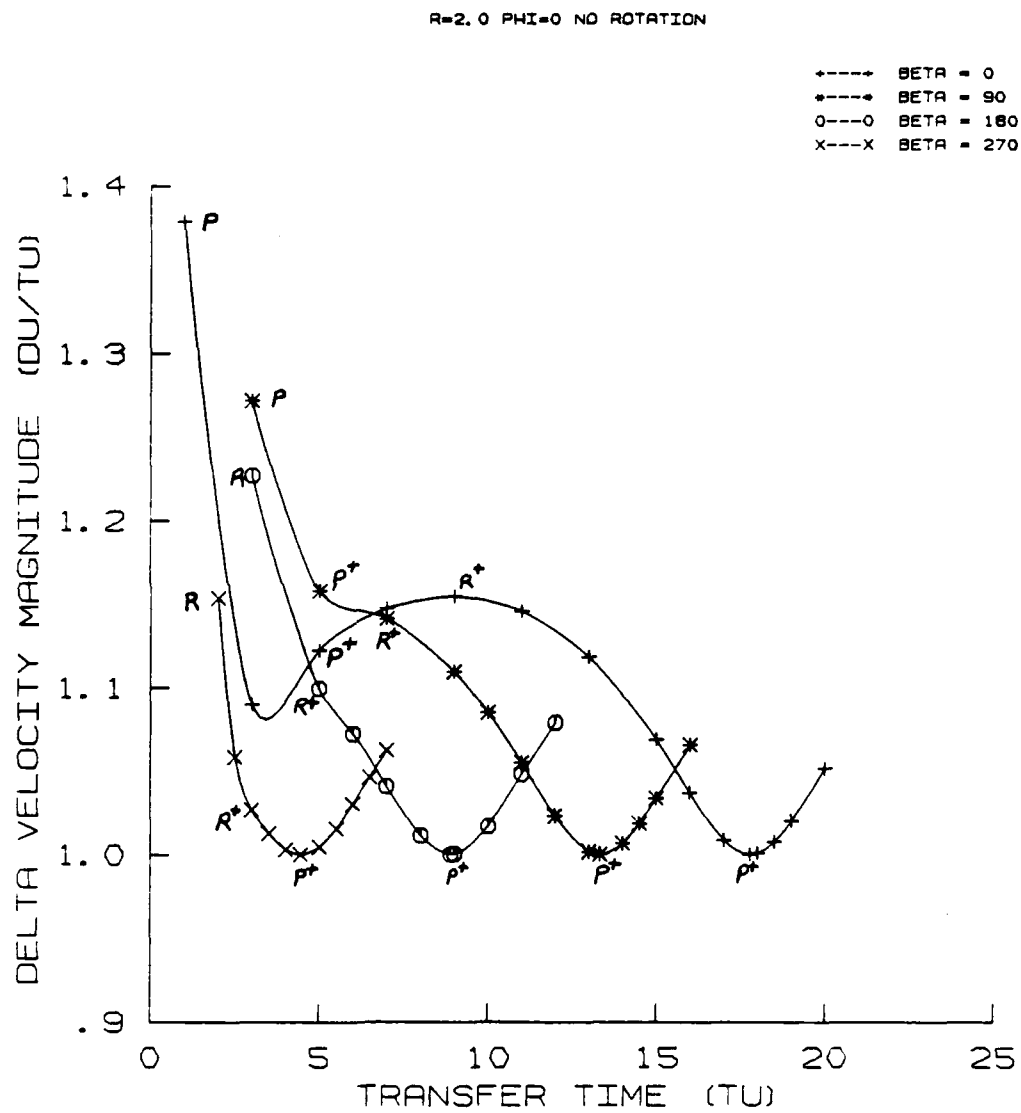Figure 4-4. Optimal Cost as a Function of Transfer Time.

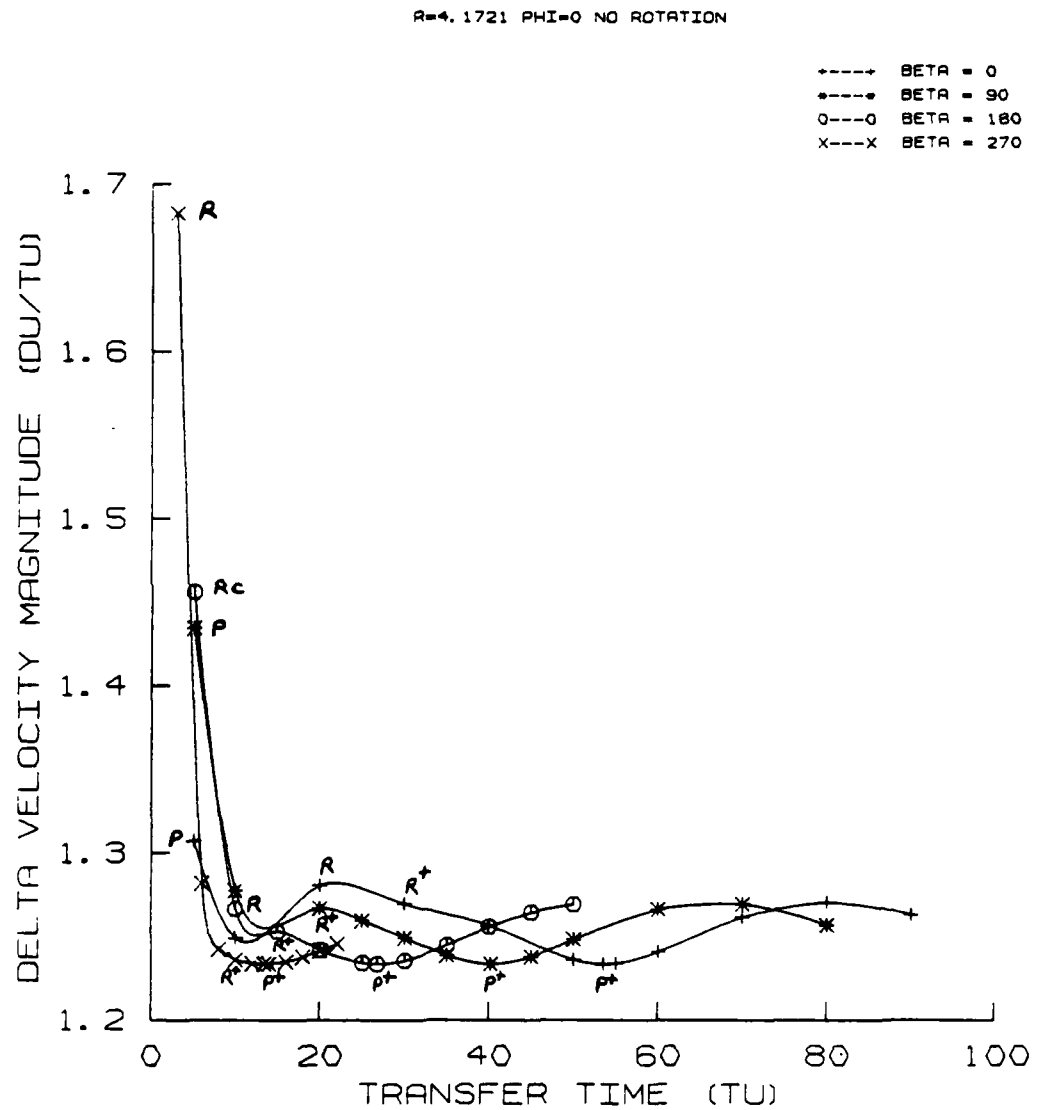Figure 4-5. Optimal Cost as a Function of Transfer Time.

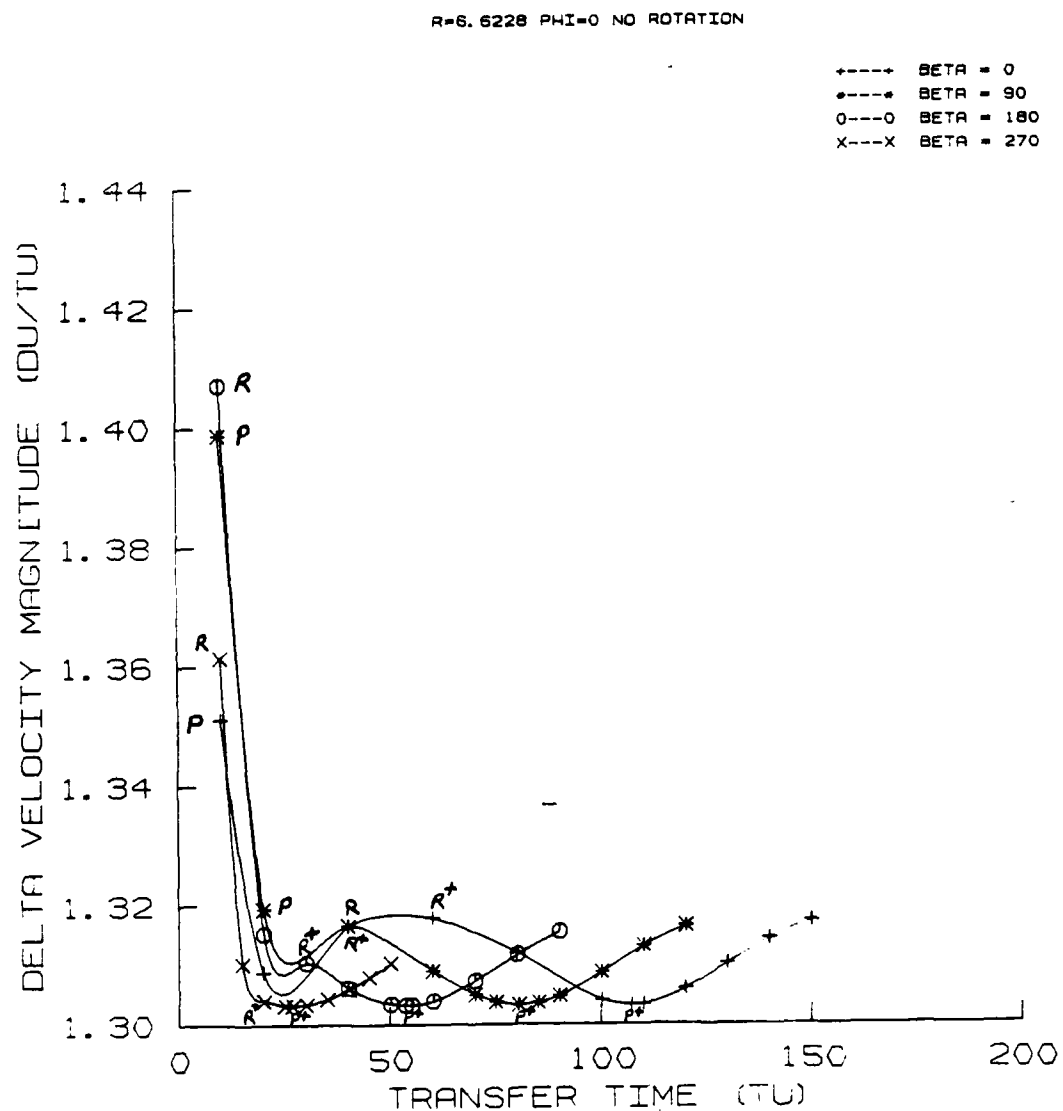Figure 4-6. Optimal Cost as a Function of Transfer Time.

Figure 4-7. Optimal Cost as a Function of Transfer Time.

impulse trajectory. To avoid clutter, only the point for the lowest transfer time is marked. The next point marked on the curve, viewing as transfer time increases, is where the optimum condition changes, e.g. from R^+ to P^+. Thus a region on a curve with no markings has the same type optimal trajectory as indicated by the last marked point to the left (lower transfer time).

Several general trends are noticeable. Retrograde, with or without a coast (depending on T_m) is optimum for times less than the minimum ΔV time, and posigrade with an initial coast is optimum for times greater than this. Only in very short flight time cases will this not be true, e.g. the time is so short that for a given geometry the launch vehicle goes through the planet on a posigrade orbit. For a given target radius, the global ΔV is the same regardless of beta. Also, as the target radius increases, the curves flatten, i.e. there is less variance in ΔV from the global minimum. Looking at Figure 4-7 for $R = 6.6228$, the absolute minimum ΔV is 1.3031 DU/TU. For $20 < t_f < 150$, the local minimum ΔV never exceeds 1.3290, only a 2% variation. Apparently, the greater the target R, the less variation there is in ΔV.

For the β and transfer times considered, only one impulse optimal solutions were found. All cases of added impulses or planet constraint violation did not have a short enough transfer time to yield multiple intercepts (see Appendix D).

Figure 4-8 shows a sample coplanar trajectory. Note that both posigrade and retrograde orbits with no coast greatly exceed the target radius of 4.1721 (5.84 and 6.23 radii respectively) and that both

Figure 4-8. Sample Trajectories.

posigrade trajectories go inside the planet's surface. The optimal

trajectory for this case was the retrograde with an initial coast.

Figure 4-9 shows sample primer time histories for the posigrade

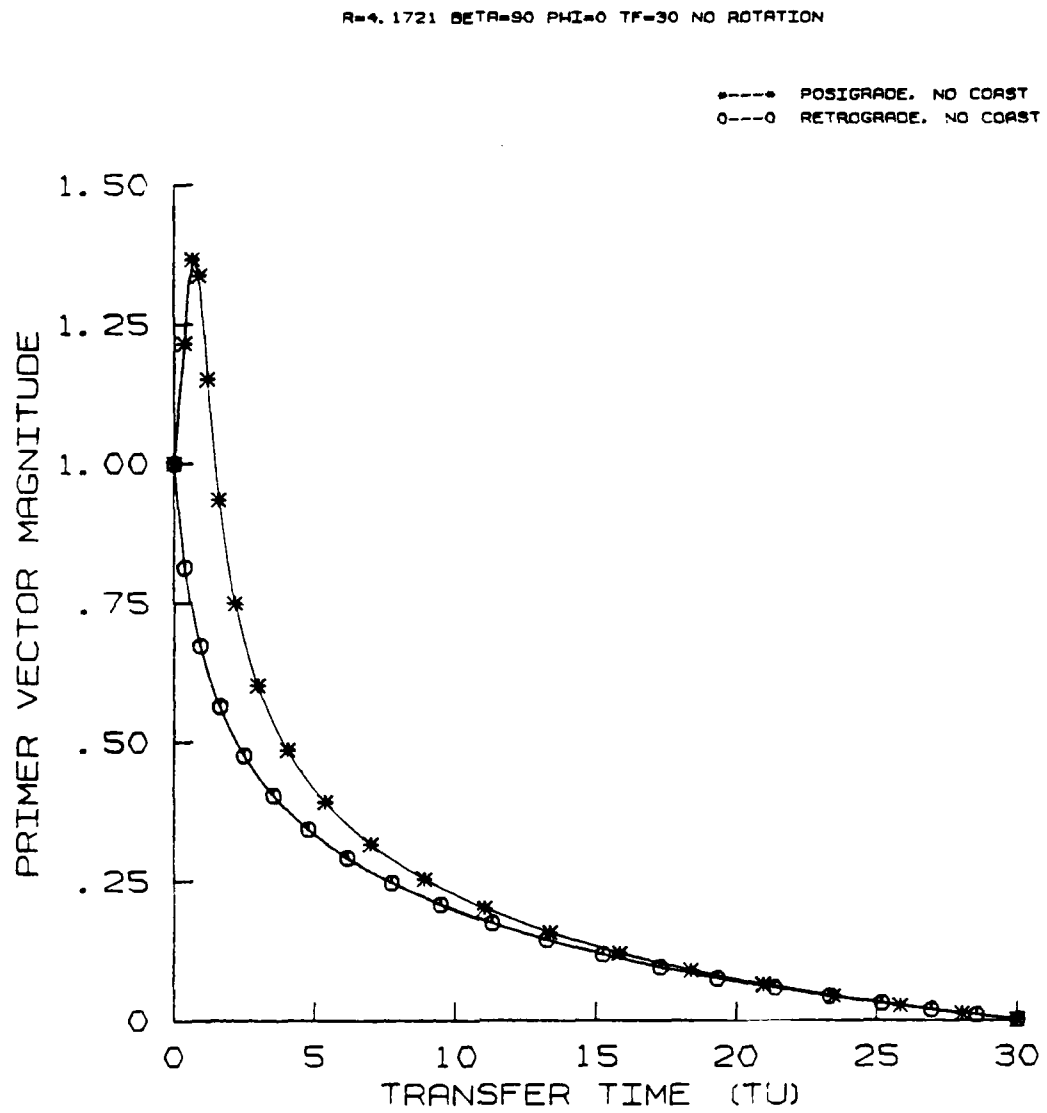and retrograde cases with no coast associated with Figure 4-8.

R=4.1721 BETA=90 PHI=0 TF=30 NO ROTATION

---- POSIGRADE. NO COAST
O---O RETROGRADE. NO COAST

Figure 4-9.   Sample Primer Time Histories.

CHAPTER 5

OPTIMAL, NONCOPLANAR, NON-ROTATING TIME-FIXED INTERCEPTS

5.1. Introduction

Gobetz and Doll (16) show how most research has concentrated on time-open problems. Fixed time interception between noncoplanar body and circular target orbit has received little attention due to the increased difficulty involved with out-of-plane motion. This chapter analyzes this area in an attempt to expand current knowledge on the effect of inclination on orbits. Results will be compared to those in Chapter 4.

5.2. Posigrade versus Retrograde

Results generally agreed with those previously found for the coplanar case. The reference time is identical to that in the previous chapter, although the trajectory is no longer rectilinear. Thus for transfer times less than the reference time, retrograde with or without initial coast is generally the local optimum. For times greater than the reference time, posigrade with an initial coast is optimal. This trend followed for all R and beta. For extremely short transfer times, with $\beta = 0°$ or $90°$, a posigrade orbit with no initial coast was optimum, as was the case for the non-inclined orbits.

5.3. Coast versus No Coast

Similar to the coplanar case, a coast often improved the cost. Again, the actual time of flight equalled the T_m with the difference

between the designated transfer time and the time of flight yielding the coast time. As previously discovered, the case with an initial coast stayed outside the planet's surface, was the local optimum, and yielded $dJ/dt_o = H = 0$.

5.4. Cost Comparison

For the non-rotating, inclined target orbit cases investigated in this chapter, the results directly paralleled those of the coplanar cases in Chapter 4. The reference time was identical, as were the times to achieve the global minimum. However, since the target orbit is no longer coplanar with the launch point, the trajectory for this global optimum is no longer rectilinear, but rather a high eccentricity ellipse in the XZ plane. The larger the target radius, the higher the eccentricity.

Figures 5-1, 5-2, 5-3, and 5-4 show the minimum fuel results for R = 1.1, 2.0, 4.1721, and 6.6228 respectively. As with the coplanar results, the global minimum ΔV is identical for a given R, regardless of beta. Posigrade and retrograde orbits follow the same trends previously noted. The curves flatten as R increases, reducing the variation in ΔV from the global minimum. Comparing the figures to the comparable ones in Chapter 4, one notes that the global minimum ΔV is higher for inclined orbits, e.g. for R = 1.1, ΔV = .6868 DU/TU versus .4844 for coplanar. This trend follows for the other target radii investigated. For R = 2, inclined versus coplanar yields 1.0248 to 1.00; R = 4.1721 yields 1.2366 versus 1.2331; and R = 6.6228 yields 1.3043 versus 1.3031.

R=1.1 PHI=28 NO ROTATION

+----+   BETA = 0
----   BETA = 90
O---O   BETA = 180
X---X   BETA = 270
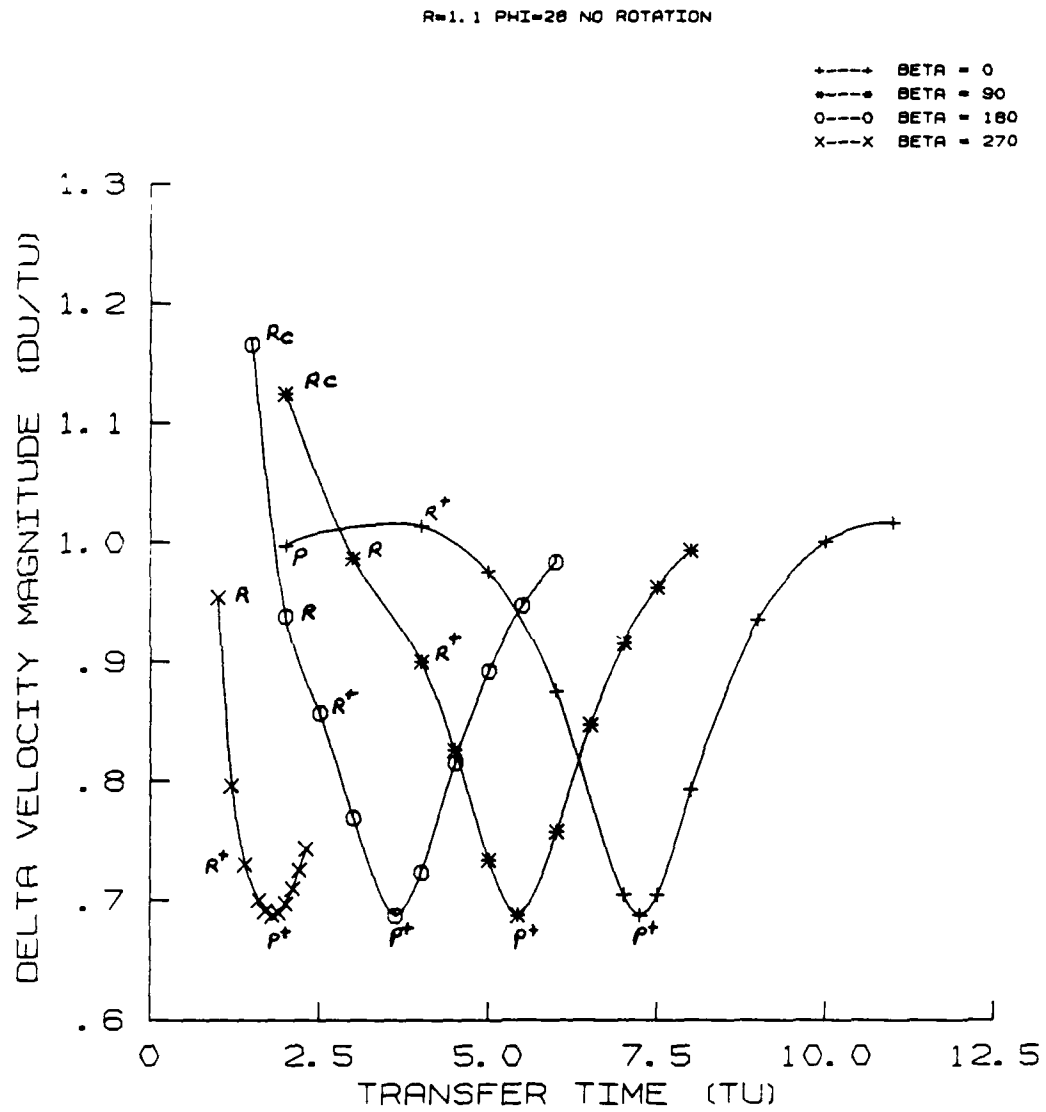
Figure 5-1.   Optimal Cost as a Function of Transfer Time.
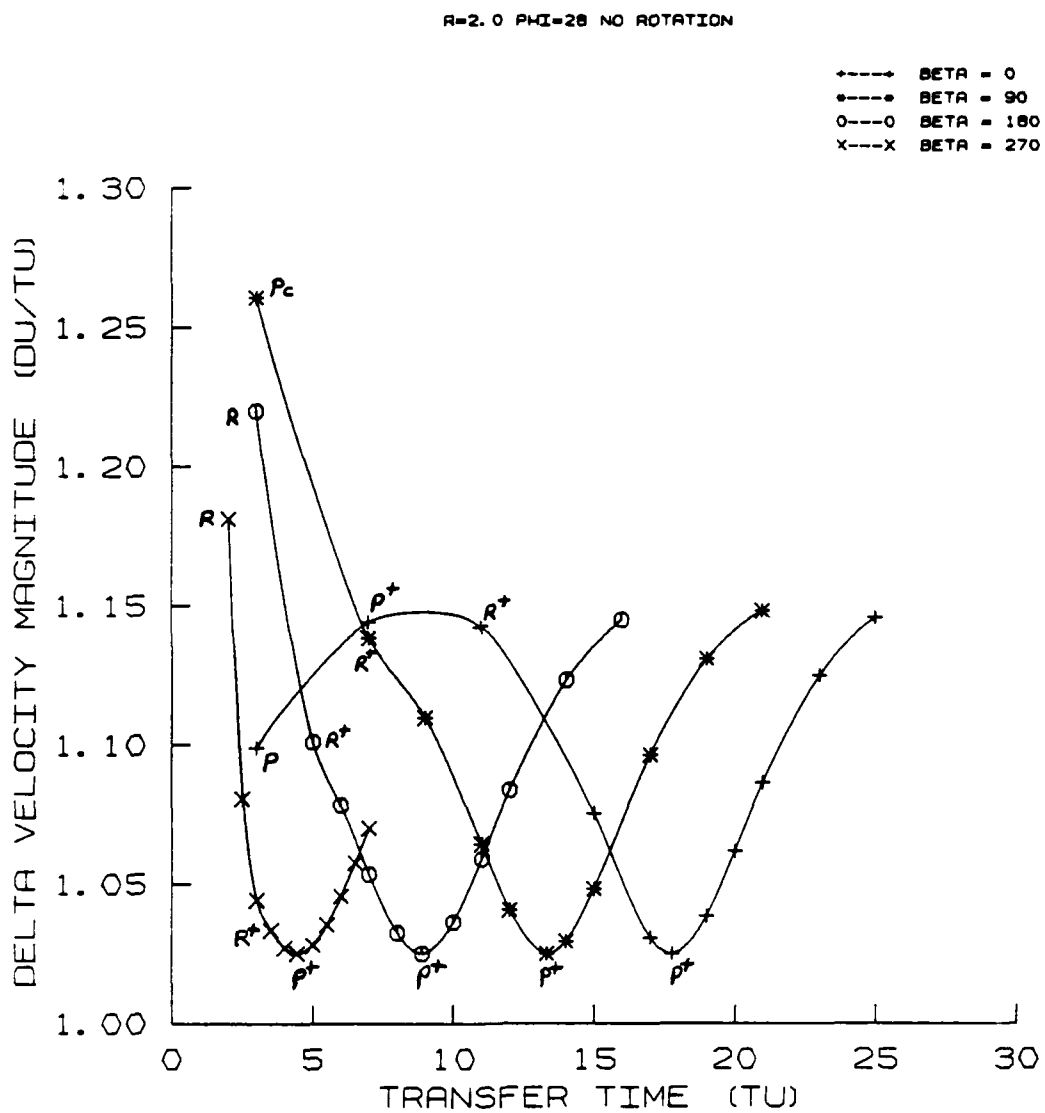
Figure 5-2. Optimal Cost as a Function of Transfer Time.
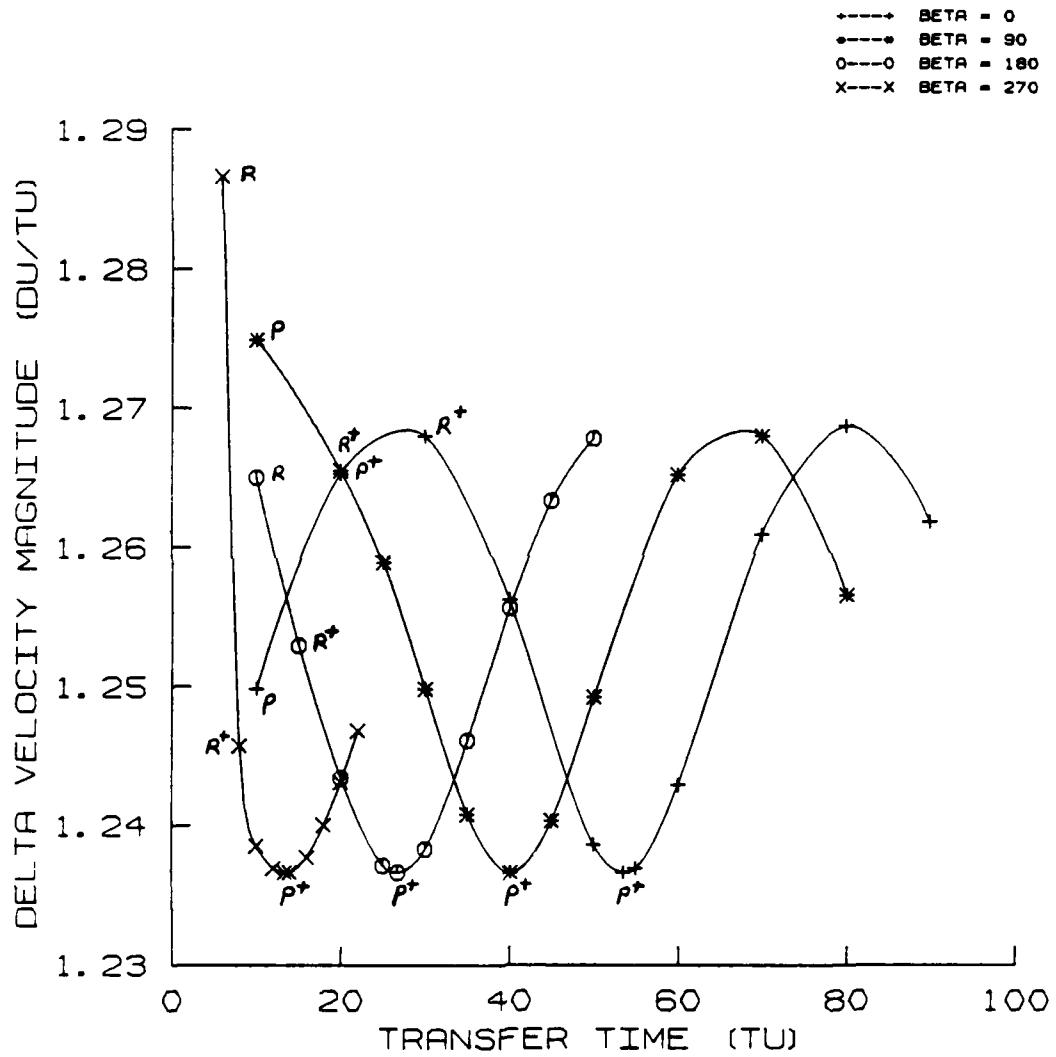
Figure 5-3. Optimal Cost as a Function of Transfer Time.
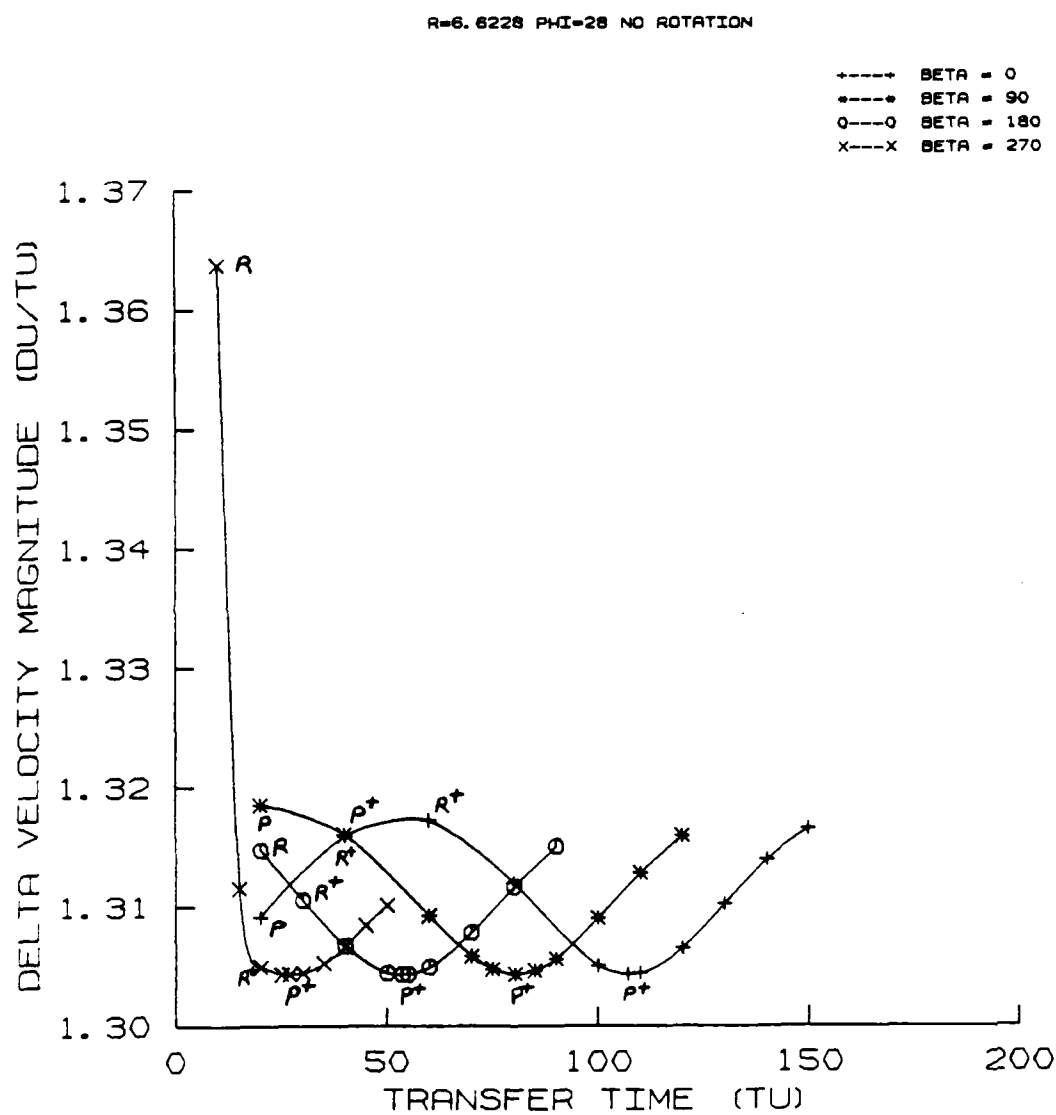
Figure 5-4.   Optimal Cost as a Function of Transfer Time.

The primer time histories are very similar to those in Chapter 4. No added impulse was optimum. Only extremely short transfer times (e.g. 1 TU for R = 1.1) caused the optimal trajectory to go through the planet surface and require multiple impulses (see Appendix D).

Figure 5-5 shows a sample trajectory for the same R, beta, and t_f as in Chapter 4. Now the problem is three dimensional, but generally similar in appearance. Again, the trajectories for posigrade and retrograde without a coast exceed the target orbit radius (5.82 and 6.22 respectively). Both posigrade orbits go inside the planet's surface. The optimum trajectory is retrograde with an initial coast.

R=4.1721   BETA=90   PHI=28   TF=30 NO ROTATION

+---+ Posigrade, No Coast
--- Posigrade, Initial Coast
o---o Retrograde, No Coast
x---x Retrograde, Initial Coast

Z

X

R = 1.0

R = 4.1721

Y

Figure 5-5. Sample Trajectories.

CHAPTER 6

OPTIMAL, COPLANAR, ROTATING, TIME-FIXED INTERCEPTS

6.1. Introduction

The conditions used to obtain the data in this chapter are

identical to those in Chapter 4 with one exception. The body from which

the interceptor is launched is now rotating. The rotation rate used

approximates that of the Earth. Intercept geometry is unchanged if

there is no wait time prior to a launch, and can be seen in Figure 4-1.

If primer theory dictates that an initial coast is optimum, the launch
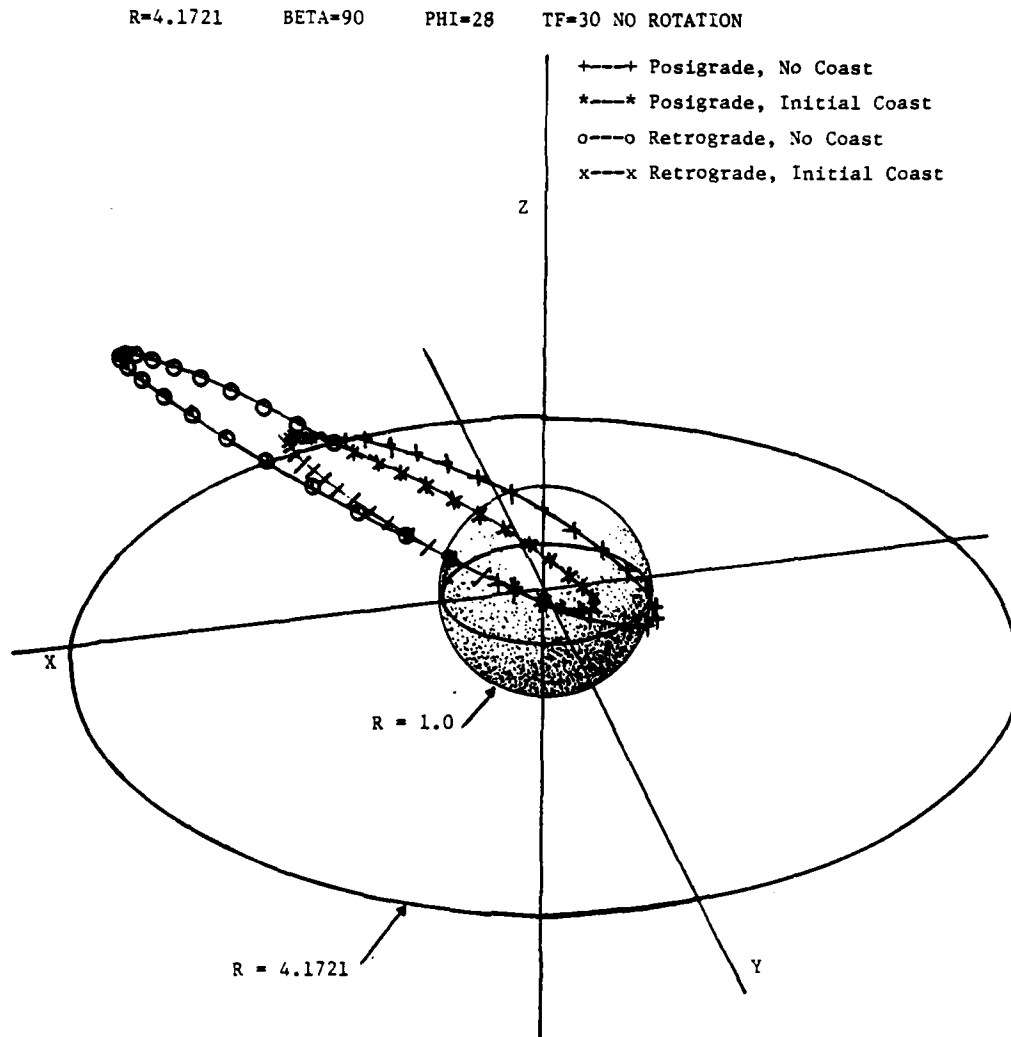
point also moves as the Earth rotates. However, the Earth rotation

rate is different from that of the target for final target radii (R)

of 1.1, 2.0, and 4.1721 (12 hour period target orbit). For the 6.6228

(geosynchronous, or 24 hour period target orbit) target radius, the

planet and target rotate at the same rate.

The same parameters were varied for this chapter as in previous

chapters. It is assumed that the planet rotation is in the same

direction as the target motion. The planet rotational angular velocity

is assumed to be along the Z axis.

As previously noted in Chapters 2 and 3, results are only a first

approximation, neglecting atmospheric effects. Thus the results of this

and the succeeding chapter are included to yield approximate optimal

Earth intercepts. As previously found in Chapters 4 and 5, all optimal

intercepts could be accomplished with a single impulse.

6.2. Posigrade versus Retrograde

Figure 6-1 shows a typical data case for R = 1.1, beta = 0° with the transfer trajectory in the same plane as the target. Similar to non-rotating results, retrograde trajectories with or without an initial coast were optimum for transfer times less than a reference time, and a posigrade trajectory with a coast was optimum for transfer times greater than this reference time. However, this can be generally seen only for R = 1.1 and 2.0.

Note that due to Earth rotation in the same direction as a posigrade transfer, posigrade orbits had lower ΔV than comparable retrograde results. Thus posigrade with no coast has a lower ΔV than retrograde with no coast. However, this ignores the planet surface constraint. Enforcing this constraint yields the results in Figures 6-2 through 6-5.

6.3. Coast versus No Coast

As for the non-rotating body cases, data analysis shows that an initial coast generally will lower the cost. One exception is for very short transfer times, where posigrade or retrograde without coast are usually optimum. The other exception is for R = 6.6228, beta = 180° and 270°, where posigrade and retrograde without coast were optimal over a wide range of transfer times. Noting that all R = 6.6228 curves are flat for transfer times past a given time (the time of flight to complete the intercept for the fixed geometry between the points), it would seem that the beta = 180° and 270° curves also show that no initial coast is required prior to this time.

In all cases, the trajectory after an initial coast yielded a local optimum primer time history, if the planet surface constraint was

R=1.1 B=0 PHI=0 Z AXIS ROTATION

+----+   POSIGRADE, NO COAST
•----•   POSIGRADE, INITIAL COAST
O---O   RETROGRADE, NO COAST
X---X   RETROGRADE, INITIAL COAST

Figure 6-1.   Sample Data Case.

R=1.1 PHI=0 Z AXIS ROTATION

Figure 6-2. Optimal Cost as a Function of Transfer Time.
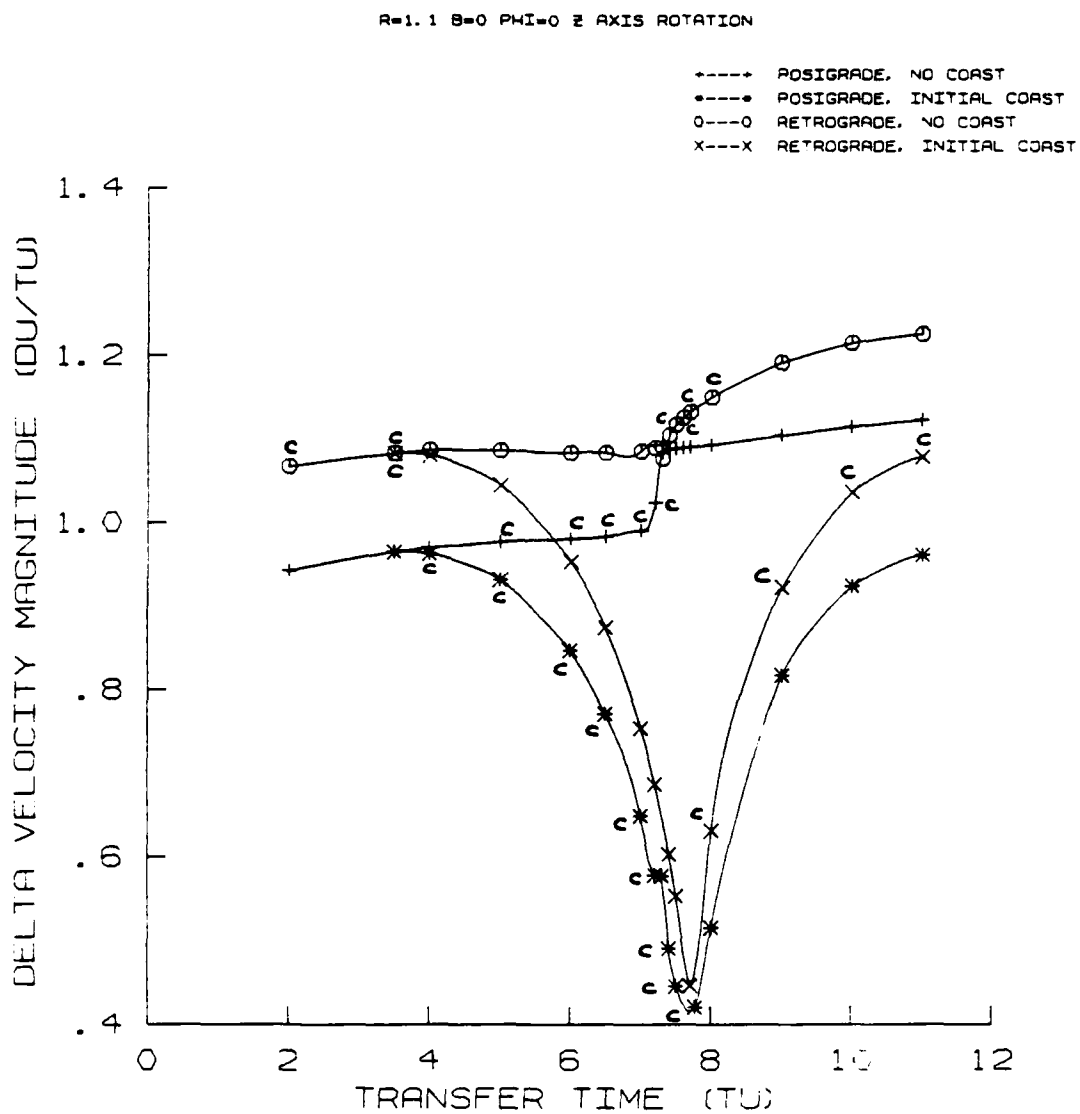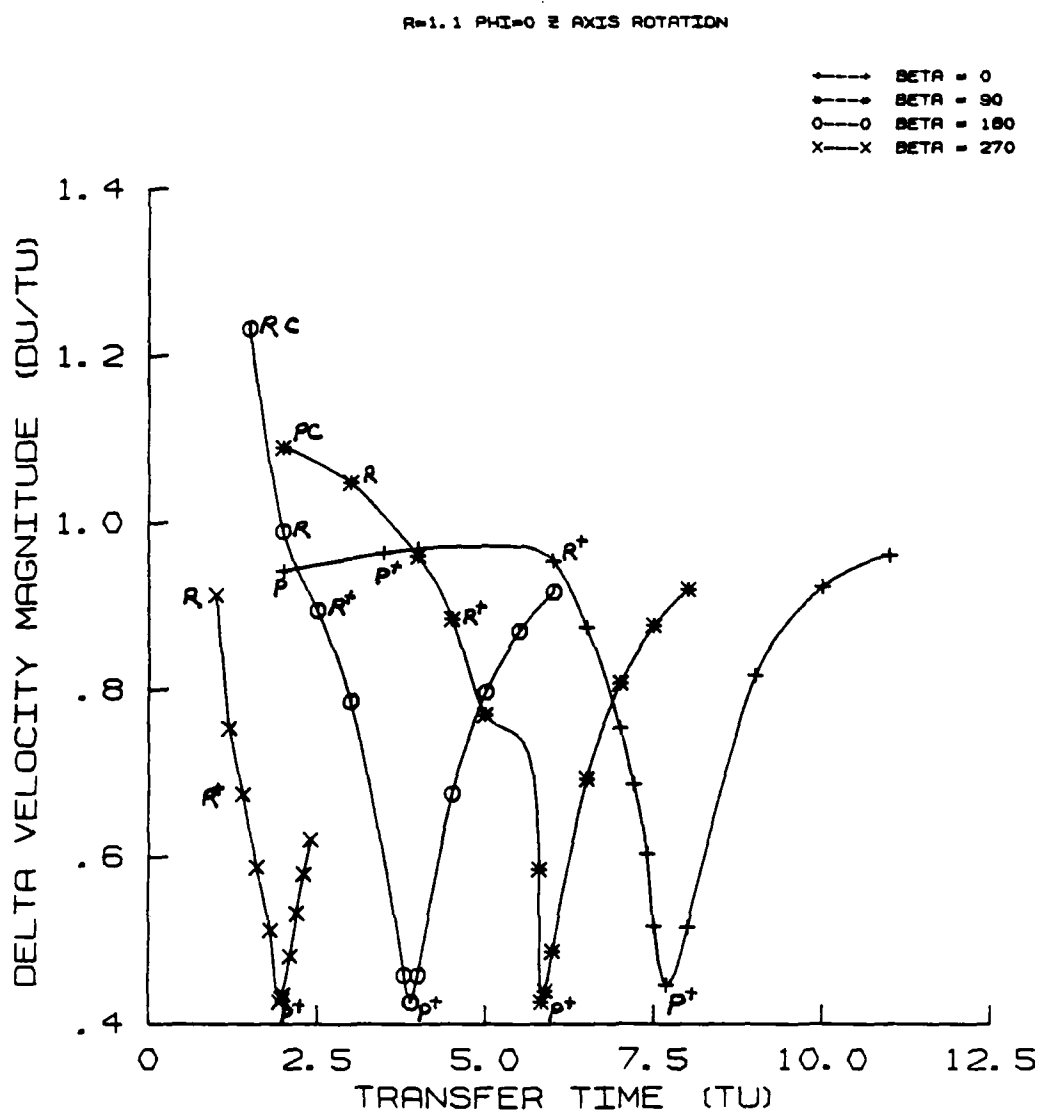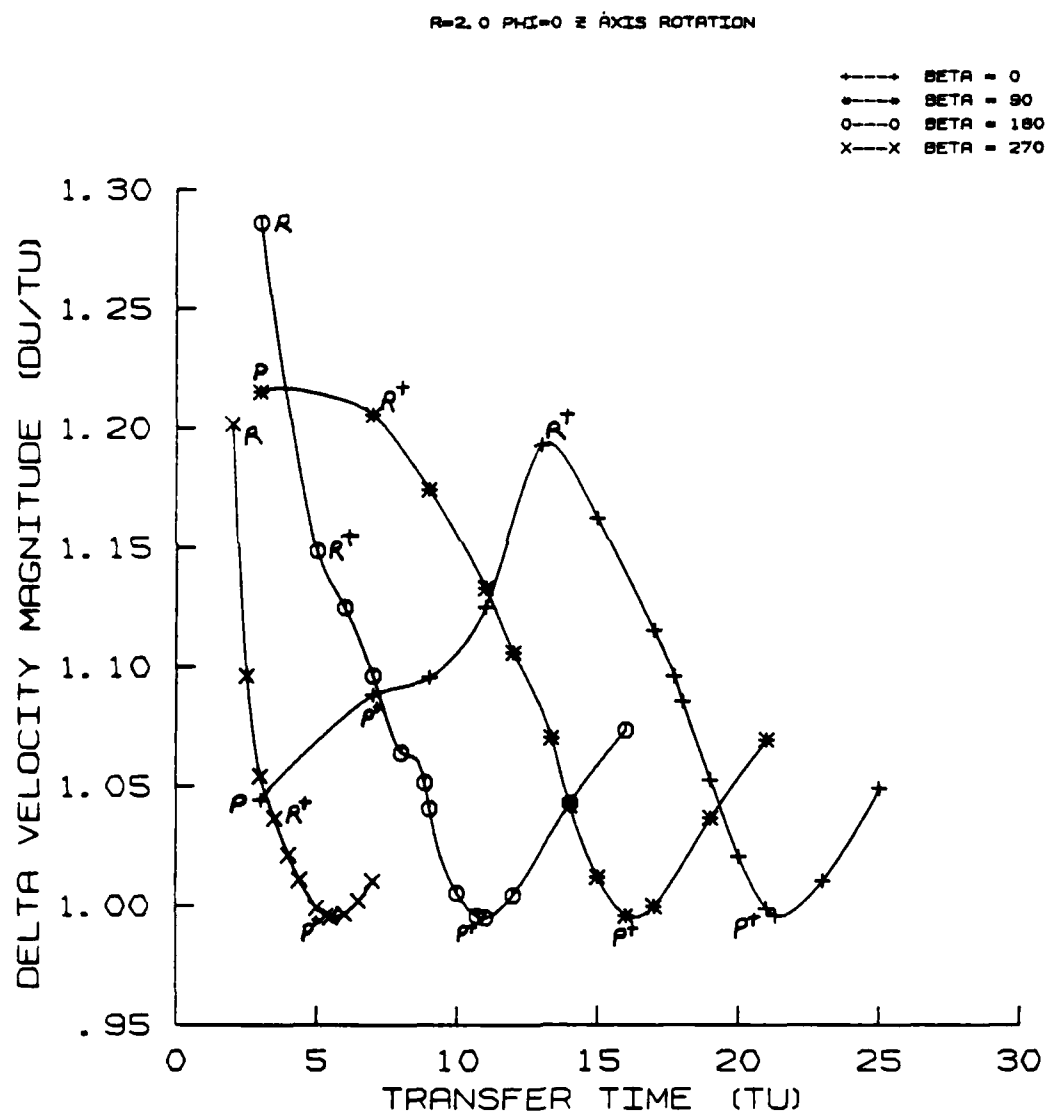
Figure 6-3. Optimal Cost as a Function of Transfer Time.

Figure 6-4. Optimal Cost as a Function of Transfer Time.

R=6.6228 PHI=0 Z AXIS ROTATION
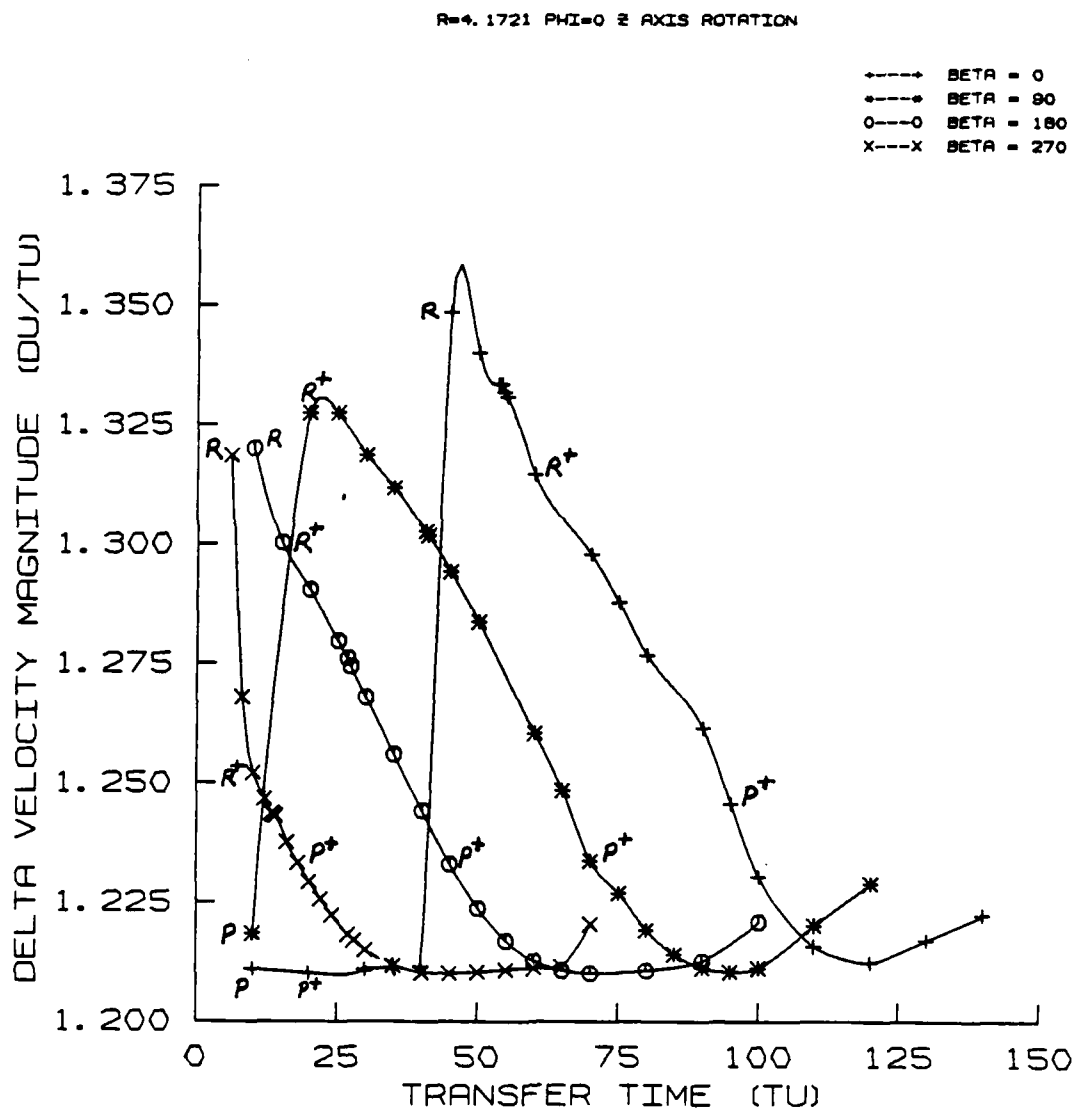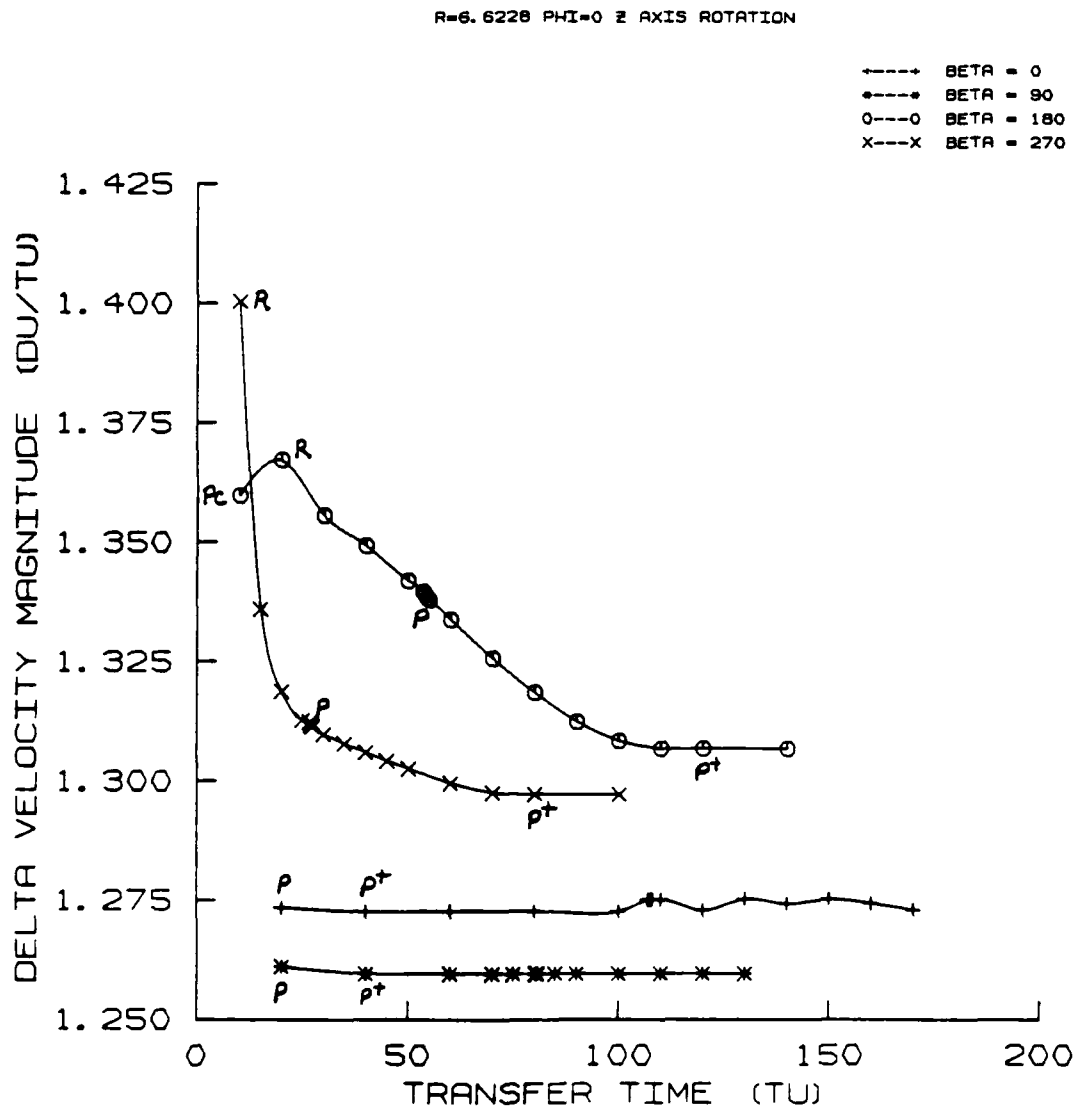

Figure 6-5.   Optimal Cost as a Function of Transfer Time.

not violated. The required cost functional, equation 3-38, $dJ/dt_o = 0$, was also met.

6.4. Cost Comparisons

The global optimum was obtained using primer vector theory. Similar to the non-rotating case, the absolute minimum ΔV occurs with an initial coast such that the trajectory is a high eccentricity ellipse (e.g. .997 for R = 1.1 and .988 for R = 2.0) with a zero intercept velocity as shown in Figure 4-3. However, since the Earth is now rotating, the optimal trajectory is no longer along the X axis, but at some point past this in the XY plane. Figures 6-2 and 6-3 for R = 1.1 and 2.0 show similar results to the non-rotating case. The time giving the absolute minimum ΔV for each beta depends on the synodic period between a point on the Earth's surface and the target body. The general trends noted for the non-rotating body in Section 4.4 are the same for these radii.

However, Figure 6-5 for R = 6.6228 does not show the same type curves. These curves asymptotically approach a limit as transfer time increases. Perhaps this is most easily demonstrated for R = 6.6228, beta = 0°. The target is always "overhead" the launch point. The interceptor must be launched downstream, or posigrade, to intercept the target with minimum ΔV. The same geometry between target and launch point, and hence the same transfer trajectory, exists for all transfer times greater than that required to accomplish the intercept. For transfer times smaller than this, a higher ΔV must be expended.

Thus, one notes that for R = 6.6228, beta = 0° and 90°, and for R = 4.1721, beta = 0°, posigrade, with or without an initial coast, is

always optimum, with a constant ΔV for sufficiently long transfer times. The other curves show a mixture of posigrade and retrograde type orbits. For R = 6.6228, each beta curve has its own minimum ΔV which is dependent on the initial geometry to obtain the minimum ΔV.

As with the non-rotating data, the minimal ΔV does increase as R increases. However, the small variation in ΔV as R increased in the non-rotating cases, generally does not apply in the rotating cases. Only in the case of the flat curves (R = 4.1721, beta = 0°, and R = 6.6228, beta = 0° and 90°) does the ΔV not vary.

Figure 6-1 shows the costs for posigrade and retrograde orbits, with and without an initial coast, for R = 1.1 and beta = 0°. Unlike the non-rotating cases, the optimal ΔV curve is not the bottom one. It is the local optimum condition closest to the bottom which does not violate the planet surface constraint. Figure 6-2 shows R = 1.1 optimal curves for the four betas tested. Note the minimum ΔV is the same for each beta, ΔV = .4256 DU/TU. This value is less than the .4264 DU/TU for the non-rotating case.

Figure 6-6 shows a sample coplanar, rotating Earth trajectory for R = 4.1721. Both posigrade and retrograde orbits with no coast do not violate the planet surface constraint, but do greatly exceed the target radius (R = 5.63 and 5.80 respectively). The retrograde orbit with a coast goes through the planet. The optimal trajectory for this case is the posigrade with an initial coast. Note that the launch points for the coasting trajectories have rotated with the Earth's surface. Since the wait times for posigrade and retrograde orbits vary slightly, the launch points are also slightly different.
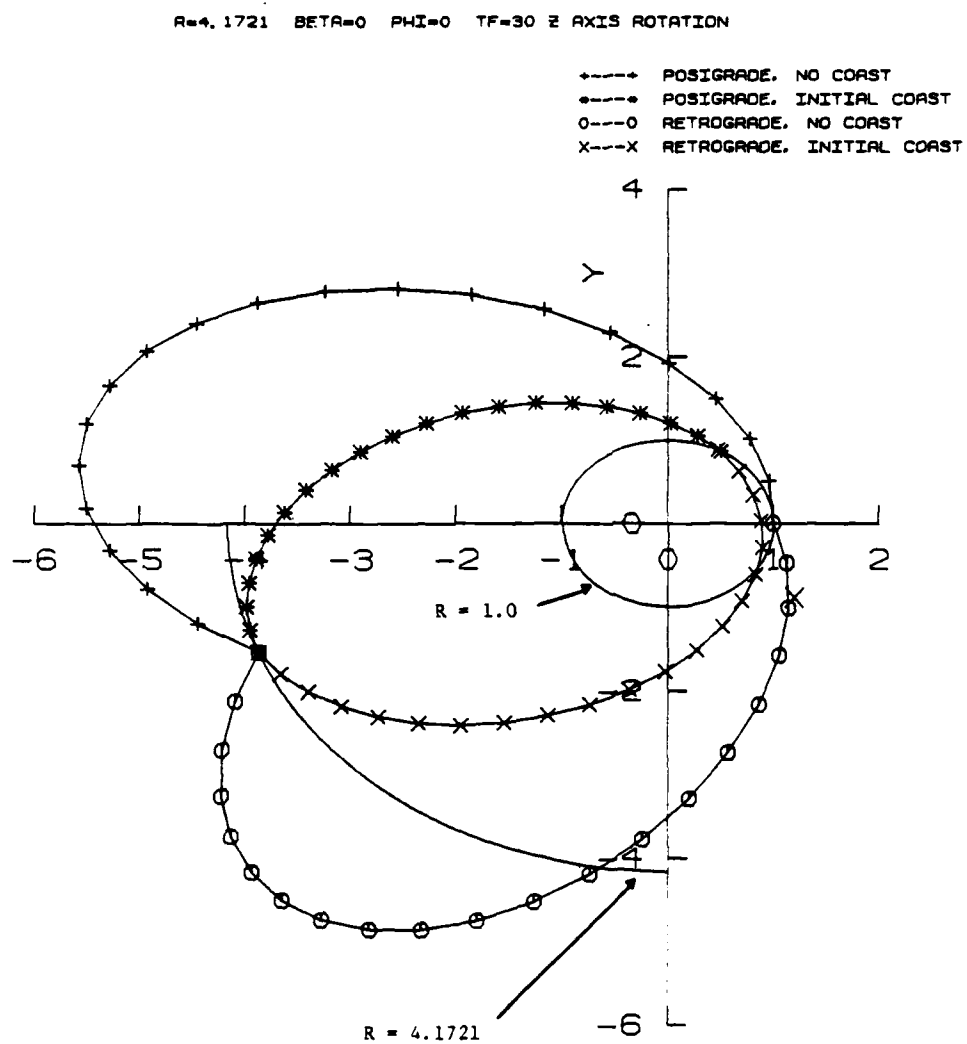
Figure 6-6. Sample Trajectories.

CHAPTER 7

OPTIMAL, NONCOPLANAR, ROTATING TIME-FIXED INTERCEPTS

7.1. Introduction

This chapter analyzes conditions identical to Chapter 6 with one exception. The launch point is now a different latitude than zero, so the intercept trajectory is not in the same plane as the target orbit. Results and conditions can be compared to Chapter 5 for a non-rotating body. The conditions applied in this chapter present the most general case analyzed in this research.

7.2. Posigrade versus Retrograde

Results generally agree with those found in Chapter 6 for a coplanar, rotating Earth. The reference time for each beta still depends on the synodic period, although the trajectory is not recti-linear (e.g. $e = .78$ for $R = 1.1$ and $e = .88$ for $R = 2.0$). For $R = 1.1$ and 2.0, retrograde, with or without an initial coast, is optimum short of the reference time, while posigrade with coast is optimum for transfer times greater than the reference time. These results can be seen in Figures 7-1 and 7-2. For short transfer times, the beta = 0° or 90°, a posigrade orbit with no initial coast is optimum.

Figures 7-3 and 7-4 show results for $R = 4.1721$ and 6.6228. The comparisons are not as predictable as with the lower radii results. Curves incorporate a mix of posigrade and retrograde orbits ranging from a flat, all posigrade curve ($R = 6.6228$, beta = 0°) to one resembling the results for the lower radii ($R = 4.1721$, beta = 180°).

Figure 7-1. Optimal Cost as a Function of Transfer Time.

R=2.0 PHI=28 Z AXIS ROTATION

```
+----+  BETA = 0
•----•  BETA = 90
0----0  BETA = 180
X----X  BETA = 270
```
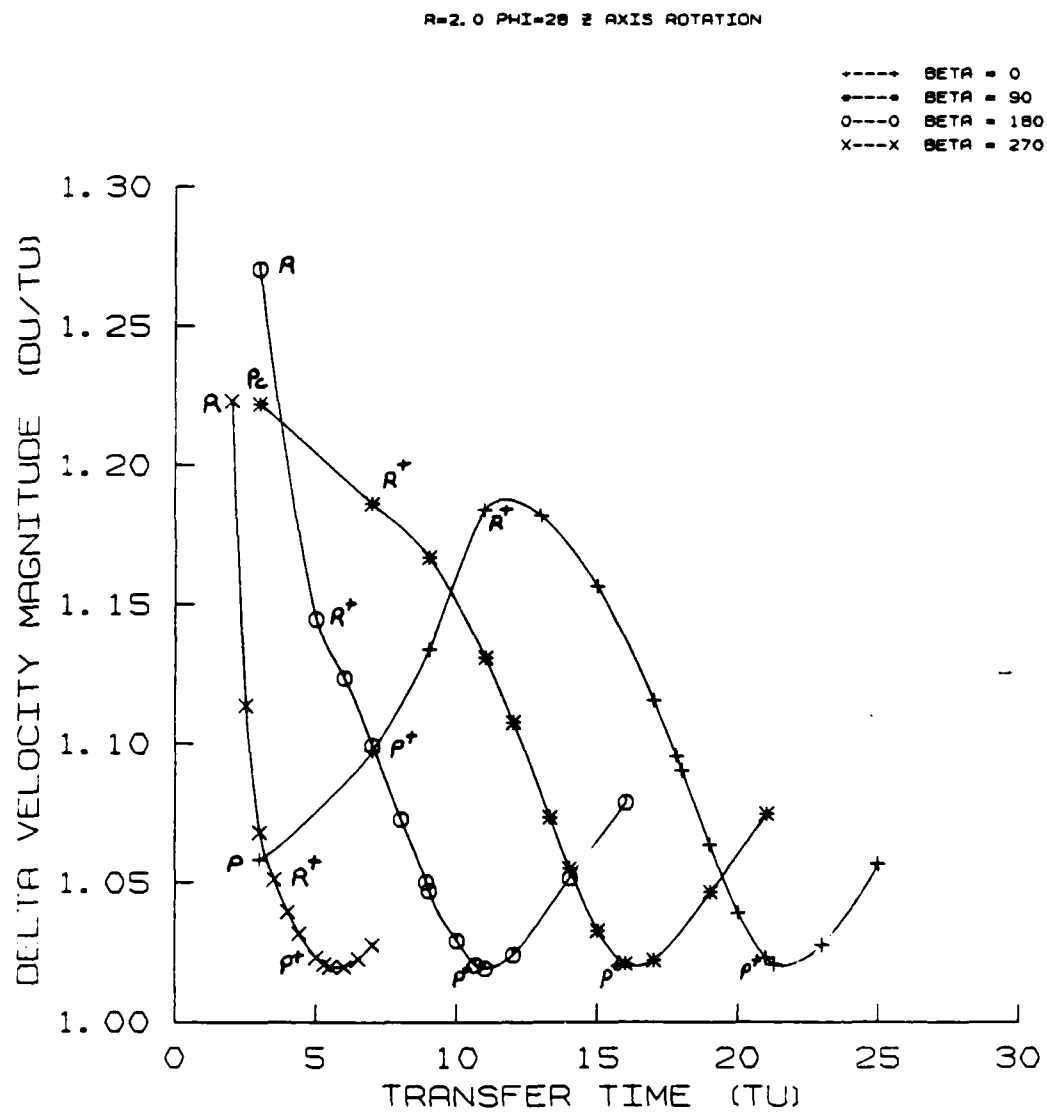

Figure 7-2.   Optimal Cost as a Function of Transfer Time.

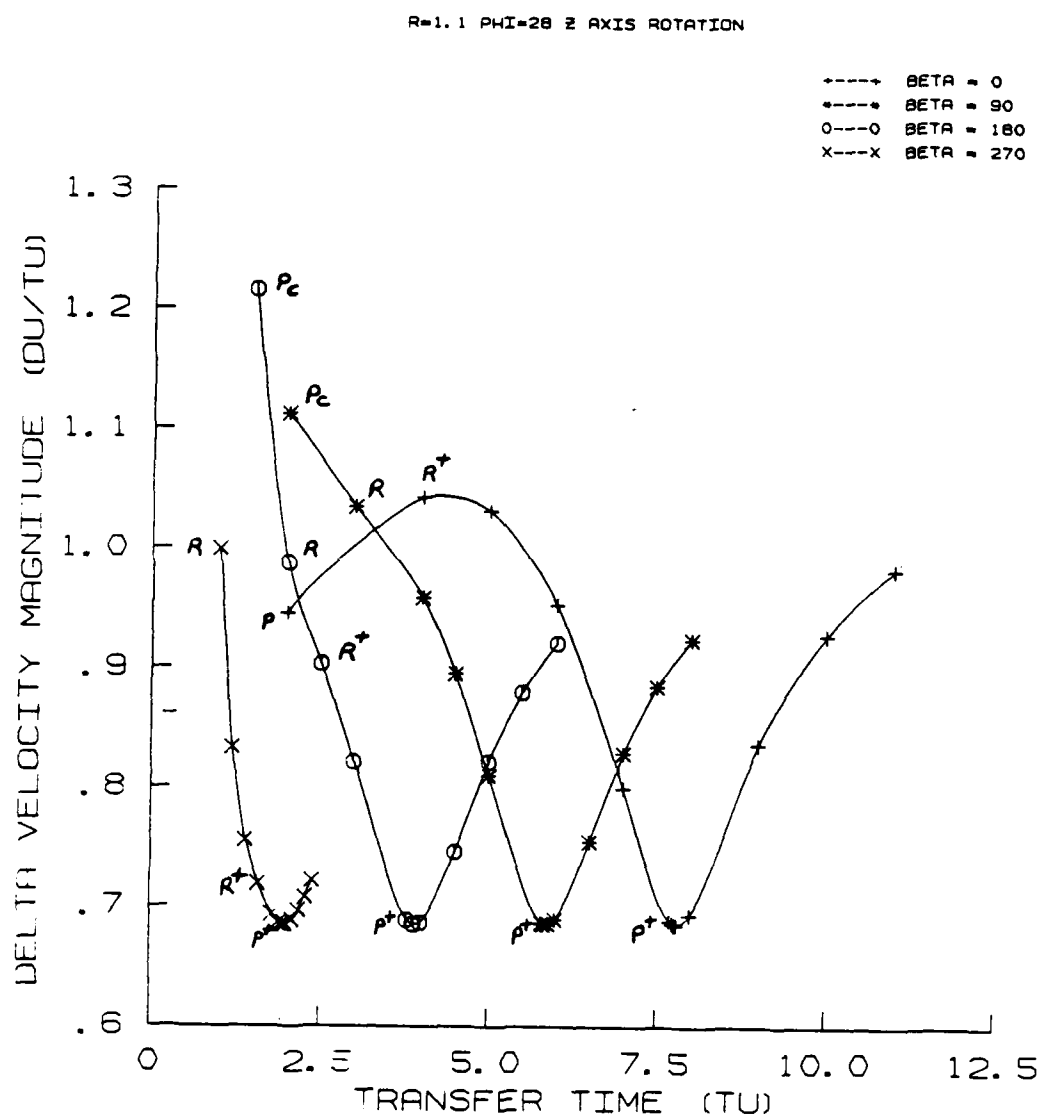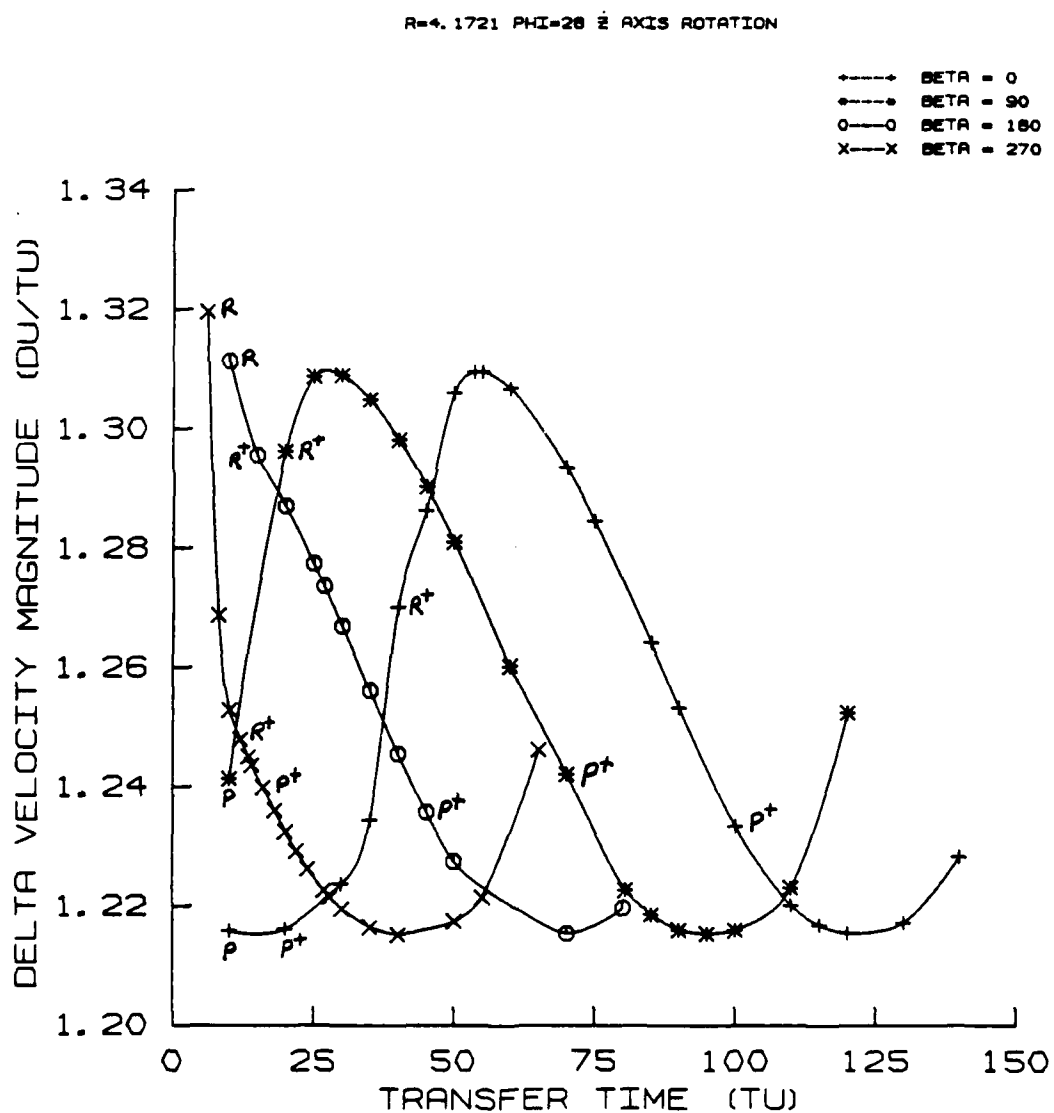Figure 7-3. Optimal Cost as a Function of Transfer Time.
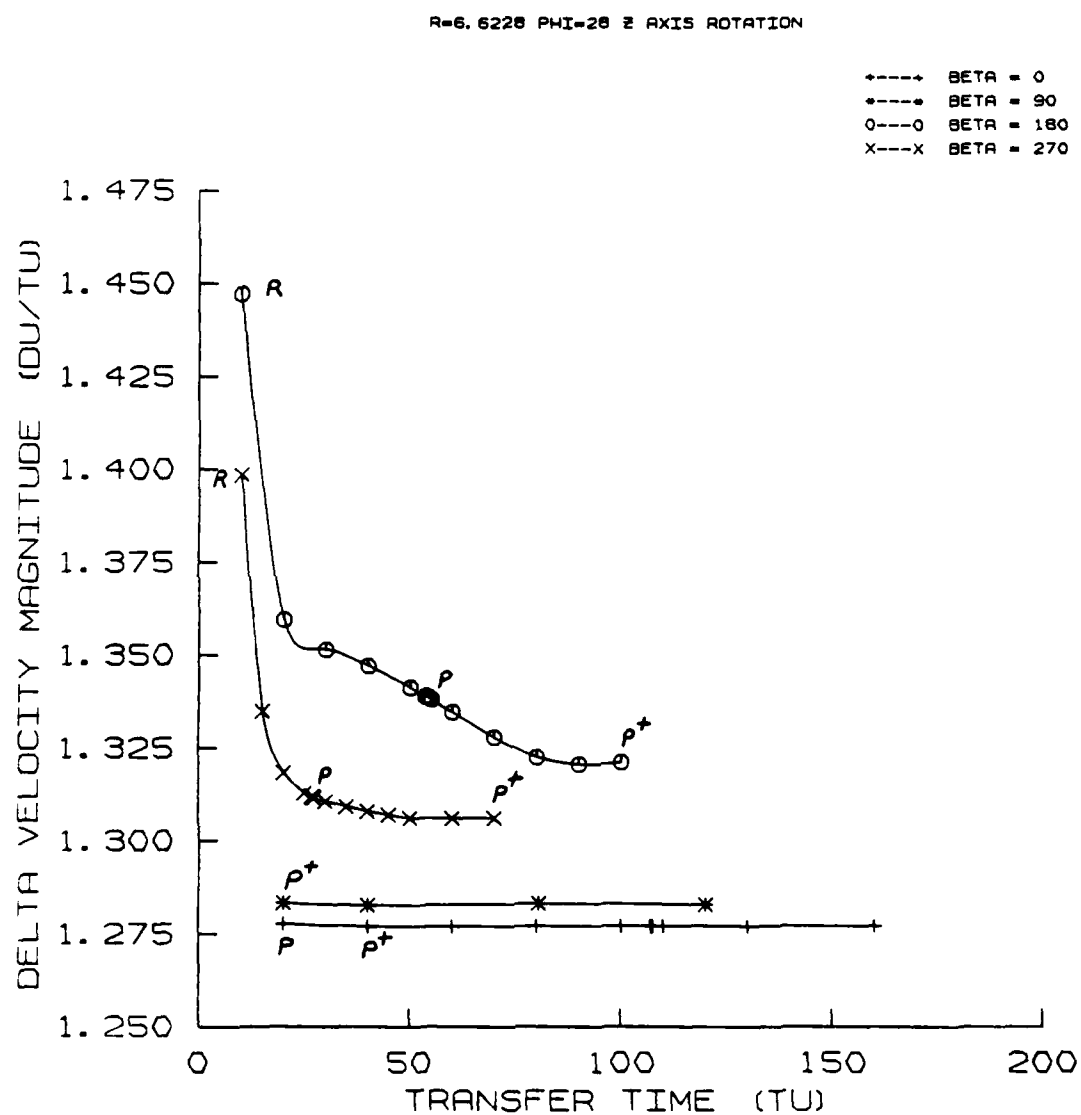
Figure 7-4. Optimal Cost as a Function of Transfer Time.

7.3. Coast versus No Coast

As previously found, an initial coast often improved the cost. Short transfer times lead to posigrade or retrograde orbits without coasts for the optimal solution. However, numerous curves have large sets of optimal solutions without an initial coast. These were for R = 1.1, beta = 90°, where there is a large set of optimal, retrograde orbits with no coast; and R = 6.6228, beta = 90°, 180°, and 270°, where there are large sets of optimal posigrade and retrograde orbits with no coast. In all optimal cases involving an initial coast, and outside the planet radius, the cost gradient, dJ/dt_o, was zero.

7.4. Cost Comparison

The rotating, inclined target orbit cases of this chapter generally agree with the coplanar cases in Chapter 6. The reference time for the global minimum is identical, but the transfer trajectory is a high eccentricity ellipse in the XZ plane, but rotated due to Earth rotation. For R = 1.1 and 2.0, the results are also similar to the non-rotating case. R = 4.1721 and 6.6228 do not show exactly the same trends. Geometry is more critical and the minimum ΔV does not always occur at the reference time. For R = 6.6228, the curves approach an asymptotic limit as transfer time increases.

As seen in Chapter 6, the minimum ΔV does increase as R increases, and the curves do not flatten as R increases. The global ΔV is higher than those for the coplanar case and optimum posigrade ΔVs are lower than comparable retrograde orbits.

Figure 7-5 shows a sample trajectory for the same R, beta, and t_f as in Chapter 6. The curves are similar to Figure 6-6, but three

R = 4.1721   BETA=0   PHI=28   TF=30 â AXIS ROTATION

+——+ POSIGRADE. NO COAST
—— POSIGRADE. INITIAL COAST
O——O RETROGRADE. NO COAST
X——X RETROGRADE. INITIAL COAST

Z

X

R = 1.0

R = 4.1721

Y
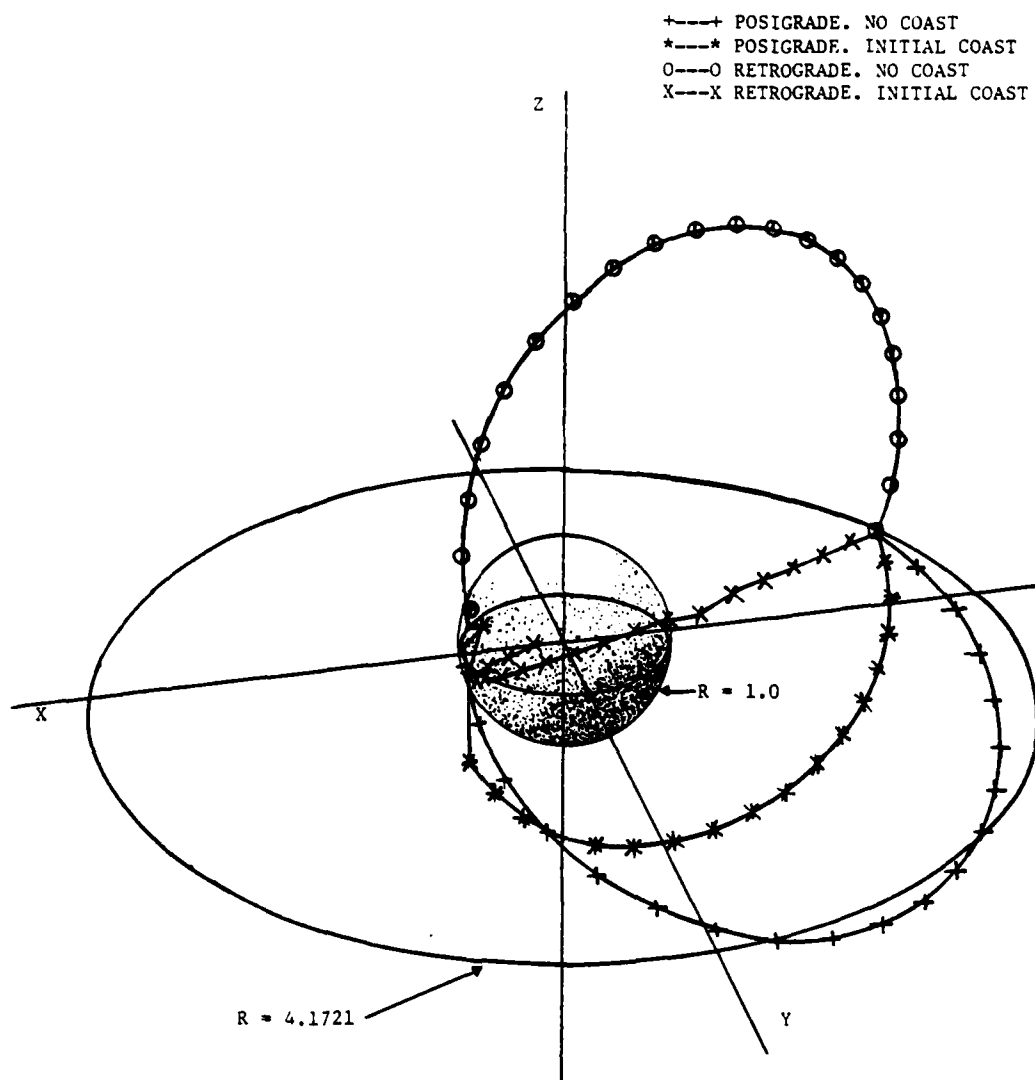
Figure 7-5.   Sample Trajectories.

dimensional. Posigrade and retrograde without an initial coast exceed the target radius (R = 5.61 and 5.86 respectively). The retrograde with an initial coast goes through the planet and violates the planet surface constraint. The optimum trajectory is the posigrade with a coast. As noted in Section 6.4, the launch points rotate as the Earth does, with a slightly different launch position for posigrade and retrograde with a coast.

CHAPTER 8

CONCLUSIONS AND RECOMMENDATIONS

8.1. Costs

The main conclusion of this research is that optimal, direct ascent, time-fixed, orbital interceptions can usually be accomplished using one impulse. This result depends on certain conditions and assumptions. The major conditions are that the intercept trajectory must remain outside the planet surface and that the transfer time must not be too small (see Appendix D).

The major assumptions qualifying the above conclusion are that there is only one central gravity field, and that single intercepts are made. Changing any of these assumptions or conditions could lead to multiple impulse trajectories.

One of the major factors to be considered which led to exceptions to this result was the planet surface constraint. Lower costs could often be achieved if the interceptor flew through the planet. Obviously, this condition is not permissible. Any time the surface constraint was violated, a minimum of two velocity changes would be necessary. The first would maintain the orbit at or above the planet surface ($\Delta V = 1.0$ DU/TU), while an additional impulse would be required to achieve the desired intercept. If the transfer time was greater than that obtained in Appendix D, i.e. greater than the minimum time required for one impulse, only one impulse would be required for an optimal trajectory. If the transfer time is less than this value, the

planet constraint would be violated, and multiple impulses would result. A theoretical approach incorporating the planet surface constraint is developed and presented in Appendix A.

Several factors contributed to the result that optimal intercepts could usually be performed with a single impulse. The flight direction could be varied between posigrade and retrograde trajectories, allowing flexibility unavailable with rendezvous problems. A retrograde trajectory for a rendezvous problem would produce unacceptably high ΔVs. Another contribution is that the launch point/target geometry changed such that an initial coast, combined with the flexibility to choose posigrade or retrograde orbits, was apparently more favorable than an added impulse. This occurred for all nonrotating cases, and for all rotating cases except near or at the geosynchronous orbit (R = 6.6228). There the body and target rotated at the same rate and the geometry was fixed. A contributing factor to the geometry change was that the body rotation rate involved was either 0, for a non-rotating body, or .0588 rad/TU for a body approximating an Earth rotation. These small rates allow relatively rapid geometry changes except for the cases previously noted.

Thus, the major contributing factors which usually allowed a single impulse to yield optimal intercept trajectories were as follows:

1. The flexibility to choose the optimal flight direction

2. The changing launch point/target relative geometry due to the low rotation rates used for the central body

3. The limiting assumptions used

4. The planet surface constraint could be satisfied for all intercepts unless the transfer time was too small (Appendix D).

This study found that to minimize the cost, an initial coast was often required, both for a rotating and non-rotating body. The ΔV cost can also be lowered by launching from a point in the same plane as the target orbit, i.e. coplanar. As the latitude between launch plane and target plane increases, the cost increases. Cost also increases with increasing target orbit radius, R.

For both rotating and non-rotating cases, the global minimum ΔV occurs at a given reference time. For a launch from a rotating body, the reference time is related to the synodic period between the rotating body and the target. For a non-rotating body, the reference time is that for interception of the target at the same longitude as the launch point. If a coplanar condition exists, the transfer trajectory for the global minimum ΔV is rectilinear with zero velocity at intercept. The sum of any coast time and the flight time for this rectilinear trajectory is the reference time. The intercept trajectory is in the XY plane, and along the X axis for the non-rotating body. For the non-coplanar case, the intercept is a high eccentricity ellipse in the XZ plane for a non-rotating body, and in a rotated XZ plane for a rotated body.

The use of primer vector theory, as developed by Lawden and others, was extremely helpful in obtaining the results in this research. In all those cases for which the planet surface constraint was satisfied, the primer vector provided the information that a neighboring trajectory containing an additional impulse would not decrease the cost. The primer vector also provided an expression for the gradient of the cost with respect to the initial time. This was useful in determining whether an initial coast was optimal and in determining the optimal value of the initial coast.

8.2. Geometry

The relationship between the launch point on the Earth's surface and the target position was also analyzed. For non-rotating bodies, and rotating bodies with target radii of 1.1 and 2.0, the results were similar. Basically, the same ΔV could be obtained regardless of the initial position (beta) of the target. Of course, this ΔV could be reached with a shorter transfer time as beta increased. Thus the transfer time for a globally optimum ΔV for beta = 270° was less than that for beta = 0°, 90°, or 180°. This relationship held for coplanar and non-coplanar trajectories.

However, the geometry relationship did not yield as universal a result for R = 4.1721 and 6.6228 for the rotating Earth case. Here, results for all betas seemed to asymptotically approach a minimum ΔV as transfer time increased. For R = 4.1721, all betas seem to converge to the same global minimum ΔV. For R = 6.6228, each beta seemed to have its own minimum ΔV differing from the other betas. Thus, for a given transfer time, each beta can give a different ΔV, with widely varying results. Especially noteworthy is the geometry involved in the geosynchronous orbit (R = 6.6228). The ΔV value is basically constant since the geometric relationship between launch point and target is invariant. Only for very short transfer times was a higher ΔV necessary to effect the intercept.

The direction of the intercept flight, posigrade or retrograde, was also critical. In general, for transfer times less than the reference time discussed in Section 8.1, retrograde with or without an initial coast was locally optimum. For transfer times greater than this

reference time the geometry changed such that posigrade with an initial coast yielded the optimum trajectory. For very short transfer times, posigrade with no coast was usually optimum. For the rotating Earth cases with R = 4.1721 and 6.6228, results were not so easily generalized. Large areas of transfer times involved posigrade or retrograde orbits with no coast at all.

8.3. Recommendations for Future Study

Several areas for further investigation would prove useful and informative. First, analysis of the rotating body for a non-Earth rotation rate could yield interesting results. The Earth rotation rate is approximately .0588 radians/TU, or a rotation period of about 17 times that of a circular orbit at the Earth's surface. Higher rotation rates should be investigated.

Second, incorporate a better model of the central body from which launch is made. Starting with the Earth, the most likely first addition would be an atmospheric model. This would introduce large effects as the launch vehicle must travel from the Earth's surface through the atmosphere to reach orbit. Drag, wind shear, and pressure and temperature gradients should all be incorporated in this model of the atmosphere. The Earth's oblateness would also be an interesting addition to the realistic model.

Third, the case of a rotating planet for which the target is not in the equatorial plane should be investigated. However, the results obtained for the nonrotating case are completely general.

Fourth, intercept between launch on a body's surface and more general target orbits, i.e. ellipses rather than circles, should be investigated. This is exceedingly more complex than surface to circular orbit transfers, but would be more general and useful in some cases.

Fifth, the inclusion of multiple intercepts should be evaluated. After making an intercept as demonstrated in this research, other intercept points could be attained in a given order. This would probably yield multiple impulse trajectories with interesting results.

Sixth, this research could be expanded to multiple gravitational fields. An example would be a launch from Earth intercepting a target in orbit around the moon.

Finally, investigation of algorithms to find multiple solutions to a given function would be useful. Non-unique optimal solutions are present for many data sets analyzed in this research. Determination of the absolute minimal optimal solution was done semi-manually by operator manipulation of input data to the computer. A better algorithm to automatically find a global minimum of a function, regardless of how many other local optimums there are, and regardless of the function or starting point for iteration, would be extremely useful.

APPENDIX A

PLANET SURFACE CONSTRAINT

This appendix is included as a reference and for general back-ground information. It was not directly used in the numerical algorithms to obtain data. However, its formulation lends insight to the problem of launching from a constraint surface rather than from one orbit to another.

A consideration in launches from a planet's surface is that the interceptor vehicle may not penetrate the surface. In order to determine the effect this has on the trajectory and the primer vector, use the notation of Bryson and Ho (8) to develop the following. Normalize the planet surface to one distance unit (DU), i.e. $R_o = 1$ DU. The new constraint can be represented as

$$\underline{r}^T \underline{r} \geq R_o{}^2 \qquad\qquad \text{A-1}$$

Rewrite this as

$$S\,(\underline{X},t) = 1/2\,(R_o{}^2 - \underline{r}^T \underline{r}) \leq 0 \qquad\qquad \text{A-2}$$

Differentiate until a control variable appears, i.e. Γ, the thrust acceleration magnitude, or $\underline{U}$, the thrust vector in the equations of state

$$\dot{X} = f\,(\underline{X},\,\underline{U},\,t) = \begin{bmatrix} \underline{V} \\ g\,(\underline{r}) + \Gamma\underline{U} \\ J \end{bmatrix} \qquad\qquad \text{A-3}$$

Thus

$$\dot{S} = -\underline{r}^T \underline{V} \qquad \text{A-4}$$

and

$$\ddot{S} = -\underline{V}^T \underline{V} - \underline{r}^T \dot{\underline{V}} = -V^2 - \underline{r}^T [\underline{g}(\underline{r}) + \Gamma \underline{U}] \qquad \text{A-5}$$

Now the constraint can be written as

$$\ddot{S} \leq 0 \qquad \text{A-6}$$

Expanding A-5 for an inverse square gravitational field and using the vis-viva equation

$$V^2 = \mu (2/r - 1/a) \qquad \text{A-7}$$

yields

$$\ddot{S} = -V^2 + \mu/r - \Gamma \underline{r}^T \underline{U} \leq 0 \qquad \text{A-8}$$

One notes that A-8 is zero if both

$$V^2 = \mu/r$$

and $\qquad \qquad \qquad \qquad \qquad \qquad \qquad \qquad \qquad$ A-9

$$\underline{r}^T \underline{U} = 0$$

Thus, $r = a$, a circular orbit of radius R_o (from vis-viva), and $\underline{r}$ is perpendicular to $\underline{U}$. Augment the Hamiltonian function with this additional constraint, using a new adjoint variable, λc. Thus from (2-10)

$$H = \underline{\lambda}_r^T \underline{V} + \underline{\lambda}_v^T (\underline{g} + \Gamma \underline{U}) - \lambda_J \Gamma + \lambda_c \ddot{S} \qquad \text{A-10}$$

For an active constraint

$$\lambda_c > 0 \text{ if } \ddot{S} = 0 \qquad\qquad \text{A-11}$$

For an inactive constraint

$$\lambda_c = 0 \text{ if } \ddot{S} < 0 \qquad\qquad \text{A-12}$$

Substitute A-5 into A-10 to obtain

$$H = (\underline{\lambda}_r^T - \lambda_c \underline{v}^T)\, \underline{v} + (\underline{\lambda}_v^T - \lambda_c \underline{r}^T)(\underline{g} + \Gamma \underline{U}) - \lambda_J \Gamma \qquad\qquad \text{A-13}$$

Define new Lagrange Multipliers as

$$\underline{\Lambda}_r = \underline{\lambda}_r - \lambda_c \underline{v}$$

and   A-14

$$\underline{\Lambda}_v = \underline{\lambda}_v - \lambda_c \underline{r}$$

Now write A-13 in simplified form as

$$H = \underline{\Lambda}_r^T \underline{v} + \underline{\Lambda}_v^T (\underline{g} + \Gamma \underline{U}) - \lambda_J \Gamma \qquad\qquad \text{A-15}$$

This is the same form as the Hamiltonian in Chapter 2 (2-10) except the Lagrange multiplier functions now include the surface constraint adjoint variable for the constraint A-6.

As was done in Chapter 2, to minimize H, align $-\underline{\Lambda}_v$ with $\underline{U}$, i.e., reintroduce the primer vector. From Chapter 2

$$\underline{\lambda}_v = -\underline{P} \qquad\qquad 2\text{-}15$$

$$\underline{\lambda}_r = \underline{\dot{P}} \qquad\qquad 2\text{-}17$$

However, now introduce a surface constrained primer vector, $\underline{\Pi}$, by defining

$$\underline{\Lambda}_v = -\underline{\Pi} \qquad\qquad \text{A-16}$$

and

$$\underline{\Lambda}_r = \underline{\dot{\Pi}} \qquad\qquad \text{A-17}$$

Introducing this nomenclature into A-14 yields

$$\underline{\dot{\Pi}} = \underline{\dot{P}} - \lambda_c \underline{V}$$

and   A-18

$$\underline{\Pi} = \underline{P} + \lambda_c \underline{r}$$

From Figure A-1, one can see that the surface constraint is violated in the nonrotating case if

$$\underline{P}_o^{\ T} \underline{r}_o \leq 0 \qquad\qquad \text{A-19}$$

To satisfy the constraint requires that

$$\underline{\Pi}\, o^T \underline{r}_o = 0 \qquad\qquad \text{A-20}$$

or using A-18,

$$\underline{P}_o^{\ T} \underline{r}_o + \lambda_c \underline{r}_o^{\ T} \underline{r}_o = 0 \qquad\qquad \text{A-21}$$

on the boundary. Solving for λ_c yields

$$\lambda_c = -(\underline{P}_o^{\ T} \underline{r}_o)/r_o^{\ 2} \qquad\qquad \text{A-22}$$

This term is positive if the surface constraint is not met. Equation A-18 can now be solved for the new, constrained primer vector given $\underline{r}_o$, $\underline{V}_o$, λ_c, and
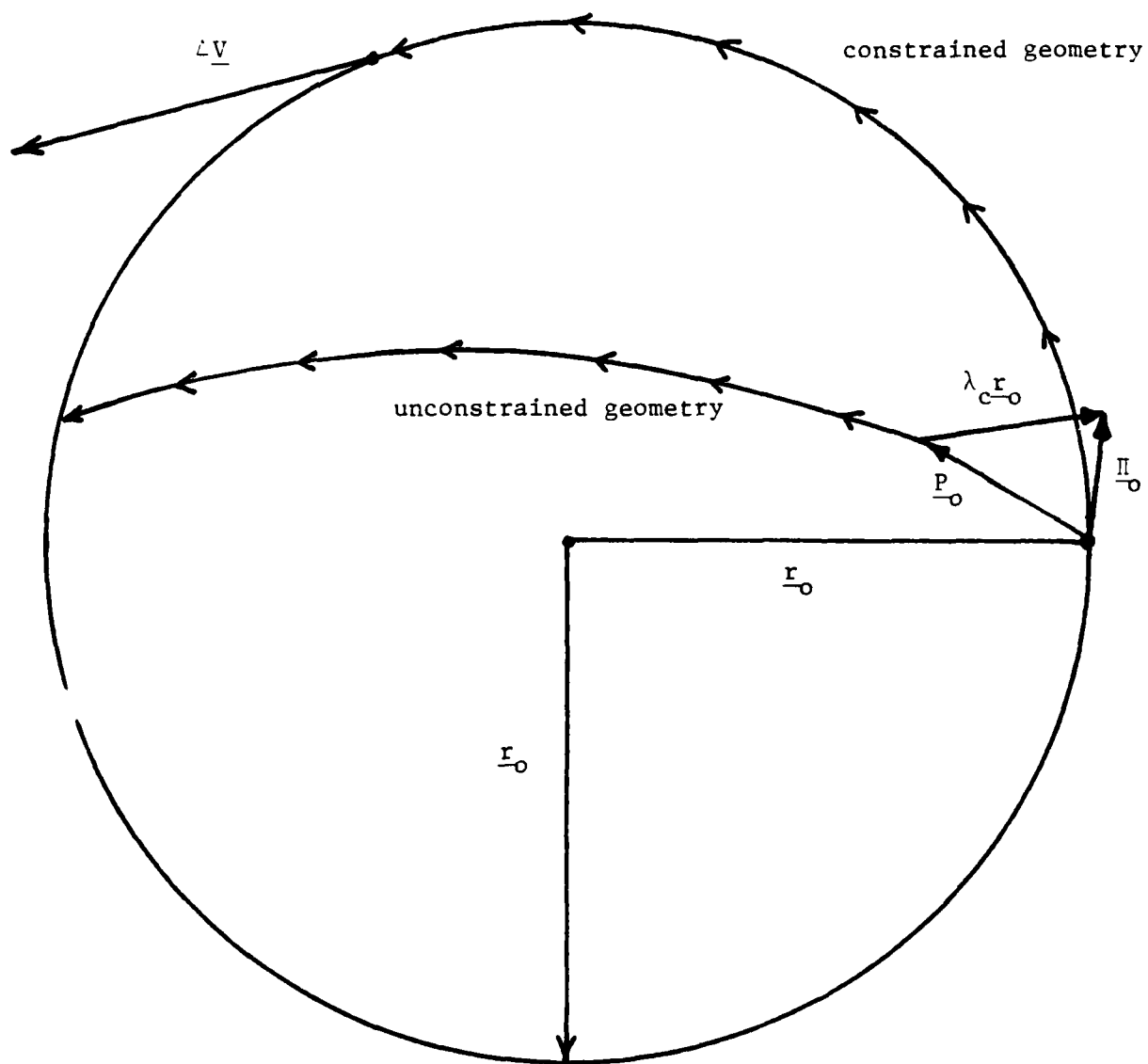
Figure A-1. Planet Surface Constraint Geometry.

$$\underline{P}_o = \Delta\underline{V}_o \ / \ |\Delta\underline{V}_o| .$$

Thus one solves the Lambert problem and obtains an initial primer and primer rate. If constraint A-19 is true, the primer must be modified by the component $\lambda_c \ \underline{r}$ to obtain the new primer, $\underline{\Pi}$. This primer will circularize the trajectory on the planet surface ($|\underline{r}| = R_o$ and $|\Delta \underline{V}_o| = 1$ DU/TU). At some appropriate time, a second $\Delta \underline{V}$ would be applied to allow interception of the required position. The theory developed in Chapters 2 and 3 would still apply with the substitution of $\underline{\Pi}$ for $\underline{P}$.

APPENDIX B

LAMBERT'S PROBLEM SOLUTION

B.1. Introduction

As with rendezvous problems, the known quantities in an intercept problem are initial position, final position, and the transfer time between the two. Lambert demonstrated that the flight time depends only on the semimajor axis of the transfer conic, the sum of the magnitudes of the terminal radii, and the chord joining these radii. Using Lambert's theorem, Battin (4) developed a convenient algorithm used in this research. This algorithm determines the trajectory and the terminal velocity vectors in terms of universal variables applicable to all types of conic orbits. The algorithm as programmed by D'Souza (13) was used in this study. Once these velocity vectors are known, the orbital elements of the transfer conic can be calculated using techniques presented in numerous references (2, 10, 18, 27).

B.2. Minimum Energy

Figure B-1 shows the geometry involved in solving Lambert's problem. Given $\underline{r}_1$ and $\underline{r}_2$, and a transfer time, there exists an orbit, having a certain value of semi-major axis, that connects P_1 and P_2 in the specified time. Writing the basic property for an ellipse, one gets

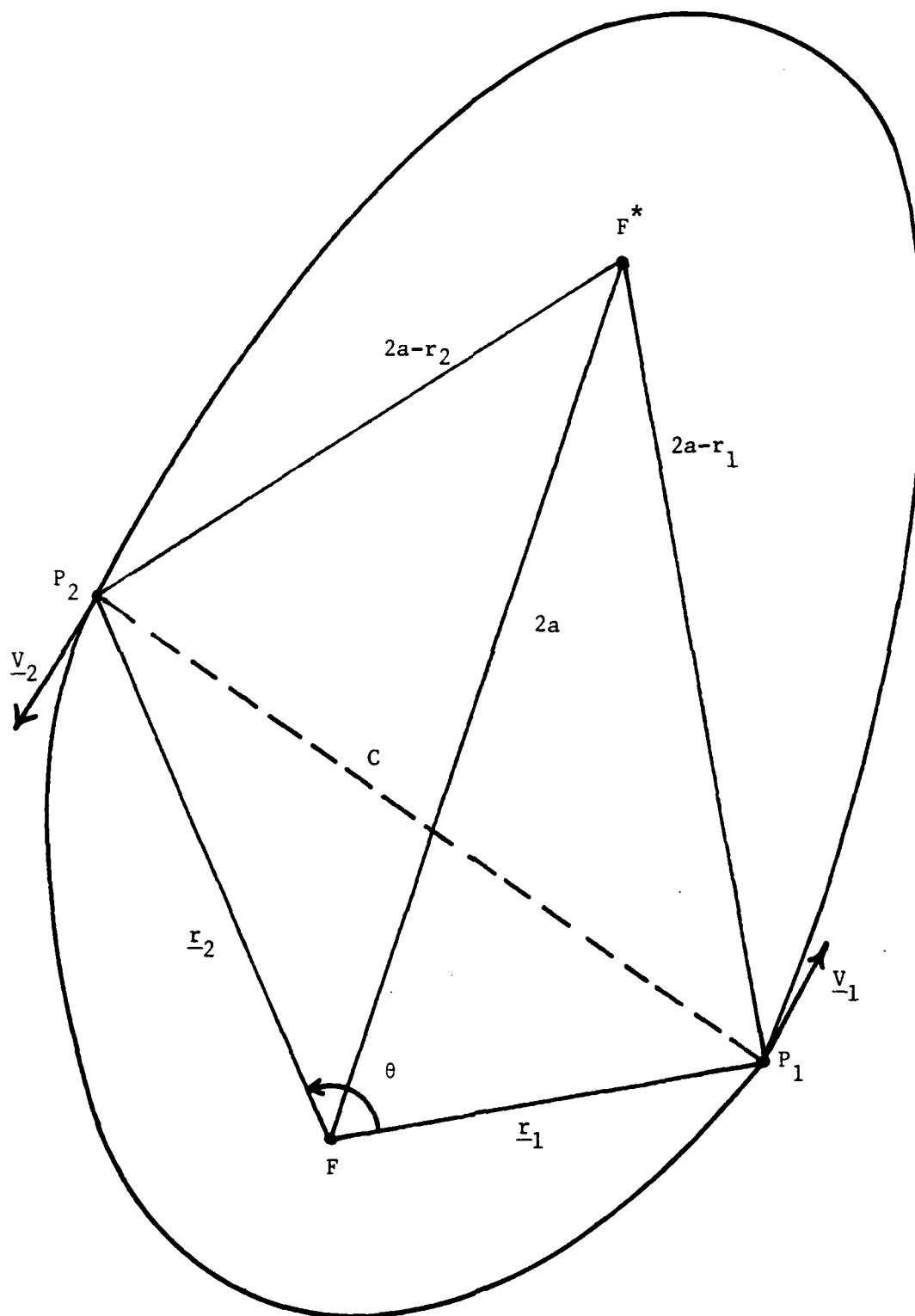$$\underline{P_1F^*} + \underline{P_1F} = \underline{P_2F^*} + \underline{P_2F} = 2a \qquad\qquad \text{B-1}$$

Figure B-1. Lambert Problem Geometry.

F*, the vacant focus, is the intersection of two circles with radii

$$P_1F* = 2a - r_1$$

and   B-2

$$P_2F* = 2a - r_2$$

By varying a, the locus of vacant focus is achieved.

There is a minimum value of a, called a_m, for which the two circles described above just touch. In this case, F* in on the chord, c. If a is too small, the circles do not touch and a transfer from P_1 to P_2 is impossible, i.e. the energy available is too low for an elliptic orbit to reach both P_1 and P_2. Thus a_m corresponds to the lowest possible energy path reaching both P_1 and P_2. A_m is obtained by noting that

$$(2a_m - r_2) + (2a_m - r_1) = c$$

or   B-3

$$a_m = (r_1 + r_2 + c)/4$$

Define the semi-perimeter, s, as

$$s = (r_1 + r_2 + c)/2$$ B-4

Thus

$$a_m = s/2$$ B-5

From the vis-viva equation

$$V_{1m}^2 = \mu(2/r_1 - 1/a_m)$$ B-6

where V_{1m} is the smallest possible speed at P_1 that will get the vehicle

to P_2. This is the condition that is critical in finding optimal intercepts for the non-rotating body cases described in Chapters 4 and 5.

B.3. Lambert Solution

Previous work has described this solution in much detail (2, 4, 10, 18, 27). This study modified the Battin algorithm (4) to calculate the terminal velocities for rectilinear orbits. The universality of the algorithm was useful, although it was found that hyperbolic orbits were optimal (and expensive) only for extremely short transfer times.

In terms of classical Lambert variables for an elliptical orbit, the time of flight for a given set of conditions $(\underline{r}_1, \underline{r}_2, t_f, a)$ is

$$t_f = \sqrt{a^3/\mu} \; [sgn(t_m-t_f)(\alpha-sin\alpha-\pi)-sgn(sin\theta)(\beta-sin\beta)] \qquad \text{B-7}$$

where θ is the transfer angle,

$$sin\alpha/2 = \sqrt{s/2a}$$

and $\qquad\qquad$ B-8

$$sin\beta/2 = \sqrt{(s-c)/2a}$$

For a minimum energy ellipse

$$sin\,\alpha_m/2 = 1 \Rightarrow \alpha_m = \Pi$$

and $\qquad\qquad$ B-9

$$sin\beta_m/2 = \sqrt{(s-c)/s}$$

Thus

$$t_m = \sqrt{s^3/8\mu} \; [\pi-sgn(sin\theta)(\beta_m-sin\beta_m)] \qquad\qquad \text{B-10}$$

The required velocities, V_1 and V_2, and the orbital elements can also be calculated using the aforementioned references.

APPENDIX C

OPTIMAL, ZERO GRAVITY, TIME-FIXED INTERCEPTION

C.1. Introduction

This problem is an interesting theoretical aside, related to the thesis topic. Gravity is assumed to equal zero. These results were not directly used in this research, but lend to an understanding of the basic problem.

C.2. Necessary Conditions for an Optimum Trajectory

From Chapter 2, the following equation of motion was introduced.

$$\underline{\dot{V}} = \underline{\ddot{r}} = \underline{g}\,(\underline{r}) + \Gamma\underline{U} \qquad\qquad C-1$$

For a no thrust, optimal coasting arc, $\Gamma = 0$. Assume that $\underline{g} = 0$. Then the solution to C-1 becomes

$$\underline{r} = \underline{a}\,t + \underline{b} \qquad\qquad C-2$$

Thus the radius vector in a zero gravity field, varies linearly with time, and the velocity vector is a constant, $\underline{a}$. Similarly. the Hamiltonian, equation 2-10, can be written as

$$H = \underline{\lambda}_r{}^T\,\underline{V} = constant \qquad\qquad C-3$$

From the Euler-Lagrange conditions (8 and equations 2-11, 2-12, and 2-13), one obtains

MICROCOPY RESOLUTION TEST CHART

NATIONAL BUREAU OF STANDARDS-1963-A

$$\dot{\underline{\lambda}}_r = \underline{0}$$

$$\dot{\underline{\lambda}}_v = -\underline{\lambda}_r \qquad\qquad C\text{-}4$$

$$\dot{\lambda}_J = 0$$

Thus,

$$\underline{\lambda}_r = \text{constant} = \underline{c}$$

$$\underline{\lambda}_v = -\underline{c}\, t + \underline{d} \qquad\qquad C\text{-}5$$

$$\lambda_J = 1$$
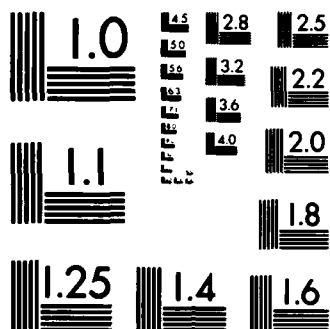
From Lawden (30), the primer vector is defined as

$$\underline{P}\,(t) = -\underline{\lambda}_v\,(t) \qquad\qquad C\text{-}6$$

Using the results in C-5

$$\underline{P}\,(t) = \underline{c}\, t - \underline{d} \qquad\qquad C\text{-}7$$

Thus

$$\underline{\dot{P}} = \underline{c} = \text{constant} = \underline{\lambda}_r \qquad\qquad C\text{-}8$$

C.3. Boundary Conditions

To solve for the constants in equations C-2 and C-7, one general assumption is made. The target (point to be intercepted) is the origin of the coordinate system used, as shown in Figure C-1.

At $t = t_o = 0$, $\underline{r} = \underline{r}_o$, and $\underline{V} = \underline{V}_o$ on the initial orbit. Similarly at $t = t_f$, $\underline{r} = \underline{0}$ since the intercept must occur at the origin, and $\underline{V} = \underline{V}_f$ which is arbitrary. Thus the intercept vehicle moves from one linear trajectory to another by application of a velocity change. Using these boundary conditions in equation C-2, one finds
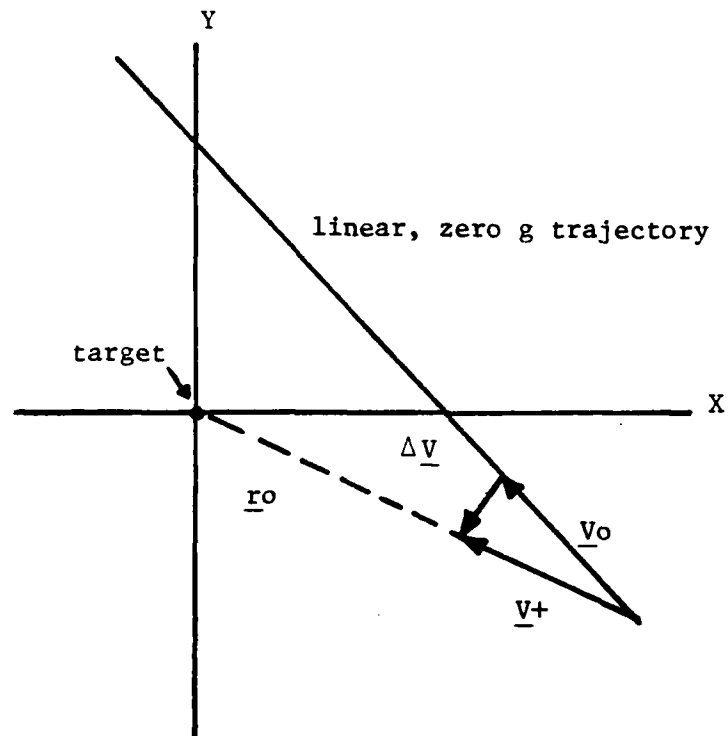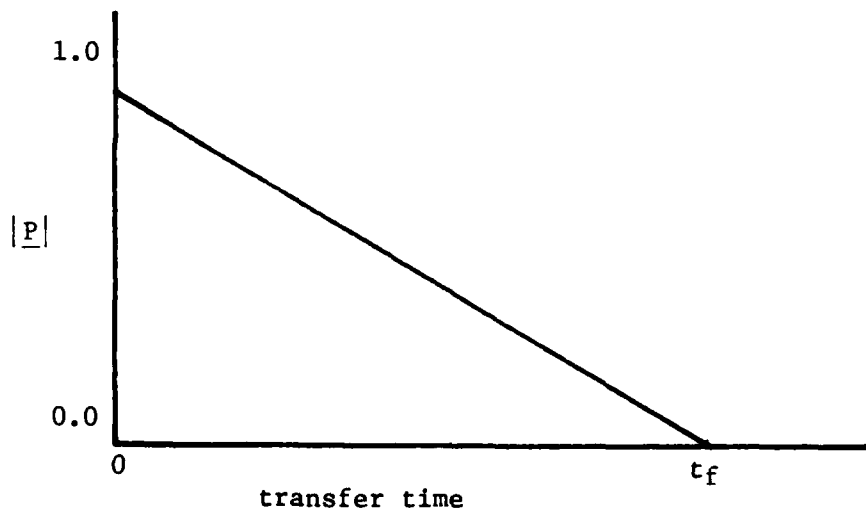
Figure C-1.   Intercept Geometry.

Figure C-2.   Primer Time History.

$$\underline{b} = \underline{r}_o$$

and $\quad \underline{a} = \underline{V}_o$ $\qquad$ C-9

Thus

$$\underline{r} = \underline{V}_o t + \underline{r}_o \qquad \text{C-10}$$

on any trajectory in a zero gravity field.

At any point, $\underline{r}$, on a general zero gravity trajectory, a $\Delta\underline{V}$ is applied to go to the origin such that

$$\underline{V}^+ = \underline{V}_o + \Delta\underline{V} \qquad \text{C-11}$$

to go to the target, or

$$\underline{r} \, I = (\underline{V}^+) \, t + \underline{r} \qquad \text{C-12}$$

or $\quad \underline{r} \, I = (\underline{V}_o + \Delta\underline{V}) t + \underline{r}$ $\qquad$ C-13

on a zero g trajectory intercepting the origin, where $\underline{r}$ I is the radius on the path to the target, starting at $\underline{r}$ with constant velocity, $\underline{V}^+$. Knowing that at $t = 0$, $\underline{r}$ I = $\underline{r}$, a point on the general zero g trajectory, and also that at $t = t_f$, $\underline{r}$ I = 0, yields the solution at the final time, t_f,

$$\underline{r} \, I = \underline{0} = (\underline{V}_o + \Delta\underline{V}) t_f + \underline{r} \qquad \text{C-14}$$

Solving for the required $\Delta\underline{V}$ yields

$$\Delta\underline{V} = -\underline{r}/t_f - \underline{V}_o \qquad \text{C-15}$$

This is the $\Delta\underline{V}$ required to go from any point $\underline{r}$, with velocity $\underline{V}_o$, on a general zero g trajectory, to the target (origin) in time t_f. Substituting C-15 into C-13 yields

$$\underline{r} \ I = \underline{r} \ (1 - t/t_f) \qquad\qquad C-16$$

C.4. Primer Vector Calculation

Use the definition of the primer vector

$$\underline{P} = -\underline{\lambda}_v = \Delta\underline{V}/|\Delta\underline{V}| \qquad\qquad C-17$$

where $|\Delta\underline{V}| = \Delta V = (\Delta\underline{V}^T\Delta\underline{V})^{1/2}$, and the known boundary conditions, to determine the constants in C-7. For an intercept trajectory $\underline{P}$ $(t_f) = \underline{0}$. Thus C-7 is rewritten as

$$\underline{P} \ (t) = \underline{c} \ (t-t_f) = \underline{d} \ (t/t_f - 1) \qquad\qquad C-18$$

Note that $t - t_f \leq 0$.

From C-17 and C-18 one can see that $\underline{P}$ is in the direction of $\Delta\underline{V}$ and $-\underline{c}$, while $\underline{\dot{P}}$ is in the direction of $-\Delta\underline{V}$ and $\underline{c}$. $\underline{P}$ and $\underline{\dot{P}}$ are in opposite directions.

To solve for the primer vector, use the initial condition $t = t_o = 0$ to obtain

$$\underline{c} = -\underline{P} \ (0)/t_f = -\Delta\underline{V}/t_f\Delta V \qquad\qquad C-19$$

Substitute C-15, evaluated at $t = t_o$, into C-19 to obtain

$$\underline{c} = 1/t_f\Delta V \ (\underline{r}_o/t_f + \underline{V}_o) \qquad\qquad C-20$$

Now that $\underline{c}$ is in terms of known quantities, a general primer vector equation can be obtained by substituting C-20 into C-18.

$$\underline{P} = \underline{r}_o \, (t - t_f)/t_f^2 \Delta V + \underline{V}_o (t - t_f)/t_f \Delta V \qquad\qquad \text{C-21}$$

This linear relation holds at both boundary conditions. At $t = t_f$, $\underline{P} = \underline{0}$, and at $t = 0$, $\underline{P} = \Delta\underline{V}/\Delta V$. The primer time history in a zero gravity field is shown in Figure C-2. From Lawden (30), the primer history shown is already optimum. No initial coast or intermediate impulse can improve ΔV.

C.5. <u>Examples</u>

Two pertinent cases arise as interesting applications of the theory just developed.

Case I

Assume $\underline{r}_o^T \, \underline{V}_o < 0.$ The minimum $\Delta\underline{V}$ will occur where

$$\Delta\underline{V}^T \underline{r}_o = 0, \qquad\qquad \text{C-22}$$

i.e. where $\Delta\underline{V}$ is perpendicular to $\underline{r}_o$. Substitute C-15 into C-22 to obtain

$$-r_o^2/t_f - \underline{r}_o^T \underline{V}_o = 0 \qquad\qquad \text{C-23}$$

Solving for t_f at this minimum $\Delta\underline{V}$ condition yields

$$T^* = t_f min = -r_o^2/\underline{r}_o^T \underline{V}_o \qquad\qquad \text{C-24}$$

Use C-24 and evaluate C-15 at t_o to obtain the minimum $\Delta\underline{V}$.

$$\Delta\underline{V} \, min = \underline{r}_o^T \, \underline{V} \, \underline{r}_o/r_o^2 - \underline{V}_o \qquad\qquad \text{C-25}$$

Look at the Hamiltonian on the trajectory to the origin for this condition.

$$H = \dot{\underline{P}}^T \underline{V} = \underline{c}^T \underline{V}^+ \qquad \text{C-26}$$

Substituting, one can obtain

$$H = -1/t_f^2 \, \Delta V \, [r_o^2/t_f + \underline{r}_o^T \underline{V}_o] \qquad \text{C-27}$$

Thus for $\underline{r}_o^T \underline{V}_o < 0$, one finds that $H < 0$ for $t < T^*$, and $H > 0$ for $t > T^*$. At T^*, $H = 0$ (the time-open optimum). This is graphically shown in Figure C-3.

If, for the time-fixed case, the transfer time, t_f is greater than T^*, the $\Delta\underline{V}$ min still occurs at T^*. If, however, the t_f is less than T^*, the $\Delta\underline{V}$ min will occur at the given t_f.

Case II

Assume $\underline{r}_o^T \underline{V}_o > 0$. Since $\Delta\underline{V}$ is never perpendicular to $\underline{r}_o$, the time-open minimum $\Delta\underline{V}$ is at $t = \infty$. At this point equation C-15 shows that $\Delta\underline{V}$ min $= -\underline{V}_o$. Given a specified final time (time-fixed), t_f, which cannot be exceeded, the minimum $\Delta\underline{V}$ occurs with a time of flight equal to the specified time, i.e. no coast. Using the analysis developed in Case 1, one obtains the time-fixed minimum conditions.

$$\text{Tmin} = t_f$$

and $\qquad \Delta\underline{V}$ min $= -\underline{r}_o/t_f - \underline{V}_o \qquad \qquad$ C-28

The Hamiltonian is identical to C-27. However, if $\underline{r}_o^T \underline{V}_o > 0$, $H < 0$ for all t. $H \to 0$ (the time-open optimum) only as $t_f \to \infty$. Figure C-4 graphically shows this.

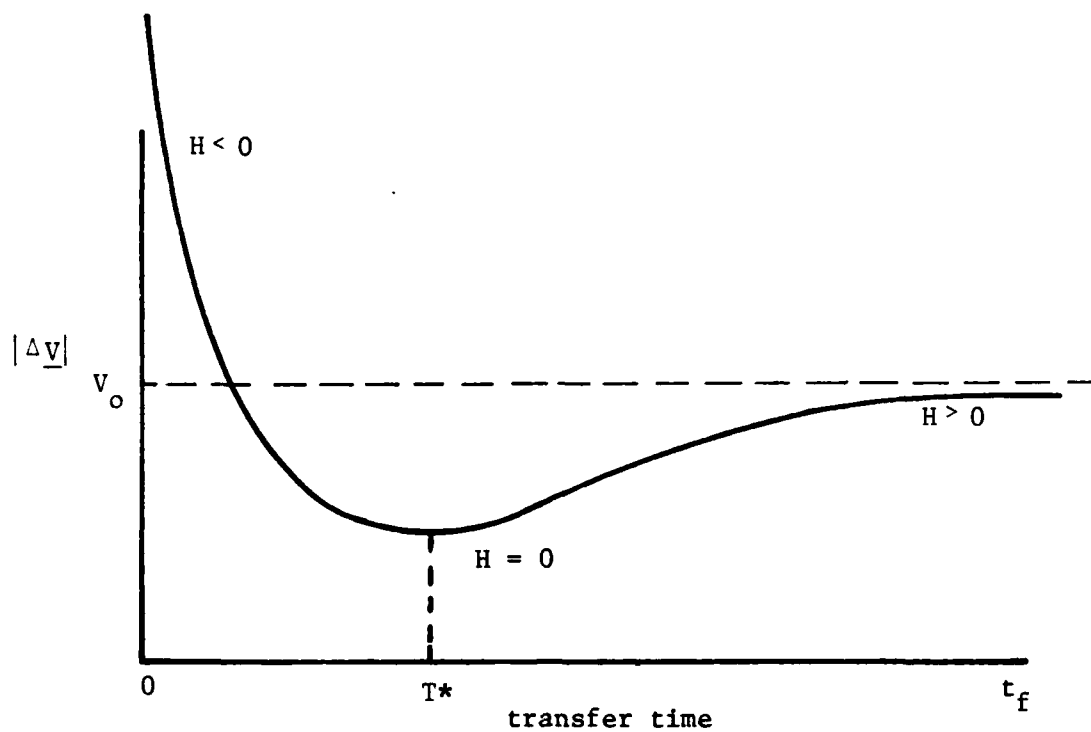Figure C-3. Optimal Cost for $\underline{r}_o{}^T \underline{V}_o < 0$.
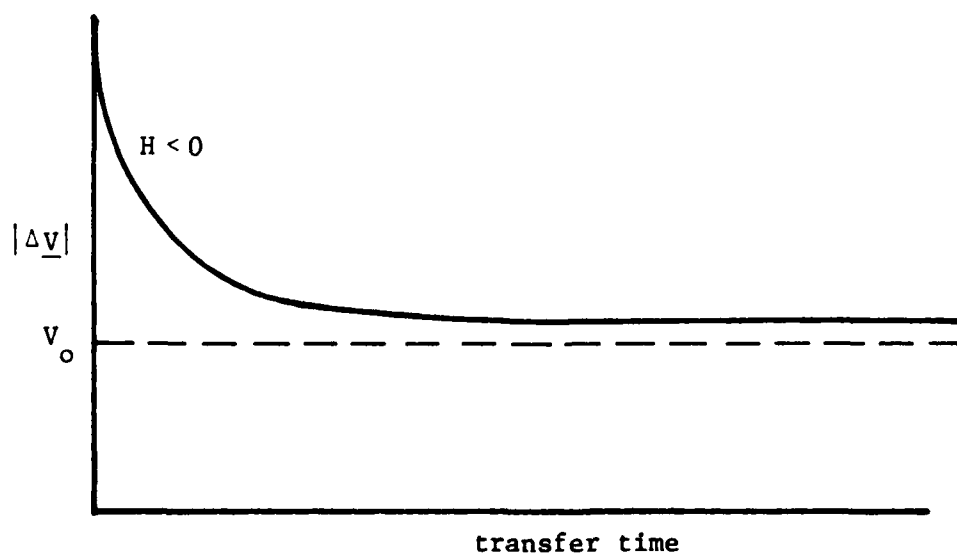

Figure C-4. Optimal Cost for $\underline{r}_o{}^T \underline{V}_o > 0$.

APPENDIX D

MINIMUM TIME FOR SINGLE IMPULSE TRAJECTORIES

D.1. Introduction

Results of this study show a single impulse to be optimal under

certain conditions, one of which was that the transfer time not be too

small for a given initial target position. In order to determine what

this minimum time for a single impulse trajectory is, the planet con-

straint must be considered. Any time the planet constraint is violated,

two (or more) impulses are required: One will maintain the orbit at or

above the planet surface, and a second will accomplish the intercept.

The condition for the launch vehicle trajectory to be tangent to the

planet surface at launch is

$$\underline{r}_o^T \underline{V}_o = 0 \qquad\qquad\qquad D\text{-}1$$

If $\underline{r}_o^T \underline{V}_o < 0$, the planet constraint is violated and more impulses would

be necessary. Thus equation D-1 represents the limiting case between one

and two impulse trajectories. It indicates that the launch point is at

the periapse of the transfer conic, i.e., $\underline{V}_o = \underline{V}_p$.

Note that the value of $\underline{V}_o$ in D-1 is not unique. Consider the

cases shown in Figure D-1. On trajectory ΓH, a Hohmann transfer is

considered (with only one impulse for an intercept). The velocity $(\underline{V}_H)$

and semi-major axis (a_H) are known, yielding a minimum transfer time,

t_H = Hohmann period/2, and the final target position is at a transfer

angle (true anomaly) of $\theta_H = 180°$ from launch. For the same final
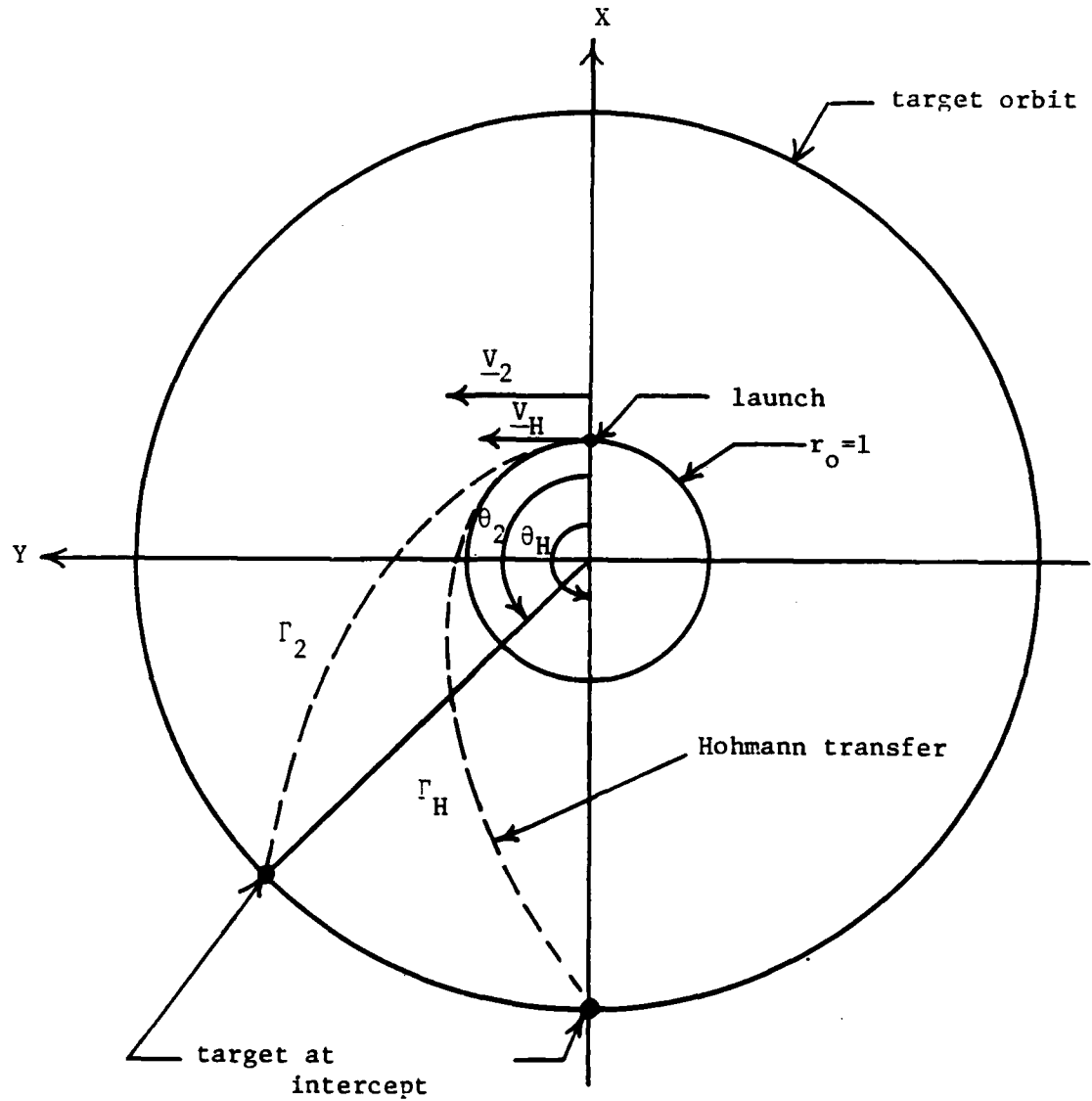
Figure D-1. Geometry for $\underline{r}_o^T \underline{V}_o = 0$.

target position and transfer time, a velocity less than the Hohmann

velocity will penetrate the planet surface but will have insufficient

energy to reach the target orbit, i.e. a < a_H. A velocity and semi-

major axis value greater than Hohmann will remain outside the planet

surface. Also, for the given final position, a time less than t_H will

violate the planet surface constraint.

For a different final position, trajectory Γ2 will have a

minimum transfer time, t_m, satisfying D-1, and an associated a and $\underline{V}_2$.

For this final target position and a time less than t_m, the trajectory

will go through the planet surface, while a time greater than t_m will

remain outside the planet.

Thus, for a given target orbit, the limiting time for a single

impulse, i.e. equation D-1, can be determined. If a nonrotating body

is considered, $\underline{V}_p = \Delta\underline{V}$, while a rotating body would yield $\underline{V}_p = \Delta\underline{V}$

$+ \underline{V}_{rot}$.

D.2. Analysis

To determine the limiting case, calculate the Hohmann transfer

conditions. Assume that $r_o = 1$, R = target orbit radius, $\mu = 1$, and

that the impulse is applied at periapse. Thus the semi-major axis is

$$a_H = (R + 1) / 2 \qquad\qquad \text{D-2}$$

Using the Vis-Viva equation, the velocity at periapse can be found.

$$V_{pH} = \sqrt{(2 - 1/a_H)} \qquad\qquad \text{D-3}$$

The eccentricity is calculated from $r_o = a(1 - e \cos E_o)$ where $E_o = 0$.

$$e_H = 1 - 1/a_H \qquad \qquad \text{D-4}$$

The time of flight from periapse to the intercept point is

$$\Delta t_H = P_H/2 = \pi\, a_H^{3/2} \qquad \qquad \text{D-5}$$

The final true anomaly is

$$\theta_H = 180° \qquad \qquad \text{D-6}$$

Finally, the position of the target at $t = t_o$ can be calculated

$$\beta_H = \theta_H - 360°\, \Delta t_H / P_R \qquad \qquad \text{D-7}$$

where P_R is the period of the orbit with radius R.

Any value of the semi-major axis less than a_H will violate the planet surface constraint. Choose successive values of $a > a_H$. Since the launch is at periapse, $\underline{h} = \underline{r}_o\ X\ \underline{V}_o = V_o\ \underline{k}$, or

$$h = V_o \qquad \qquad \text{D-8}$$

Solve the following equations for each a:

$$e = 1 - 1/a \qquad \qquad \text{D-9}$$

$$V_o = \sqrt{2 - 1/a} = \sqrt{1 + e} \qquad \qquad \text{D-10}$$

$$\theta = \cos^{-1}\left[1/e\ (V_o^2/R - 1)\right] \qquad \qquad \text{D-11}$$

$$E = \cos^{-1}\left[1/e\ (1 - R/a)\right] \qquad \qquad \text{D-12}$$

$$\Delta t = (E - e\, \sin E)\, a^{3/2} \qquad \qquad \text{D-13}$$

$$\beta = \theta - 360°\, \Delta t / P_R \qquad \qquad \text{D-14}$$

In the limit, a $\to \infty$, yielding a parabolic transfer, and e = 1.
Calculate the quantities in equations D-10, D-11, and D-14. Use
Barker's equation for a parabola in place of D-13, i.e.

$$\Delta t = [\tan \theta/2 + 1/3 \tan^3 \theta/2] P^{3/2} \qquad\qquad \text{D-15}$$

where $P = 2r_p = 2$ for a parabola.

D.3. Results

By successively picking values of a from that for a Hohmann
transfer to that for a parabolic transfer, and performing the calcula-
tions indicated in Section D.2, a curve of transfer angle versus the
minimum time for one impulse can be obtained. Figure D-2 shows the
results for the four target radii used in this study. It is a graph of
the minimum time for one impulse versus transfer angle, or final true
anomaly, for either a posigrade or retrograde trajectory, and is
symmetric about $\theta = 180°$. Thus, for a given θ, i.e. final target
position, the intersection of a vertical line with the curve for a
given R is the t_m. If $t > t_m$, i.e. "above" the curve for each R, one
impulse is possible. If $t < t_m$, i.e. "below" the curve for each R,
the planet surface constraint is violated and two impulses are required.
For example, on the R = 6.6228 curve in Figure D-2, choose a transfer
angle of 150.2°. If the given transfer time is greater than t_m = 12.77 TU,
a single impulse trajectory is optimal. If t < 12.77 TU, two or more
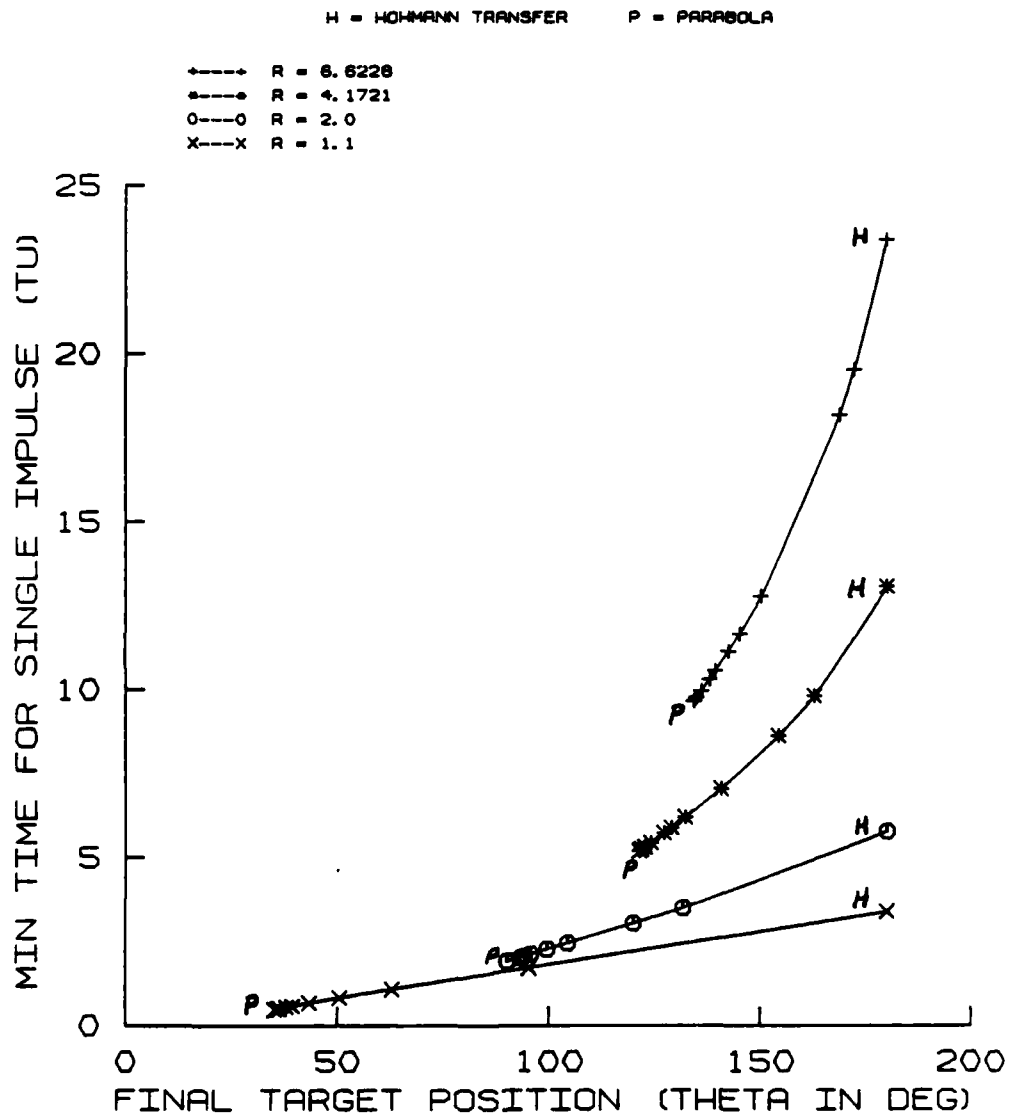impulses would be required.

Figure D-2. One Impulse Minimum Time Versus True Anomaly.

REFERENCES AND SELECTED BIBLIOGRAPHY

1. Baker, J. M. "Orbit Transfer and Rendezvous Maneuvers between Inclined Circular Orbits." Journal of Spacecraft and Rockets, Vol. 8, No. 8, Aug. 1966, pp. 1216-1220.

2. Bate, R. R., Mueller, D. D., and White, J. E. Fundamentals of Astrodynamics. Dover Publications, Inc., New York, 1971.

3. Battin, R. H. Astronautical Guidance. McGraw-Hill, 1964.

4. Battin, R. H., and Vaughan, R. M. "An Elegant Lambert Algorithm." Journal of Guidance, Control and Dynamics, Vol. 7, No. 6, Nov.-Dec. 1984, pp. 662-670.

5. Billik, B. H., and Roth, H. L. "Studies Relative to Rendezvous between Circular Orbits." Astronautic Acta, Vol. 13, No. 1, Jan.-Feb. 1967, pp. 23-35.

6. Boden, Daryl G., and Kruczynski, Leonard R. "Multiple-Intercept Trajectories." Paper 81-155, AAS/AIAA Astrodynamics Specialist Conference, Aug. 3-5, 1981.

7. Breakwell, J. V., and Dixon, J. F. "Minimum-Fuel Rocket Trajectories Involving Intermediate-Thrust Arcs." Journal of Optimization Theory and Applications, Vol. 17, No. 6, Dec. 1975, pp. 465-479.

8. Bryson, A. E., and Ho, Y. C. Applied Optimal Control. Hemisphere Publishing Corporation, New York, 1975.

9. Carstens, J. P., and Edelbaum, T. N. "Optimal Maneuvers for Launching Satellites into Circular Orbits of Arbitrary Radius and Inclination." ARS Journal, Vol. 31, No. 7, Jul. 1961, pp. 943-949.

10. Chiu, J. H. "Optimal Multiple-Impulse Nonlinear Orbital Rendezvous." Ph.D. thesis, University of Illinois at Urbana-Champaign, Department of Aeronautical and Astronautical Engineering, 1985.

11. Conte, S. D., and deBoor, C. Elementary Numerical Analysis, An Algorithmic Approach. McGraw-Hill Book Company, New York, 1980.

12. Davidon-Fletcher-Powell IBM Scientific Subroutine Package (SSP) FMFP.

13. D'Souza, C. N. "A Comparison of Algorithms for the Solution of Lambert's Problem." M.S. Thesis, University of Illinois at Urbana-Champaign, Department of Aeronautical and Astronautical Engineering, 1984.

14. Edelbaum, T. N. "How Many Impulses?" Astronautics and Aeronautics, Vol. 5, No. 11, Nov. 1967, pp. 64-69.

15. Glandorf, D. R. "Lagrange Multipliers and the State Transition Matrix for Coasting Arc." AIAA Journal, Vol. 7, No. 2, Feb. 1969, pp. 363-365.

16. Gobetz, F. W., and Doll, J. R. "A Survey of Impulsive Trajectories." AIAA Journal, Vol. 7, No. 5, May 1969, pp. 801-834.

17. Gravier, J. P., Marchal, C., and Culp, R. D. "Optimal Impulsive Transfers Between Real Planetary Orbits." Journal of Optimization Theory and Application, Vol. 15, No. 5, May 1975, pp. 587-604.

18. Gross, Larry R. "Optimal Multiple-Impulse Direct Ascent Rendezvous." Ph.D. Thesis, University of Illinois at Urbana-Champaign, Department of Aeronautical and Astronautical Engineering, 1972.

19. Gross, Larry R., and Prussing, J. E. "Optimal Multiple-Impulse Direct Ascent Fixed-Time Rendezvous." AIAA Journal, Vol. 12, No. 7, Jul. 1974, pp. 885-889.

20. Grund, E., and Pitkin, E. T. "Iterative Method for Calculating Optimal Finite-Thrust Orbit Transfers." AIAA Journal, Vol. 10, No. 2, Jan. 1972, pp. 221-223.

21. Haviland, R. P., and House, C. M. "Nonequatorial Launching to Equatorial Orbits and General Nonplanar Launching." AIAA Journal, Vol. 1, No. 6, Jun. 1963, pp. 1336-1341.

22. Jezewski, D. J. "N-Burn Optimal Analytic Trajectories." AIAA Journal, Vol. 11, No. 10, Oct. 1973, pp. 1373-1376.

23. Jezewski, D. J. "Optimal Two-Impulse Transfer Between Specified Terminal States of Keplerian Orbits." Optimal Control Applications and Methods, Vol. 3, 1982, pp. 257-267.

24. Jezewski, D. J. "Primer Vector Theory and Applications." NASA, TR R-454, 1975.

25. Jezewski, D. J. "Primer Vector Theory Applied to the Linear Relative Motion Equations." Optimal Control Applications and Methods, Vol. 1, 1980, pp. 387-401.

26. Jezewski, D. J., and Rozendaal, H. L. "An Efficient Method for Calculating Optimal Free-Space N-Impulse Trajectories." AIAA Journal, Vol. 6, No. 11, 1968, pp. 2160-2165.

27. Kaplan, M. H. Modern Spacecraft Dynamics and Control. John Wiley and Sons, New York, 1976.

28. Kirpichnikov, S. N. "Optimal Trajectories Between Material Points Moving on the Same Orbit." Cosmic Research, Vol. 14, No. 4, Jul.-Aug. 1966, pp. 460-471.

29. Korkowski, J. A. "Minimum Three-Impulse Earth to Circular Orbit Transfer." M.S. Thesis, University of Illinois at Urbana-Champaign, Department of Aeronautical and Astronautical Engineering, 1978.

30. Lawden, D. F. Optimal Trajectories for Space Navigation. Butterworths, London, 1963.

31. Lion, P. M., and Handelsman, M. "The Primer Vector on Fixed-Time Impulsive Trajectories." AIAA Journal, Vol. 6, No. 1, Jan. 1968, pp. 127-132.

32. Liu, F. C., and Plexico, L. D. "Improved Linear Solution of Optimal Multi-Impulse Fixed-Time Rendezvous Between Circular Orbit." Journal of Spacecraft and Rockets, Vol. 19, No. 6, Nov.-Dec. 1982, pp. 521-528.

33. Pines, S. "Constants of the Motion for Optimal Thrust Trajectories in a Central Force Field." AIAA Journal, Vol. 7, No. 2, Feb. 1969, pp. 2010-2014.

34. Prussing, J. E. "A Performance Comparison of Several Numerical Minimization Algorithms." Final Report, 1972 Graduate College Faculty Summer Fellowship Program, University of Illinois, Department of Aeronautical and Astronautical Engineering, 1972.

35. Prussing, J. E. "Illustration of the Primer Vector in Time-Fixed Orbit Transfer." AIAA Journal, Vol. 7, No. 6, Jun. 1969, pp. 1167-1168.

36. Prussing, J. E. "Optimal Four-Impulse Fixed-Time Rendezvous in the Vicinity of a Circular Orbit." AIAA Journal, Vol. 7, No. 5, May 1969, pp. 928-935.

37. Prussing, J. E. "Optimal Multiple-Impulse Orbital Rendezvous." Sc.D. Thesis, Sep. 1967, Department of Aeronautics and Astronautics, Massachusetts Institute of Technology.

38. Prussing, J. E. "Optimal Two- and Three-Impulse Fixed-Time Rendezvous in the Vicinity of a Circular Orbit." AIAA Journal, Vol. 8, No. 7, Jul. 1970, pp. 1221-1228.

39. Prussing, J. E. "Optimal Spacecraft Trajectories." Class notes, University of Illinois, 1983.

40. Prussing, J. E., and Chiu, J. H. "Optimal Multiple-Impulse Time-Fixed Rendezvous between Circular Orbits." Journal of Guidance, Control and Dynamics, to appear.

41. Robbins, H. M. "An Analytical Study of the Impulsive Approximation."
    AIAA Journal, Vol. 4, No. 8, Aug. 1966, pp. 1417-1423.

42. Sameh, A. "Introduction to Numerical Methods." Computer Science/
    Math 257 class notes, University of Illinois, undated.

43. Vinh, N. X. "Integration of the Primer Vector in a Central Force
    Field." Journal of Optimization Theory and Applications, Vol. 9,
    No. 1, 1972, pp. 51-58.

VITA

William G. Heckathorn was born on March 8, 1946 in Steubenville, Ohio. He graduated from Dreux American High School, Dreux Air Force Base, France in May 1964. He earned Bachelor of Aeronautical and Astronautical Engineering and Master of Science degrees from The Ohio State University in 1969 and 1970, respectively. He is a member of Tau Beta Pi, the national engineering honorary. His engineering experience has covered systems engineering projects, including the APG-63 radar system; the BQM-34A, BQM-34F, MQM-107, and HAHST drones; fuel enhancement testing on NKC-135 aircraft; performance testing of F-4C aircraft; and systems management of innumerable aircraft, systems, and special projects.

END

10-86

DTIC